TÉCNICO LISBOA

Inter-Cell Interference Impact on LTE Performance in Urban Scenarios

Diogo Xavier Azevedo de Almeida

Thesis to obtain the Master of Science Degree in

Electrical and Computer Engineering

Examination Committee

Chairperson: Prof. Fernando Duarte Nunes

Supervisor: Prof. Luís Manuel de Jesus Sousa Correia

Member of Committee: Prof. António José Castelo Branco Rodrigues

Member of Committee: Eng. Marco Paulo Almeida Serrazina

October 2013

To my family and friends

Acknowledgements

My first acknowledgement goes to Prof. Luís M. Correia, who has always been keen on doing master thesis in collaboration with network operators or manufacturers, so that students can work on real life issues and provide some guidelines for better solutions. I will never forget his guidance, support and professionalism, which contributed to shape my work ethics and attitude, and his advices about my future as a professional. I would also like to thank the support provided by Daniel Sebastião, who was responsible to dedicate some of his time to help me improve my work. My special thanks are also extended to other members of the Group for Research on Wireless (GROW), such as Carla Oliveira, Ema Catarré, Lúcio Ferreira, Michal Mackowiak, Mónica Branco, Sina Khatibi and Vera Almeida, for their advices and companionship during some leisure moments. Being part of GROW was an excellent opportunity to sharpen my presentation skills and to keep in touch with the most promising telecommunications topics that will outline the future of wireless communications.

Special acknowledgements are also given to Eng. Diana Caiado, Eng. Marco Serrazina, Eng. Pedro Lourenço and Eng. Ricardo Batista, who followed my work from Vodafone's point of view and helped me with their advices and support during the measurements campaign.

For their friendship, mutual sharing of information and advices, I would like to thank Dinis Rocha, Joana Fernandes and Ricardo Santos, who shared GROW's MSc Students room with me. I would also like to extend this acknowledgement to other GROW's MSc Students, who were also part of the mutual sharing of knowledge – Jaime Pereira, Joana Falcão, João Martins and Pedro Martins. For his help during the transition of his work to mine, as both of us were doing a master thesis with Vodafone at a common short period of time, I would also like to thank André Pires.

My gratitude also goes out to the following Professors, who were never reluctant to share their knowledge and advices: Prof. Adolfo Cartaxo, Prof. António Rodrigues, Prof. Carlos Fernandes, Prof. Fernando Pereira, Prof. Jorge Fernandes, Prof. Leonel Sousa, Prof. Luís Caldas de Oliveira and Prof. Teresa Mendes de Almeida (who was my tutor during my first two years of college).

Last, but not least, I would like to thank my Father, Mother, Sister and Grand-Mother, for being both family and friends, and to my college friends, especially the ones which have accompanied my journey as a college student through the best and hardest times: Ângelo Dias, Bernardo Costa, Carlos Martins, Darpan Dayal, David Doutor, Dharmine Jamnadas, Diogo Cândido, Diogo Rolo, João Fole, Joel Martins, Lucas Balthazar, Márcia Santos, Martina Fonseca, Pedro Miguel and Pedro Ramos.

Abstract

The main objective of this thesis was the evaluation of LTE performance in urban scenarios concerning inter-cell interference via antenna aspects. A detailed analysis of the effect of the antenna's electrical and mechanical downtilts, height, and output power on interference minimisation was addressed for the 800, 1 800 and 2 600 MHz frequency bands in dense urban (centre of Lisbon) and urban (off-centre of Lisbon) environments. A stochastically generated line of sight occurrence, a contiguous spectrum distribution and a received power based association of users to sectors was considered in a simulator intended to represent a real network as close as possible. Two separate studies were performed: in the low load scenarios analysis, results obtained via simulation were compared with measurements, while in the high load scenarios analysis it was found that output power and electrical downtilt provide the best improvements on the number of users served per sector (up to 11.6% improvement) and user's throughput (up to 27.3% higher throughput), respectively, over the reference scenario. Interference margins were also calculated, ranging from 18.53 dB at 2 600 MHz to 32.95 dB at 800 MHz, in the centre of Lisbon.

Keywords

LTE, inter-cell interference, downtilt, radiation pattern, sector, line of sight

Resumo

O objetivo principal desta dissertação foi a avaliação do desempenho do LTE em cenários urbanos no que toca à interferência inter-celular através de aspetos de antenas. Uma análise detalhada do efeito das inclinações elétrica e mecânica, altura, e potência de emissão das antenas na minimização da interferência teve lugar para as bandas de frequências de 800, 1 800 e 2 600 MHz em ambientes urbanos densos (centro de Lisboa) e urbanos (periferia de Lisboa). Considerou-se uma geração estocástica da ocorrência de linha de vista, uma distribuição espectral contígua e uma associação de utilizadores a sectores baseada na potência recebida num simulador destinado a representar uma rede real da forma mais próxima possível. Foram feitos dois estudos distintos: numa análise de cenários de baixa carga, os resultados obtidos por simulação foram confrontados com medidas, enquanto na análise dos cenários de alta carga verificou-se que a potência de emissão e a inclinação elétrica levam às maiores melhorias do número de utilizadores servidos por sector (até 11.6%) e do ritmo binário dos utilizadores (até 27.3%), respetivamente, em relação ao cenário de referência. Calcularam-se também margens de interferência, que variam desde 18.53 dB em 2 600 MHz até 32.95 dB em 800 MHz, no centro de Lisboa.

Palavras-chave

LTE, interferência inter-celular, inclinação, diagrama de radiação, sector, linha de vista

Table of Contents

List of Figures

List of Tables

List of Acronyms

2G	Second-Generation
3G	Third-Generation
3GPP	3rd Generation Partnership Project
4G	Fourth-Generation
ACK	ACKnowledgement
AM	Acknowledged Mode
AMC	Adaptive Modulation and Coding
ANACOM	Autoridade Nacional de Comunicações
AWGN	Additive White Gaussian Noise
BPSK	Binary Phase Shift Keying
BS	Base Station
CFI	Control Format Indicator
CP	Cyclic Prefix
CQI	Channel Quality Indicator
DCI	Downlink Control Information
DL	Downlink
E-UTRA	Evolved Universal Terrestrial Radio Access
EDGE	Enhanced Data Rates for Global Evolution
EIRP	Effective Isotropic Radiated Power
eNodeB	evolved Node B
EPA	Extended Pedestrian A
EPC	Evolved Packet Core
ETU	Extended Typical Urban
EVA	Extended Vehicular A
FDD	Frequency Division Duplex
FFR	Fractional Frequency Reuse
FTP	File Transfer Protocol
GBR	Guaranteed Bit Rate
GSM	Global System for Mobile Communications
HARQ	Hybrid Automatic Repeat reQuest
HSDPA	High Speed Downlink Packet Access
HSPA	High Speed Packet Access
HSPA+	HSPA Evolution
HSUPA	High Speed Uplink Packet Access

HSS	Home Subscription Server
HTTP	HyperText Transfer Protocol
ICIC	Inter-Cell Interference Coordination
IMS	IP Multimedia Sub-system
IP	Internet Protocol
ITU	International Telecommunication Union
LoS	Line of Sight
LTE	Long Term Evolution
LTE-A	LTE-Advanced
M2M	Machine to Machine
MAC	Medium Access Control
MBR	Maximum Bit Rate
MCS	Modulation and Coding Scheme
MIMO	Multiple-Input Multiple-Output
MM	Mobility Management
MME	Mobility Management Entity
NACK	Negative ACKnowledgement
NLoS	Non Line of Sight
OFDM	Orthogonal Frequency Division Multiplexing
OFDMA	Orthogonal Frequency Division Multiple Access
OLPC	Open Loop Power Control
P-GW	Packet Data Network Gateway
PBCH	Physical Broadcast Channel
PC	Personal Computer
PCC	Policy and Charging Control
PCFICH	Physical Control Format Indicator Channel
PCRF	Policy and Charging Resource Function
PDCCH	Physical Downlink Control Channel
PDSCH	Physical Downlink Shared Channel
PDU	Protocol Data Unit
PHICH	Physical HARQ Indicator Channel
PRACH	Physical Random Access Channel
PSS	Primary Synchronization Signal
PUCCH	Physical Uplink Control Channel
PUSCH	Physical Uplink Shared Channel
Qi	ith Quarter
QAM	Quadrature Amplitude Modulation
QCI	QoS Class Identifier
QoS	Quality of Service
QPSK	Quadrature Phase Shift Keying

RACH	Random Access Channel
RB	Resource Block
RE	Resource Element
RF	Radio Frequency
RLC	Radio Link Control
RRM	Radio Resource Management
RS	Reference Signal
RSRP	Reference Signal Received Power
S-GW	Serving Gateway
SAE-GW	System Architecture Evolution Gateway
SC-FDMA	Single Carrier Frequency Division Multiple Access
SFR	Soft Frequency Reuse
SINR	Signal-to-Interference plus Noise Ratio
SNR	Signal-to-Noise Ratio
SSS	Secondary Synchronization Signal
TB	Transport Block
TDD	Time Division Duplex
TE	Terminal Equipment
TTI	Transmission Time Interval
UE	User Equipment
UICC	Universal Integrated Circuit Card
UL	Uplink
UL-SCH	Uplink Shared Channel
UMTS	Universal Mobile Telecommunications System
USIM	Universal Subscriber Identity Module
VoIP	Voice-over-IP
WCDMA	Wideband Code Division Multiple Access

List of Symbols

θ	Angle between the pointing direction of the antenna and the direction defined by the antenna and the UE (LoS) / building (NLoS), in the vertical plane
θ_{3dB}	Vertical half-power beamwidth
θ_{etilt}	Electrical antenna downtilt
θ_{mtilt}	Mechanical antenna downtilt
$\theta_v{}'$	Angle between the vertical direction of the antenna (neglecting any existing tilt) and the direction defined by the antenna and the UE (LoS) / building (NLoS), in the vertical plane
ϕ	Angle of incidence of the signal in the buildings, on the horizontal plane
ρ_N	SNR
ρ_{IN}	SINR
φ	Angle between the pointing direction of the antenna and the direction defined by the antenna and the UE, in the horizontal plane
φ'	Angle between the pointing direction of the antenna (neglecting any existing tilt) and the direction defined by the antenna and the UE, in the horizontal plane
φ_{3dB}	Horizontal half-power beamwidth
A_m	Front-to-back attenuation
B_N	Noise bandwidth
B_{RB}	Bandwidth of an RB
d	Distance between the BS and the UE
d_{co}	Cut-off distance
d_{max}	Distance of the UE farther away from its serving sector antenna
F	Noise figure
f	Carrier frequency of the signal
G	Gain of the transmitting antenna
G_{max}	Maximum gain of the antenna
G_r	Gain of the receiving antenna
H_B	Height of the buildings
h_b	Height of the BS antenna
h_m	Height of the UE
I	Interfering power
k	Boltzmann's constant
L_0	Free space propagation path loss

L_c	Losses in the cable between the transmitter and the antenna
L_p	Path loss from the COST-231 Walfisch-Ikegami model
$L_{p,total}$	Path loss
L_{rm}	Attenuation due to diffraction from the last rooftop to the UE
L_{rt}	Attenuation due to propagation from the BS to the last rooftop
L_u	Losses due to the user
M_{FF}	Fast fading margin
M_{SF}	Slow fading margin
N	Noise power
$N_{b/sym}$	Number of bits per symbol
N_I	Number of interfering signals reaching the receiver
N_{MIMO}	MIMO order
N_{RB}	Number of RBs
$N_{sub/RB}$	Number of sub-carriers per RB
$N_{sym/sub}$	Number of symbols per sub-carrier
P_{EIRP}	Effective isotropic radiated power
P_{LoS}	LoS probability
P_r	Power available at the receiving antenna
P_{Rx}	Power at the input of the receiver
P_{Tx}	Transmitter output power
R_b	Throughput
R_{sector}	Sector antenna's range
SLA_v	Sidelobe attenuation
T	Temperature of the receiver
T_{RB}	Time duration of an RB
w_B	Distance between buildings' centres
w_s	Width of the streets

List of Software

C++ Builder XE3	C++ App Development Environment
FileZilla	FTP client
Google Earth	Geographical information program
MapBasic 11.5	Programming software and language for the creation of additional tools and functionalities for MapInfo
MapInfo Professional 11.5	Geographical information system software
Microsoft Excel 2010	Spreadsheet application
Microsoft Word 2010	Word processor
TEMS Discovery 3.0.2	Drive-test analysis software
TEMS Investigation 13.1.33	Software for verification of wireless networks
Wolfram Mathematica 8	Computational software

Chapter 1

Introduction

This chapter provides a brief overview of the mobile communications systems evolution, in terms of technology and consumer demand, with a strong particular focus on LTE. It also discusses the motivation for this work and the structure of the thesis.

1.1 Overview

Over the past years, several mobile communications systems were introduced, in order to fulfil consumer demand needs. Those needs have changed throughout the years – the most significant change was the transition of a clear dominance of voice traffic, to a clear dominance of data traffic, as it can be seen in Figure 1.1.

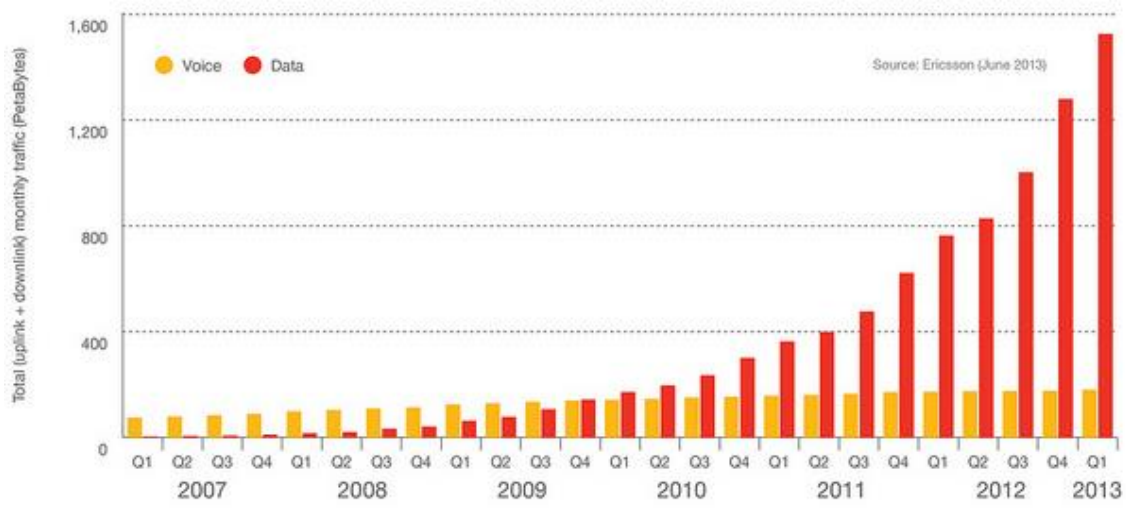

Figure 1.1. Global total traffic in mobile networks, 2007-2013 (extracted from [Eric13]).

Wide-area wireless networks have experienced a rapid evolution in terms of data rates, but wireline networks are still able to provide the highest data rates, according to [HoTo11]. As such, wireless networks must be able to provide increasingly higher data rates to match the user experience that wireline networks provide, because customers are used to wireline performance and they expect the wireless networks to offer comparable performance. Wireless technologies, however, are able to offer personal broadband access, which is independent of the user's location – they provide mobility in nomadic or full mobile use cases. They can also provide low-cost broadband coverage compared to new wireline installations, if there is no existing wireline infrastructure.

Global System for Mobile Communications (GSM) was originally designed to carry voice traffic. Later on, data capability was added. Data use has increased, but the traffic volume in second-generation (2G) networks, such as GSM, is clearly dominated by voice. The introduction of third-generation (3G) networks, such as Universal Mobile Telecommunications System (UMTS), boosted data use considerably. UMTS data growth is driven by high-speed radio capability, flat-rate pricing schemes, and simple device installation, and its introduction has marked the transition of mobile networks from voice-dominated to packet-data-dominated networks.

The definition of the targets for 3rd Generation Partnership Project (3GPP) Long Term Evolution (LTE), often called the fourth-generation (4G), started in 2004. Although the evolution of UMTS, High Speed Packet Access (HSPA), was not yet deployed, work for the next radio system started, because it takes more than five years from system target settings to commercial deployment using interoperable standards, which means that system standardisation must start early enough to be ready in time. LTE

development was driven by wireline capability evolution, need for more wireless capacity, need for lower cost wireless data delivery (higher efficiency), and competition from other wireless technologies.

Several requirements were defined for LTE, as it was supposed to be able to provide a performance superior to that of existing 3GPP networks based on UMTS/HSPA. Peak user throughput should present a minimum of 100 Mbit/s in the downlink (DL) and 50 Mbit/s in the uplink (UL), which is ten times more than that of HSPA Release 6. Latency must also be reduced to improve performance for the end user, and terminal power consumption must be minimised to enable a higher usage of multimedia applications without a constant need to recharge the battery. There should also be frequency flexibility with available allocations from below 1.5 MHz up to 20 MHz.

Time schedules of 3GPP specifications and its commercial deployments are shown in Figure 1.2, where 3GPP dates refer to the approval of the specifications. UMTS' Wideband Code Division Multiple Access (WCDMA) Release 99 specification work was completed at the end of 1999, being followed by the first commercial deployments during 2002, right after the ones for GSM's Enhanced Data Rates for Global Evolution (EDGE). High Speed Downlink Packet Access (HSDPA) and High Speed Uplink Packet Access (HSUPA) standards were completed in March 2002 and December 2004, respectively, and their commercial deployments followed in 2005 and 2007. The first phase of HSPA Evolution (HSPA+) was completed in June 2007, deployments starting during 2009. The LTE standard was approved at the end of 2007, while backwards compatibility studies started in March 2009. The first commercial LTE networks started during 2010. The next step is LTE-Advanced (LTE-A), which had its specification approved in December 2010.

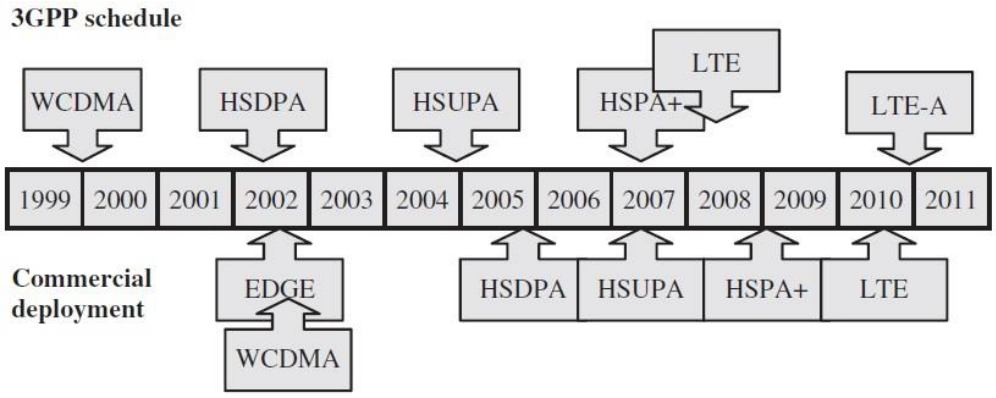

Figure 1.2. Schedule of 3GPP standards and their commercial deployments (extracted from [HoTo11]).

Every new generation of technologies pushes peak data rates higher, which are summarised in Figure 1.3. It should be noted that each new 3GPP technology is designed for smooth interworking and coexistence with the existing ones. For example, LTE supports bi-directional handovers between LTE and GSM, and between LTE and UMTS. GSM, UMTS and LTE can share network elements, such as those of the core network. Also, some of the 3G network elements can be upgraded to support LTE, and the existence of a single network platform supporting both UMTS/HSPA and LTE is possible

The growing availability of mobile broadband has raised users' expectations of mobile network quality,

which turned mobility an integral part of their everyday lives. It is, therefore, crucial to provide coverage, sufficient quality and speed to run applications anywhere and anytime.

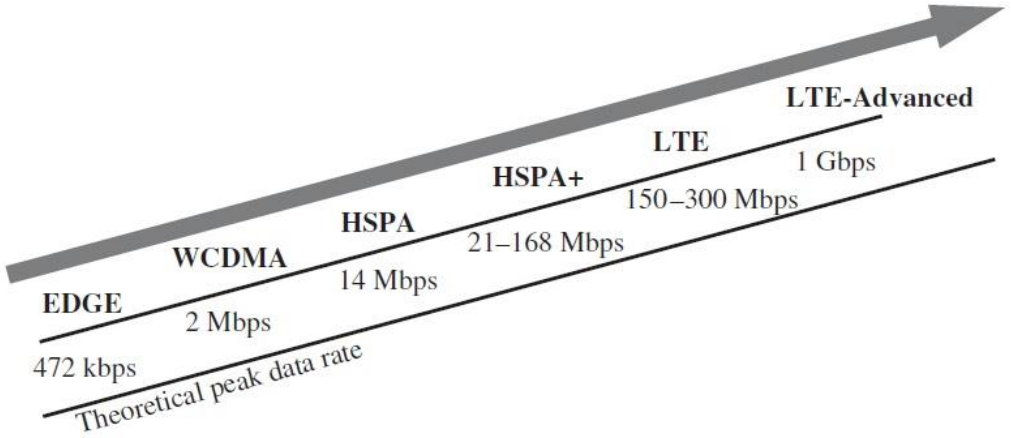

Figure 1.3. Peak data rate evolution of 3GPP technologies (extracted from [HoTo11]).

Concerning the adoption of technologies and products, and according to [Eric13], around 50% of all mobile phones sold in the first quarter (Q1) of 2013 were smartphones – this suggests that there is a strong momentum for smartphone uptake in all regions, taking also into account that 40% of the mobile phones sold in the full year of 2012 were smartphones. However, of all mobile phone subscriptions, only 20 to 25% are associated with smartphones, which means that there is considerable room for further uptake.

LTE is growing strongly, with around 20 million new subscriptions added in Q1 2013. In the same period, around 30 million GSM/EDGE-only subscriptions and 60 million UMTS/HSPA subscriptions were added. Total smartphone subscriptions reached 1.2 billion at the end of 2012, and are expected to grow to 4.5 billion in 2018. Mobile subscriptions are increasing for Personal Computers (PCs), mobile routers and tablets, which have large screen sizes. They are expected to grow from 300 million in 2012 to around 850 million in 2018, exceeding the number of fixed broadband subscriptions.

When talking about dissimilarities between different regions of the globe, it is worth referring that it is expected that almost all handsets in Western Europe and North America in 2018 will be smartphones, while in Middle East, Africa and Asia Pacific regions, it will be only 40 to 50%.

Figure 1.4 shows mobile subscriptions categorised by technology, where subscriptions are defined by the most advanced technology that the mobile phone and network are capable of. LTE is currently being deployed in all regions, and will reach around 2 billion subscriptions in 2018. The rapid migration to more advanced technologies in developed countries means global GSM/EDGE-only subscriptions will decline after 2012-2013. On a global scale, GSM/EDGE will continue to lead in terms of subscriptions until the later years of the forecast period. This happens because new and less affluent users entering networks in global markets will be likely to use the cheapest mobile phones and subscriptions available. Also, it takes time for the installed base of phones to be upgraded.

As a mature market, Western Europe will show little growth in subscriptions. UMTS/HSPA is the current dominant technology in the region and, by 2018, LTE will penetrate around 35% of the total

subscriptions base. Data services were rolled out early in this region, initially accessed via dongle or PC. However, the drive for LTE has not yet been as strong in Europe as it was in North America, for example, partly because there are many well-developed 3G networks in that region.

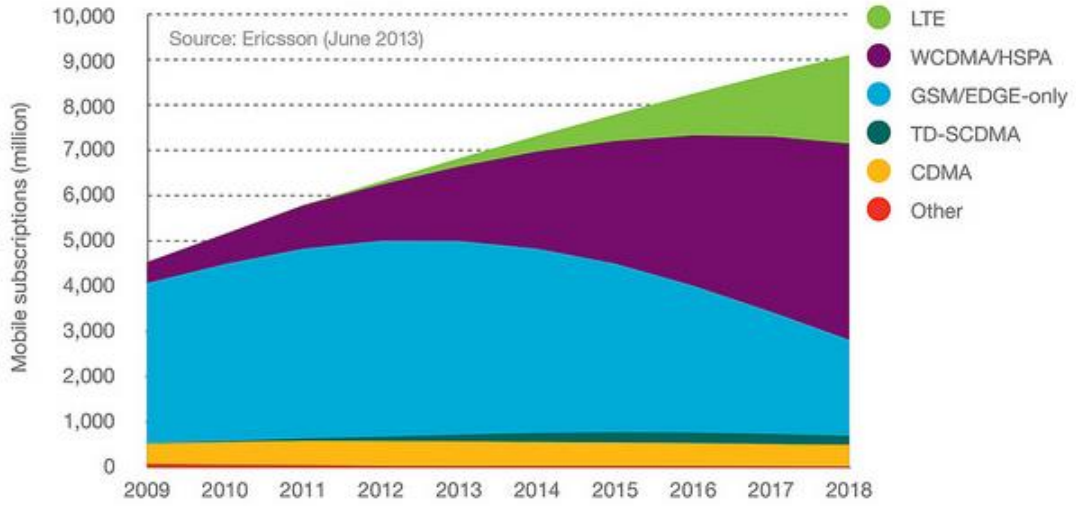

Figure 1.4. Mobile subscriptions by technology, 2009-2018 (extracted from [Eric13]).

Data traffic doubled between Q1 2012 and Q1 2013, which can be seen in Figure 1.1, while voice traffic only grew 4% in the same period. It is expected that video will account for around half of global mobile data traffic by 2018.

During 2013, overall mobile data traffic is expected to continue the trend of doubling each year. Mobile PCs dominate traffic in most regions, except in North America. However, smartphone traffic is growing faster, due to the high growth in subscriptions. In the later years of the forecast period (which ends in 2018), data traffic will be split fairly equally between mobile phones on the one hand, and tablets, mobile routers and mobile PCs on the other. Also, mobile data traffic will grow considerably faster than fixed one over the same period. However, in absolute volume, fixed data traffic will remain dominant.

1.2 Motivation and Contents

The accelerating traffic growth originated from a crescent subscriber demand forces mobile network operators to increase network capacity. However, spectrum availability is scarce and, as such, its allocation costs are very high. In order to increase capacity, operators can use several approaches, such as the following:

- increase spectral efficiency, which can be achieved by the usage of new technologies, such as LTE (and eventually LTE-A), because LTE is more efficient than 3G networks in carrying data in a given amount of radio spectrum – this means that the cost to the operator of carrying data on an LTE network should be several factors lower than for 3G [LeSC13];
- adopt the minimum frequency reuse factor of 1, which means that the same spectrum is used everywhere in the network;

- deploy increasingly smaller cell sizes, capable of serving huge capacity to a relatively small coverage area.

Even though these approaches increase the necessary capacity density where needed, most of them come at a great price: inter-cell interference levels become higher, especially in cell-edge areas, where coverage may be provided by more than one Base Station (BS). This higher interference causes a degradation of the Signal-to-Interference plus Noise Ratio (SINR), network performance and user experience, as it is stated in [Paol12]. This makes it crucial to develop networks where inter-cell interference can be minimised, using one or both of the following techniques:

- classical, which essentially deal with the tweaking of some parameters of the system, such as the tilting of the antennas, their height and their output power;
- advanced, which deal with complex frequency reuse schemes and allocation restrictions.

The main objective of this thesis is the evaluation of LTE performance in urban scenarios, concerning inter-cell interference. The first group of techniques referred above is studied in this thesis: a detailed analysis of performance is provided, addressing the pattern for antenna's electrical and mechanical downtilt, height of the antennas and transmitter output power.

This thesis was done in collaboration with Vodafone Portugal – Comunicações Pessoais, S.A., which belongs to a multinational network operator, and conclusions taken as a result of the developed work are intended to give some guidelines to the operator, essentially on how can inter-cell interference be minimised. Measurements performed under the scope of this work were done with equipment supplied by Vodafone, and using its own deployed network. Support for the analysis of the measured results was also provided by Vodafone. The network that supports all the analyses performed in this thesis is based on Vodafone's, and all analyses are based on the three frequency bands that Vodafone uses to provide coverage.

Five different chapters provide the general understanding of the work performed, methods used and results obtained. The present chapter provides a general understanding of mobile communications systems and their adoption throughout the world, which justifies the need to be constantly developing new systems and new techniques that improve performance of existing ones.

Chapter 2 provides the theoretical basis of the work, being a crucial element for the understanding of subsequent chapters. It provides a superficial description of LTE's network architecture, presenting the main elements that are part of it. A radio interface description follows, where aspects that distinguish LTE from previously deployed 3GPP systems are highlighted. Coverage and capacity considerations are provided, including a summary of theoretical peak data rates achieved using different configurations for LTE. The main focus of this thesis is then theoretically explained – inter-cell interference issues are presented, and models used to study and minimise it are summarised in a so called state of the art. In the end of the chapter, services and applications considerations are explored, including Quality of Service (QoS) requirements and priorities, and traffic models that illustrate the different nature of traffic that is served by network operators.

The models used to study performance are described in Chapter 3. Particular relevance is given to a

stochastically generated Line of Sight (LoS) occurrence, Signal-to-Noise Ratio (SNR) and SINR computations, throughput and capacity analysis, coverage determination and, last but not least, antennas' radiation patterns and how they are affected by either electrical or mechanical downtilt are presented and explained. Theoretical models' implementation in the simulator is then described, where the entire simulator workflow is illustrated and then textually detailed. An assessment of the models is provided, so that it is ensured that results given by the simulator are relevant.

The analysis of the results extracted via simulation is provided in Chapter 4. Results obtained via measurements in the city of Lisbon are also compared with them, so that an extra assessment of the models can be provided. Two separate and major analyses are distinctly provided: a low load results analysis takes measurements and simulations done under a low load scenario into account, while a high load scenarios analysis shows how inter-cell interference affects overall system performance in a reference scenario, which is then tweaked in order to study the effect of the variation of some parameters in the results. Electrical and mechanical downtilts, height of the BS antennas and transmitter output power are the variables under scrutiny in this thesis.

Obtained results are then looked at in a global perspective and some conclusions are taken from them, followed by suggestions for future work – this is all presented in Chapter 5. A summary of all the work performed is also provided, so that one can have a general understanding of the thesis and the conclusions obtained in the end.

Some auxiliary studies performed under the scope of this work are provided as annexes. In Annex A, frequency allocations in Portugal are shown, and information about their correlation with LTE coverage and capacity purposes is provided. Considerations on how the link budget should be calculated are provided in Annex B. It also makes use of the path loss that the signal suffers when travelling in the propagation medium, which is modelled by the COST-231 Walfisch-Ikegami model, summarised in Annex C. In Annex D, a set of equations that give throughput as a function of SINR (done under the scope of this work), and vice-versa, is presented. The user's manual intended to aid the understanding of the simulator's user interface is provided in Annex E. Finally, in Annex F, some important results and figures done as a result of the measurements performed in the city of Lisbon are included.

Chapter 2

LTE Aspects

This chapter provides an overview of the basic concepts of an LTE network, such as its network architecture, radio interface and coverage and capacity issues. Then, a synopsis of interference related aspects, including a brief state of the art, and a study of services and applications, and their related traffic models, are provided.

2.1 Basic Concepts

This section provides a general understanding of LTE, including its architecture, radio interface and capacity and coverage issues, being based on [HoTo11] and [SeTB11].

2.1.1 Network Architecture

There are many representations of an LTE network, as its implementation may take place when other networks are already employed. However, one can represent a simple, yet functional, LTE network that does not interact with legacy systems. The representation of such an LTE network is presented in Figure 2.1, where the architecture is divided into four main domains: the User Equipment (UE), the Evolved UTRAN (E-UTRAN), the Evolved Packet Core (EPC), and the Services domain.

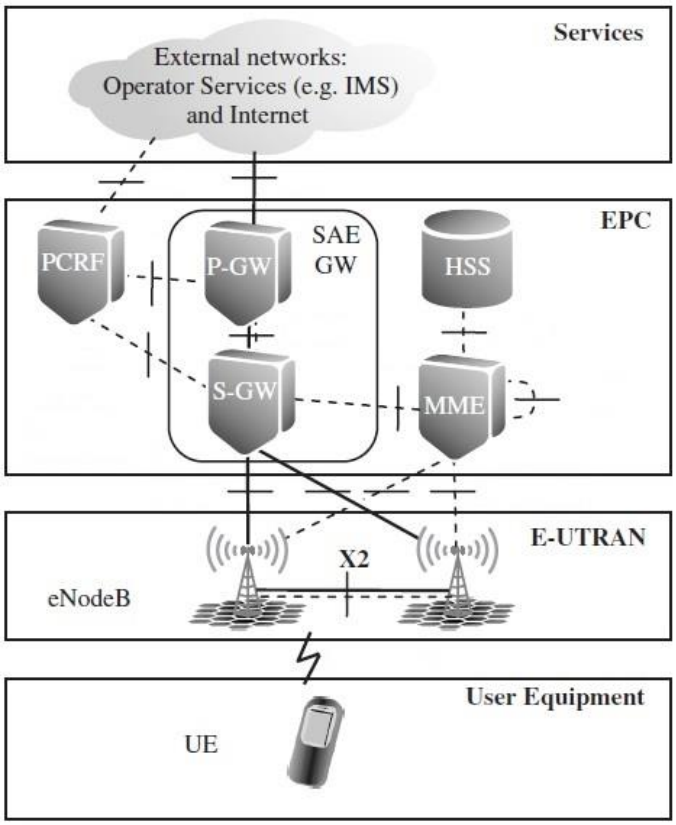

Figure 2.1 Simplified system architecture for E-UTRAN only network (adapted from [HoTo11]).

On a general perspective, the UE, the E-UTRAN and the EPC together are called the Evolved Packet System (EPS), representing the Internet Protocol (IP) Connectivity Layer.

The UE represents the end user's equipment, and it includes both the Universal Subscriber Identity Module (USIM) and the Terminal Equipment (TE). The USIM is used to authenticate and identify the user and to originate security keys that protect the radio interface transmissions, being an application placed into a removable smart card called the Universal Integrated Circuit Card (UICC).

The UE connects to the EPC via the so-called evolved Node Bs (eNodeBs), which support the radio access of the network and are connected to each other through the X2 interface, outlining the

E-UTRAN. The eNodeB represents the termination point of all radio protocols towards the UE, and relays data between the radio connection and the corresponding IP based connectivity towards the EPC. Many Control Plane functions are under the scope of the eNodeB, such as:

- Radio Resource Management (RRM), which controls the usage of the radio interface, by allocating resources based on requests, prioritisation and scheduling of traffic according to the required QoS, and by frequent monitoring of the resources usage;
- Mobility Management (MM) which, based on radio signal level measurements, performed both at the UE and at the eNodeB, decides whether or not to handover UEs between cells, including the exchange of handover signalling between other eNodeBs and the Mobility Management Entity (MME).

Concerning the EPC, one should note that, unlike the core networks of other previous 3GPP networks, it does not have a circuit switched domain, its main elements being the following:

- the MME, which is the main control element and is responsible for providing some functions in the basic System Architecture Configuration, such as authentication and security, mobility management, subscription profile management and service connectivity;
- the SAE-GW (System Architecture Evolution Gateway), also part of the EPC, which represents the combination of the S-GW (Serving Gateway, responsible for User Plane tunnel management and switching), and the P-GW (Packet Data Network Gateway, described as the edge router between the EPS and external packet data networks);
- the PCRF (Policy and Charging Resource Function), which is responsible for Policy and Charging Control (PCC);
- the HSS (Home Subscription Server), which is a database server that records the location and all permanent data of the user.

To conclude the network architecture description, it should be noted that the Services domain may include services that are not provided by the mobile network operator, such as those provided directly through the internet, and IMS (IP Multimedia Sub-system) based operator ones. The latter are provided on top of the IP connectivity provided by the lower layers – for example, to support the voice service through Voice-over-IP (VoIP).

2.1.2 Radio Interface

When discussing LTE's radio interface, some important topics need to be addressed, such as multiple access techniques, resource allocation, frequency bands, modulation schemes, data and control channels, and Multiple-Input Multiple-Output (MIMO).

Concerning the multiple access technique, one has Orthogonal Frequency Division Multiple Access (OFDMA) in DL, in order to minimise the receiver's complexity and to enable frequency domain scheduling with resource allocation flexibility, and Single Carrier Frequency Division Multiple Access (SC-FDMA) in UL, to optimise the range and power consumption of the UE.

LTE's OFDMA transmission in the frequency domain consists of several narrow, mutually orthogonal

sub-carriers that fill the system bandwidth with steps of 15 kHz. Users can be allocated to any of the sub-carriers, which enable frequency domain diversity due to the momentary interference and fading differences in different parts of the system bandwidth. However, there is at least one practical limitation: the signalling resolution due to the resulting overhead implies that the allocation should not be done on an individual sub-carrier basis. Resource allocation is based on Resource Blocks (RBs), each consisting of 12 sub-carriers, thus, resulting in a 180 kHz minimum bandwidth allocation, in both DL and UL. In the time domain, the largest unit is the 10 ms radio frame, which is subdivided into 1 ms sub-frames that constitute the basic unit of resource allocation. Each of the sub-frames is split into two 0.5 ms slots (RBs), each having seven Orthogonal Frequency Division Multiplexing (OFDM) symbols when the normal/short Cyclic Prefix (CP) length is used, or six when the extended CP length is considered. A sub-carrier for a duration of one OFDM symbol is termed a Resource Element (RE) and is the smallest unit of resource, which means that an RB comprises 84 REs whenever a normal CP length is used. Some REs are reserved for special purposes, such as synchronisation signals, Reference Signals (RSs), control signalling and critical broadcast system information, whereas the remaining ones are used for data transmission. Figure 2.2 shows the basic time-frequency resource structure of LTE, which is applicable for Frequency Division Duplex (FDD) in paired radio spectrum or for a standalone DL carrier, assuming that all sub-frames are available for DL transmission.

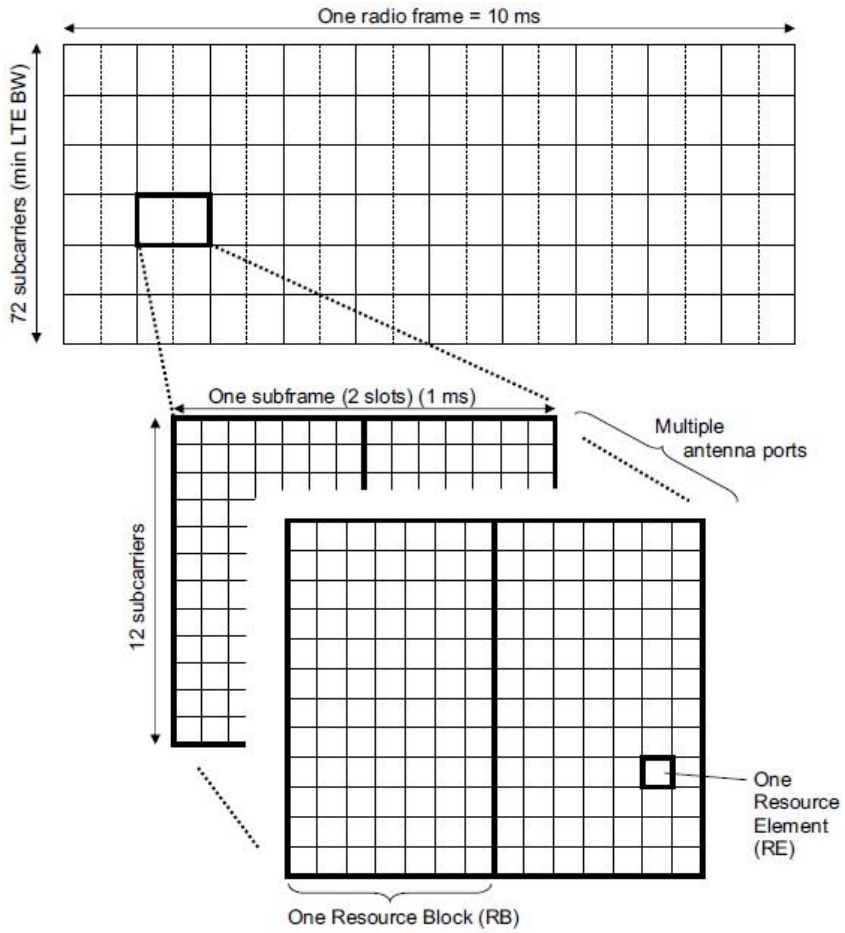

Figure 2.2. Basic time-frequency resource structure of LTE for the normal CP case (extracted from [SeTB11]).

From [3GPP10c], it can be seen that there are three basic types of resource allocation in the DL:

- Resource Allocation Type 0, which is based on a set of consecutive RBs called Resource Block Groups (RBGs). The number of RBs per RBG depends on the system bandwidth, being illustrated in Table 2.1.
- Resource Allocation Type 1, which is RBG Subset based, where an RBG Subset consists of a set of RBGs. The number of RBG Subsets also depends on system bandwidth, and is equal to the number of RBs in an RBG (Table 2.1). One of the main drawbacks of Resource Allocation Type 1 is that it is not possible to allocate all RBs, since only one subset can be assigned to a UE and no subset is able to cover all RBs.
- Resource Allocation Type 2, based on Virtual Resource Blocks (VRBs), which are contiguously allocated in a localised or distributed way. Localised VRB allocations for a single UE vary from one VRB up to the maximum number of VRB spanning the system bandwidth. Distributed VRBs allocations vary from one VRB up to 16 VRBs when the number of RBs available in DL goes from 50 to 110 and MIMO is considered, according to [Ku11].

Table 2.1. Number of RBs in an RBG as a function of the number of RBs available in DL (extracted from [3GPP10c]).

Number of available RBs in the DL	**RBG size**
≤10	1
11–26	2
27–63	3
64–110	4

Resource Allocation Type 2 considers a virtually contiguous RB allocation. This means that, even though the Medium Access Control (MAC) layer allocates RBs in a contiguous way, they may be mapped in a different way at the physical layer, depending on the conversion type (localised or distributed): when localised is considered, both virtual allocation and physical allocation correspond to an RB contiguous allocation, while when distributed is considered, virtual allocation is contiguous, but physical allocation is not.

The UL user specific allocation is continuous to enable single-carrier transmission, and the transmission bandwidth (for DL and UL) can range from 1.4 to 20 MHz, depending on the available spectrum. Figure 2.3 provides an illustration of the referred multiple access techniques.

The transmission bandwidths must fit in frequency bands that are allocated to network operators, based on the spectrum availability and the investment that operators are willing to do. In order to provide high coverage, lower frequency bands are used, while higher frequency bands are deployed to provide high capacity. The 800 MHz band (identified in Annex A), previously used to offer terrestrial TV broadcasting in Europe, is being used to provide LTE coverage. In this band, there are 30 MHz available for LTE FDD, which enables a three operator scenario with 10 MHz each. On the other hand, the 2 600 MHz band (also identified in Annex A) is used to provide capacity, as the coverage area that it provides is smaller than the one provided by lower frequency bands, due to the fact that signal

attenuation increases with frequency. In this band, 60 MHz are available for LTE FDD, which enables a three operator scenario with 20 MHz each – as such, this band is of particular importance to network operators, as its available bandwidth is best suited to provide extra capacity. The 1 800 MHz band (identified in Annex A as well) provides up to 20 MHz of additional capacity – although the operators bought 14 MHz each in the auction described in Annex A, they already had 6 MHz in that band allocated to GSM1800 purposes [Voda13]. So, many implementations for the 1 800 MHz band can be considered, such as 10 MHz for LTE1800 and 10 MHz for GSM1800, 15 MHz for LTE1800 and 5 MHz for GSM1800, or 20 MHz for LTE1800, for example.

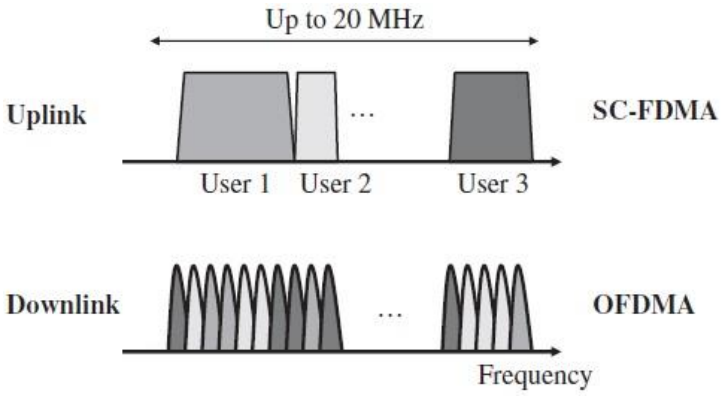

Figure 2.3. LTE multiple access techniques (extracted from [HoTo11]).

Regarding the available modulation methods for user data, Quadrature Phase Shift Keying (QPSK) and QAM (Quadrature Amplitude Modulation) in 16QAM and 64QAM variants are implemented. QPSK and 16QAM are available in all devices, whereas the availability of 64QAM in UL depends on UE's capabilities. Table 2.2 summarises all the available UE's categories, which are characterised by different modulation and MIMO support, as well as different peak throughputs, for DL and UL. In theory, an OFDM system could use a different modulation for each sub-carrier, but that would result in an excessive overhead, in order to have channel quality and signalling information with such a granularity. In control channels, either Binary Phase Shift Keying (BPSK) or QPSK is used for transmission.

Table 2.2. UE's categories in LTE (adapted from [Corr13]).

<table>
<tr><th rowspan="2">Category</th><th colspan="2">DL</th><th colspan="2">UL</th><th colspan="2">MIMO support</th></tr>
<tr><th>Peak throughput [Mbit/s]</th><th>Modulation schemes</th><th>Peak throughput [Mbit/s]</th><th>Modulation schemes</th><th>2×2</th><th>4×4</th></tr>
<tr><td>1</td><td>10</td><td rowspan="5">QPSK, 16QAM, 64QAM</td><td>5</td><td rowspan="3">QPSK, 16QAM</td><td>No</td><td rowspan="4">No</td></tr>
<tr><td>2</td><td>50</td><td>25</td><td rowspan="4">Yes</td></tr>
<tr><td>3</td><td>100</td><td>50</td></tr>
<tr><td>4</td><td>150</td><td>50</td><td rowspan="2">QPSK, 16QAM, 64QAM</td></tr>
<tr><td>5</td><td>300</td><td>75</td><td>Yes</td></tr>
</table>

Concerning LTE's physical layer, one should note that dedicated resources are not reserved for a single user; instead, resource usage is based solely on dynamically allocated shared resources. For

the UE to communicate with an eNodeB supporting one or more cells, it must first identify the DL transmission from one of these cells and synchronise with it. This is achieved by the detection of two specially designed physical channels that are broadcast in each cell: the Primary Synchronisation Signal (PSS) and the Secondary Synchronisation Signal (SSS), which enable time and frequency synchronisation, provide the UE with the physical layer identity of the cell and the CP length, and inform the UE whether the cell uses FDD or Time Division Duplex (TDD). In the case of initial synchronisation, after the detection of the synchronisation signals, the UE decodes the Physical Broadcast Channel (PBCH), from which critical system information is obtained. In the case of neighbour cell identification, the UE does not decode the PBCH; instead, it simply makes quality-level measurements based on the RS transmitted from the newly detected cell and decides if a cell reselection should be made. Afterwards, the UE must estimate the DL radio channel in order to be able to perform coherent demodulation of the information-bearing parts of the DL signal.

In LTE, user data in DL is transported in the Physical Downlink Shared Channel (PDSCH), which is also used for broadcast system information not carried on the PBCH, and for paging messages. The transmission of data in the PDSCH is made in units known as Transport Blocks (TBs), each of which corresponds to a MAC layer Protocol Data Unit (PDU). TBs may be passed down from the MAC layer to the physical one once per Transmission Time Interval (TTI), which corresponds to the sub-frame duration of 1 ms.

In what concerns DL control channels, one has the Physical Control Format Indicator Channel (PCFICH), the Physical HARQ (Hybrid Automatic Repeat reQuest) Indicator Channel (PHICH) and the Physical Downlink Control Channel (PDCCH). The PCFICH carries a Control Format Indicator (CFI), indicating the number of control OFDM symbols used for transmission of control channel information in each sub-frame. The PHICH indicates whether a correct transmission on the Physical Uplink Shared Channel (PUSCH) was received by the eNodeB (the HARQ indicator is set to 0 for a positive Acknowledgement – ACK – and 1 for a Negative Acknowledgement – NACK). The PDCCH carries a message responsible for resource assignments and other control information for one or more UEs known as Downlink Control Information (DCI).

Regarding UL, the transmission can only be scheduled if the UE's UL transmission timing is synchronised. Therefore, the Random Access Channel (RACH) is of major importance as an interface between non-synchronised UEs and the orthogonal transmission scheme of the UL radio access. The Physical Random Access Channel (PRACH) is where the RACH procedure is done. The UL physical layer transmissions are also mediated by the PUSCH, which carries the user data from the Uplink Shared Channel (UL-SCH) transport channel, and the Physical Uplink Control Channel (PUCCH), which is responsible for control signalling.

LTE systems adjust the transmitted information data rate using both modulation scheme and channel coding rate options, to match the prevailing radio channel capacity for each user, based on a DL channel conditions prediction. That prediction is supported by the Channel Quality Indicator (CQI) feedback transmitted by the UE in UL, which indicates the data rate supported by the channel, taking the SINR and the characteristics of the UE's receiver into account.

Power control, which is only specified for UL, also plays an important role at the UE level, as it balances the need for sufficient transmitted energy to satisfy the required QoS, against the need to minimise interference on other users of the system and to maximise the battery life of the UE.

As part of the first LTE Release (Release 8), MIMO operation including spatial multiplexing, pre-coding and transmit diversity was introduced. Spatial multiplexing, in its essence, consists of sending signals from two or more different antennas with different data streams. As the signal is processed, the receiver separates the data streams, increasing the peak data rates by a factor of 2, or 4 if one considers a 4×4 antenna configuration. Pre-coding refers to the fact that the signals transmitted from the different antennas are weighted in order to maximise the received SNR. Transmit diversity consists of sending the same signal from multiple antennas with some coding, so that gains from independent fading between the antennas can be exploited.

2.1.3 Coverage and Capacity

LTE system performance is presented as an improvement from legacy systems, due to the fact that orthogonal multiple access schemes (OFDMA and SC-FDMA) are used, as well as the requirement to support DL transmission with up to two or four spatial layers via MIMO. The former aspect enables the exploitation of frequency-domain multi-user diversity gain, while the latter enhances both the peak data rate and the cell average and cell-edge spectral efficiencies.

LTE's high peak data rates are achieved by using the maximum bandwidth of 20 MHz (in the first releases), 64QAM modulation and MIMO transmission. QPSK modulation carries 2 bits per symbol, whereas 16QAM and 64QAM carry 4 and 6 bits per symbol, respectively. 2×2 MIMO doubles the peak bit rate up to 12 bits per symbol. So, QPSK 1/2 (coding rate) carries 1 bps/Hz, while 64QAM, with a unitary coding rate and considering a 2×2 MIMO configuration, carries 12 bps/Hz.

LTE achievable peak data rates are calculated taking into account a normal CP usage and the correspondence between bandwidth and available number of RBs for data shown in Table 2.3, being shown in Table 2.4, for DL, and Table 2.5, for UL. If signalling and control overheads were considered, the represented peak data rates would be lower. One should also take into account that not all UEs support the represented peak throughputs, as it is illustrated in Table 2.2.

Table 2.3. Number of RBs associated to each bandwidth (extracted from [Corr13]).

Bandwidth [MHz]	1.4	3	5	10	15	20
Number of RBs	6	15	25	50	75	100

As it can be seen, the bit rate increases with the bandwidth (which corresponds to an increasing number of RBs), with the order of the coding scheme and rate, as well as with the number of antennas used to send and receive the signals.

An analysis of coverage is provided in Annex B, taking into account that it is influenced by the link budget associated to the communication between BS and UE.

Table 2.4. Downlink peak bit rates, in Mbit/s (adapted from [HoTo11]).

Resource blocks			Bandwidth [MHz]					
Modulation and coding	**Bits/symbol**	**MIMO usage**	**1.4**	**3.0**	**5.0**	**10**	**15**	**20**
QPSK ½	1.0	-	1.0	2.5	4.2	8.4	12.6	16.8
16QAM ½	2.0	-	2.0	5.0	8.4	16.8	25.2	33.6
16QAM ¾	3.0	-	3.0	7.6	12.6	25.2	37.8	50.4
64QAM ¾	4.5	-	4.5	11.3	18.9	37.8	56.7	75.6
64QAM 1/1	6.0	-	6.0	15.1	25.2	50.4	75.6	100.8
64QAM ¾	9.0	2 × 2 MIMO	9.1	22.7	37.8	75.6	113.4	151.2
64QAM 1/1	12.0	2 × 2 MIMO	12.1	30.2	50.4	100.8	151.2	201.6
64QAM 1/1	24.0	4 × 4 MIMO	24.2	60.5	100.8	201.6	302.4	403.2

Table 2.5. Uplink peak bit rates, in Mbps, considering no MIMO (adapted from [HoTo11]).

Resource blocks		Bandwidth [MHz]					
Modulation and coding	**Bits/symbol**	**1.4**	**3.0**	**5.0**	**10**	**15**	**20**
QPSK ½	1.0	1.0	2.5	4.2	8.4	12.6	16.8
16QAM ½	2.0	2.0	5.0	8.4	16.8	25.2	33.6
16QAM ¾	3.0	3.0	7.6	12.6	25.2	37.8	50.4
16QAM 1/1	4.0	4.0	10.1	16.8	33.6	50.4	67.2
64QAM ¾	4.5	4.5	11.3	18.9	37.8	56.7	75.6
64QAM 1/1	6.0	6.0	15.1	25.2	50.4	75.6	100.8

2.2 Interference

In this section, an outline of interference is provided, along with a brief discussion about interference models used in LTE, and their related state of the art.

2.2.1 Basic Aspects

Interference levels tend to impact on the performance of all mobile communications systems, especially when these work with a frequency reuse factor of 1 to maximise the spectral efficiency.

Interference can be classified as inter-cell interference, when the UE receives signals from more than one eNodeB, or as intra-cell one, when the different UEs under the coverage of the same eNodeB interfere with each other, Figure 2.4, [Paol12].

The usage of SC-FDMA in UL provides an orthogonal transmission by the different UEs, which

minimises intra-cell interference in LTE, when compared with previous 3GPP systems. As such, only inter-cell interference is highlighted in this thesis. However, when calculating inter-cell interference, one should know that not all of the sub-carriers emitted by different eNodeBs and received at the same UE interfere with each other – only the subcarriers with the same frequency have a negative impact on system performance.

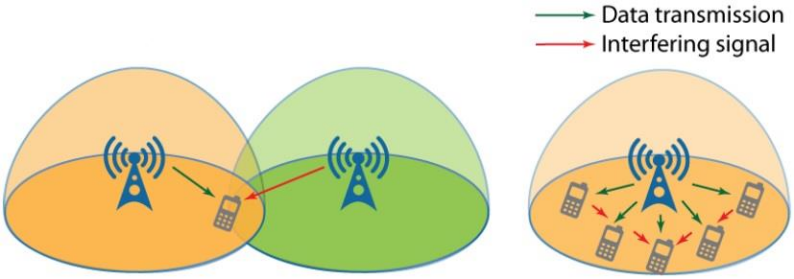

(a) Inter-cell interference (b) Intra-cell interference

Figure 2.4. Inter-cell and intra-cell interference (adapted from [Paol12]).

According to [SeTB11], LTE was primarily designed to provide high-speed data services with good spectral efficiency, hence, the appeal to use a frequency reuse factor of 1, also called Universal Frequency Reuse, where the same frequencies are used in all the cells of the system. The Reuse-1 frequency reuse scheme provides the best throughput for users in the cell-centre, as they are the ones that experience the higher SINR, while deteriorating the service quality for cell-edge users, which experience a significantly lower SINR [Khan09].

Data and control channels can experience a significant level of interference from neighbour cells, reducing the achievable spectral efficiency, especially at the cell-edge. To mitigate this problem, there are many mechanisms that are interference related, such as Inter-Cell Interference Coordination (ICIC), Coordinated Multi-Point (CoMP), Multi-User MIMO (MU-MIMO) and Single-User MIMO (SU-MIMO) [Paol12].

ICIC relies on frequency domain sharing between cells and transmitter powers adjustment. The signalling that carries interference and scheduling information is standardised, being included in the X2 interface between the eNodeBs. Although it is often stated that the frequency reuse factor used in LTE is 1, some ICIC techniques may avoid the reutilisation of the frequency used in a given cell in the nearby ones at the same time, which ends up being the same as having a system with a higher frequency reuse factor.

One of the other ICIC roles is to manage Fractional Frequency Reuse (FFR), which is a new technique defined in LTE releases after Release 8 (where power control in the DL is not considered). When FFR is employed, each cell is divided in inner and outer parts, and users are then treated differently by the eNodeB scheduler, depending on whether they are cell-centre or cell-edge users. In the inner part, where users experience a low interference level and also require less power to communicate with the serving eNodeB, a frequency reuse factor of one is used. In the outer part, a frequency reuse factor higher than one is used. When the eNodeB allocates a user in a given part of the frequency band and in the outer part of the cell, system capacity is optimised if the neighbouring

cells do not transmit in the same part of the spectrum, or if they transmit in the same band only at low power, to users in the inner parts of those cells [SeTB11].

CoMP relies on many tools introduced in LTE Release 11, which minimise inter-cell interference when one or more UEs are located at the cell-edge and receive signals from more than one BS. Coordinated transmission and reception between the BSs and the UEs is exploited in order to improve cell-edge performance.

MU-MIMO is a functionality introduced in LTE-A, where a BS can transmit to up to 8 UEs concurrently using the same spectrum, by directing an adaptive beam to the UE (beamforming). When using SU-MIMO, the BS concurrently transmits to and receives from a single UE over up to 4 layers (Release 10) [Paol12].

In the UL, fractional power control is applied to improve the throughput near the eNodeB and reduce inter-cell interference at the cell-edge. Power control can also be performed jointly with frequency-domain resource allocation, by means of allocating more RBs to UEs near the cell-centre, in order to enhance the data rate, while cell-edge UEs are allocated fewer RBs. PUCCH and PUSCH are mapped onto different RBs in the frequency domain, meaning that independent interference management techniques, such as power control, can be applied for control and data channels [SeTB11].

The antenna tilt, which is defined as the angle of the main beam of the antenna below or above the horizontal (azimuth) plane, has great influence on inter-cell interference, as it changes the signal power distribution along the cell. Positive and negative angles are referred to as downtilt and uptilt respectively, and the tilt can be adjusted mechanically and/or electrically, which is represented in Figure 2.5.

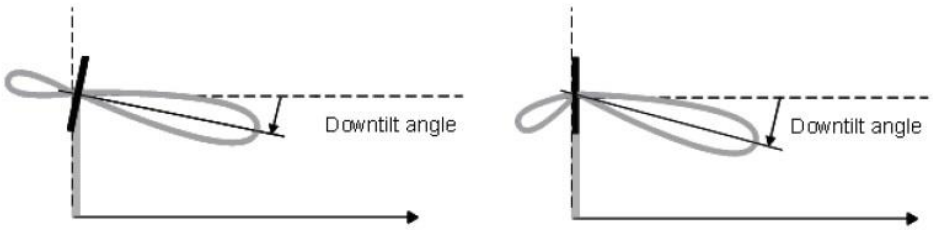

(a) Mechanical downtilt (b) Electrical downtilt

Figure 2.5. Mechanical downtilt versus electrical downtilt (extracted from [YiHH09]).

The electrical tilt changes the phase delivered to the antenna's radiation elements and, as such, may remove the need for tower climb and BS site visits, as the tilt angle may be controlled via the network management system, which reduces the operational cost. However, the electrical tilt range is limited compared to the mechanical one [ZMSR08].

2.2.2 Interference Models

Concerning the interference models used in LTE, and the problem under study in this thesis (inter-cell interference impact on LTE performance in urban scenarios), there are many studies already done

that address performance gains achieved by the usage of ICIC techniques, different frequency reuse schemes, and different antenna tilt types and values.

An analysis of the ICIC potential in terms of throughput, delay and UE energy consumption gains that are theoretically possible by using multi-cell power control and scheduling is done in [FKRR09]. Simulations were performed, and showed that the measured cell-edge throughput of narrowband, “circuit switched” like users benefit from gains up to 50 to 60% with ICIC algorithms. The largest throughput gains are achieved when the UE path gain relation to the own cell vs. the neighbour cell is taken into account in the allocation order. Concerning packet switched, TCP like traffic, the throughput gains were not the most relevant, but instead the gains in delay and UE power consumption. The primary reason evoked was the burst behaviour of such traffic, where the traffic flow is interleaved with random idle periods, which create the opportunity to regain the lost bandwidth due to potential collisions by scheduling further RBs to users. Even though such retransmissions increase the delay of the packet and the UE power consumption, typically there is no impact in the throughput. This contrasts with “circuit switched” like traffic, for which the scheduler is assumed to assign a periodically recurring set of RBs, matching the behaviour of voice traffic. In those cases, the bandwidth lost as a result of a collision cannot be compensated by scheduling extra resources.

In [PoPo10], a numerical methodology for calculation of interference generated by co-channel cells is provided. It can be used in many scenarios for different frequency channel assignments in cellular systems. The analytical quantification proposed was used to compare the level of co-channel interference in three different scenarios: cellular system with universal frequency reuse, cellular system with cells organised in clusters with the size of 3 and cellular system with implemented ICIC based on fractional frequency reuse. It was analytically concluded that users in their own cells experience less interference when using fractional frequency reuse, instead of universal frequency reuse. Also, it was concluded that the interference introduced in the system when using a frequency reuse factor of 3 was the smallest, but it required, by definition, a three times larger spectrum usage than fractional frequency reuse. It was also concluded that SINR is approximately 10 dB higher when using fractional frequency reuse instead of universal frequency reuse, for both LoS and NLoS environments. All the results achieved in this study were based on the assumption that the area occupied by cell-centre users and the area occupied by cell-edge users in each cell were the same size.

An interference modelling and evaluation is presented in [TGBC11]. The study was carried out using the load factor, which represents the traffic density of each cell of the network, and two frequency reuse schemes: the frequency reuse 1 scheme, where the whole available bandwidth is used in each cell/sector, and the frequency reuse 3 scheme, in which the entire bandwidth is divided into 3 non-overlapping groups and assigned to 3 co-site sectors within each cell. The study used the Hata propagation model to measure the radio signal propagation in a medium sized city in France. Traffic load at different times was considered in order to represent, in a realistic way, the traffic growth and demand during the day. Three scenarios were selected with low, average and high traffic demands. For the calculation of the number of outage users (non-covered users), a two steps cycle of network

stabilisation was defined, in which the estimation of the Reference Signal Received Power (RSRP) was used as a first approach, followed by an estimation of the SINR. It was concluded that, concerning coverage, the number of outage users in LTE is sensitive to the choice of the frequency band reuse pattern. The tests confirmed that the frequency reuse 3 scheme shows better results than the reuse 1 scheme, and allowed the research team to validate their interference model. It also showed the huge impact of frequency pattern on the network capacity due to radio resource limitations.

In [PaNS11], the use of realistic pre-computed interference patterns for LTE UL performance analysis and testing is proposed, instead of traditional methods that rely of additive white Gaussian noise (AWGN) interference sources. The interference patterns are generated via a system-level simulator taking into account a given set of scenario parameters such as cell configuration, user configurations and traffic models. The generated interference patterns can be employed to benchmark the performance of any LTE UL system both in lab simulations and field trials for practical deployments. The presented methodology is stated to offer the advantage of reproducibility and repeatability of lab tests and field trials, being beneficial for researchers and developers to benchmark the performance of their algorithms over a realistic and reproducible set of conditions.

In [ZMSR08], a performance evaluation of BS antenna mechanical downtilt in LTE networks and the interaction performance with the fraction Open Loop Power Control (OLPC) are provided, with a focus on UL and under LoS conditions. For the cell specific path loss compensation factor α equal to 0.6 and 1.0 respectively, there are about 75% and 37.5% increases in terms of cell coverage, and about 47% and 39% increases in terms of cell capacity. It is also shown that the network has the optimal performance in terms of average SINR per user at an antenna downtilt of 12° to 16°. Concerning cell coverage and capacity, the downtilt angle of 16° has the optimal overall performance. The maximum outage throughput is obtained when using a broadcast cell specific parameter of -58 dBm in an $\alpha = 0.6$ scenario and -106 dBm in an $\alpha = 1.0$ scenario.

A comparison of DL performance impacts of electrical and mechanical antenna downtilts by means of network simulation is provided in [YiHH09]. System performance was investigated using a snapshot simulator with 3D antenna modelling, and both mechanical and electrical downtilt were simulated for different downtilt angles. The 5%- and 50%-tiles SINR was used to statistically describe the coverage and capacity performance respectively. The results show that electrical downtilt provides better performance in case of an interference limited system, while performance difference is insignificant for noise limited cases. It is also worth noticing that optimal downtilt angles in mechanical and electrical tilt techniques are slightly different from each other, and that coverage and capacity criteria may lead to slightly different optimal tilt angles in an interference limited system with short inter-site distance.

A similar kind of analysis is done in [AtJo10], which shows how LTE DL system performance is affected by different combinations of electrical and mechanical tilts of the eNodeB antenna. Models of radiation patterns and a simple model of system performance were validated against measured patterns and a dynamic system simulator. Concerning coverage, the results show that the choice of a tilt method, or combination of tilt methods, has insignificant impact, and the optimal combination of

electrical and mechanical tilts is insensitive to the choice of a tilt method. In terms of capacity, pure electrical tilt is optimal for cell-edge and mean throughput, while equal amounts of electrical and mechanical tilts are optimal for peak rate, holding for a wide range of elevation and azimuth bandwidths. The differences in optimal throughput between different combinations of tilt methods are at most 25%, and cell-edge performance is the most sensitive to tilt type combination. Overall, the conclusion confirms the previously known results, which stated that total tilt has a strong impact on both coverage and capacity.

In [EcKG11], a heuristic variant of the gradient ascent algorithm is proposed to improve the overall and sector edge spectral efficiency by changing the vertical antenna tilts of BSs. The results show that the average sector spectral efficiency can be improved by 10%, while the sector edge spectral efficiency can even be improved by 100%. As such, the algorithm can be favourably employed for an automatic adjustment of antenna tilts in an operational system, even in case of cell outages, and will therefore reduce network operating costs.

Finally, some theoretical models for understanding heterogeneous cellular networks are provided in [GMRM12] and [DGBA12]. In [DGBA12], a tractable, flexible and accurate model for a DL heterogeneous cellular network (HCN) is developed. It is considered that the HCN consists of several tiers of randomly located BSs, where each tier may differ in terms of average transmit power, supported data rate and BS density. It is also assumed that a UE connects to the strongest candidate BS, the resulting SINR is greater than 1 when in coverage, and Rayleigh fading, in order to derive an expression for the probability of coverage (equivalently outage) over the entire network under both open and closed access. For external validation, a comparison against an actual LTE network (for a single tier) is performed, with the other tiers being modelled as independent Poisson Point Processes, and shows that the model is accurate to within 1 to 2 dB. One of the conclusions of this work is that, for interference-limited open access networks, and at a given SINR, adding more tiers and/or BSs neither increases nor decreases the probability of coverage or outage when all the tiers have the same target-SINR.

These studies provide a background and a guideline to the work performed in this thesis, which offers, among others, some suggestions on what is the optimal solution, in terms of minimum inter-cell interference, for a given scenario.

2.3 Services and Applications

Traffic information is important for the development of simulation scenarios, as the lack of realistic traffic models leads to unreliable results. In order to characterise traffic in UMTS, 3GPP specified four different QoS classes, which are summarised in Table 2.6.

The main difference between Conversational, Streaming, Interactive and Background is how delay sensitive the traffic is. While the Conversational class is meant for traffic that is very delay sensitive,

the Background class is the most delay insensitive of them all, as it is described in [3GPP11b]. Although these classes were not specifically done for an LTE system analysis, they do provide some insights about the four different natures of traffic, which offers a general view of the traffic classes.

Table 2.6. UMTS QoS classes (extracted from [3GPP11b]).

Service class	Conversational	Streaming	Interactive	Background
Real time	Yes	Yes	No	No
Symmetric	Yes	No	No	No
Guaranteed rate	Yes	Yes	No	No
Delay	Minimum Fixed	Minimum Variable	Moderate Variable	High Variable
Buffer	No	Yes	Yes	Yes
Bursty	No	No	Yes	Yes
Example	Voice	Video Streaming	Web Browsing	SMS, E-Mail

In LTE, the QoS is an important indicator, as all provided services are packet based, including voice (VoIP). It is possible to have multiple applications running in a UE at the same time, each one having different QoS requirements. For example, a UE can be involved in a VoIP call while downloading a File Transfer Protocol (FTP) file. VoIP is more delay and delay jitter sensitive than FTP, which requires a much lower packet loss rate. The support of multiple QoS requirements involves different bearers that are set up within the EPS, each being associated with a QoS. These bearers can be classified into Minimum Guaranteed Bit Rate (GBR) and Non-GBR ones, based on the nature of the QoS they provide.

GBR bearers can be used for applications that have an associated GBR value for which dedicated transmission resources are permanently allocated (for example, by an admission control function in the eNodeB) at bearer establishment or modification. An example of such an application is VoIP. Bit rates higher than the GBR may be allowed if resources are available, which implies the definition of a Maximum Bit Rate (MBR) parameter responsible to set up an upper limit on the bit rate that can be expected from a GBR bearer.

Non-GBR bearers do not guarantee any particular bit rate, hence, its usage in applications such as web browsing or FTP transfer. For these bearers, no bandwidth resources are allocated permanently to the bearer.

It is the eNodeB's responsibility to ensure that, in the access network, the necessary QoS for a bearer over the radio interface is met. Each bearer has an associated QoS Class Identifier (QCI), which is characterised by priority, packet delay budget and acceptable packet loss rate. The label of each QCI for a bearer determines the way it is handled in the eNodeB. A few QCIs have been standardised so that vendors can all have the same understanding of the underlying service characteristics, and thus provide the corresponding treatment, which includes queue management, conditioning and policing strategy. This approach ensures that an operator can expect uniform traffic handling behaviour

throughout its network, regardless of the manufacturers of the eNodeB equipment. The set of standardised QCIs and their corresponding characteristics is shown in Table 2.7.

Table 2.7. Standardised QCIs for LTE (extracted from [SeTB11]).

QCI	Resource type	Priority	Packet delay budget [ms]	Packet error loss rate	Example services
1	GBR	2	100	10^{-2}	Conversational voice
2	GBR	4	150	10^{-3}	Conversational video (live streaming)
3	GBR	5	300	10^{-6}	Non-conversational video (buffered streaming)
4	GBR	3	50	10^{-3}	Real time gaming
5	Non-GBR	1	100	10^{-6}	IMS signalling
6	Non-GBR	7	100	10^{-3}	Voice, video (live streaming), interactive gaming
7	Non-GBR	6	300	10^{-6}	Video (buffered streaming)
8	Non-GBR	8	300	10^{-6}	TCP-based (e.g. WWW, e-mail) chat, FTP, P2P file sharing, progressive video, etc.
9	Non-GBR	9	300	10^{-6}	

The priority and packet delay budget (and, to some extent, the acceptable packet loss rate) from the QCI label are responsible for the Radio Link Control (RLC) mode configuration, and how the scheduler in the MAC handles packets sent over the bearer (e.g. in terms of scheduling policy, queue management policy and rate shaping policy). For instance, a packet with a higher priority can be expected to be scheduled before a packet with lower priority. In the case of bearers with a low acceptable loss rate, an Acknowledged Mode (AM) can be used within the RLC protocol layer to ensure that packets are delivered successfully across the radio interface [SeTB11].

Concerning traffic models, one should understand that those that take advantage of an LTE usage tend to be the ones that demand higher data rates and low latency. However, and considering a long term perspective, one should provide a performance overview of a representative set of services and applications that should include the ones supported by legacy systems that will be replaced by LTE in the future.

To model VoIP traffic, the two-state active-inactive (ON-OFF) Markov voice activity model is considered in [Corr06] and [Khan09]. Two states are considered – silence or inactive state and talking or active state.

According to [Corr06] and [Khan09], traffic associated with FTP is considered as best effort traffic, where an FTP session is a sequence of file transfers separated by reading times. The size of the file to be transferred and the time interval between the end of the download of the previous file and the user request for the next one (reading time) are the two main FTP session parameters. The file size is statistically characterised as having a truncated lognormal distribution, while the reading time is exponentially distributed. The FTP traffic model assumes transmission in DL, although it can be

extended to be applied in UL.

In [Khan09], a typical HyperText Transfer Protocol (HTTP) web browsing session is divided into active and inactive periods, representing web-page downloads and the intermediate reading times, respectively. The active and inactive periods are a result of human interaction, where the packet call (web-page download) represents a user's request for information and the reading time corresponds to the time required to digest the web-page. A packet call is also divided into active and inactive periods, which, unlike a packet session, are attributed to machine interaction rather than human one. A user's request is handled by fetching the initial HTML page using an HTTP GET request, followed by the retrieval of each of the embedded objects (i.e., pictures, advertisements, etc.). These retrievals are represented by the active period within the packet call, while the parsing time and protocol overhead are represented by the inactive periods within a packet call. Web-browsing traffic is characterised by the main object size (with a truncated lognormal distribution) the embedded object size (also with a truncated lognormal distribution), the number of embedded objects (with a truncated Pareto distribution), the reading time (with an exponential distribution) and the parsing time (also with an exponential distribution). In [Corr06], it is considered that the number of packet calls per session, the reading time between packet calls, and the number of packets within a packet call are geometrically distributed random variables, whereas the inter-arrival time between packets (within a packet call) is inverse Gaussian distributed and the size of a packet is Pareto distributed. According to [LeGu07], the HTML object size, the embedded object size and the parsing time have a truncated lognormal distribution, the number of embedded objects has a Gamma distribution, the embedded object IAT (time between the arrival of one embedded object and the arrival of the consecutive embedded object) is Weibull distributed, the reading time has a lognormal distribution and the request size (the size of the HTTP requests) has a uniform distribution.

The e-mail service is modelled by a two-state ON-OFF Markov model in [Corr06], with periods modelled by an exponential distribution. The packet call inter-arrival time is Pareto distributed.

Regarding video streaming, [Khan09] assumes that each frame of the video arrives at a regular interval determined by the number of frames per second. Each video frame is decomposed into a fixed number of slices, and each one of them is transmitted as a single packet. The size of these packets is modelled as a truncated Pareto distribution. The video encoder introduces encoding delay intervals between the packets of a frame, which are also modelled by a truncated Pareto distribution.

Interactive gaming is another service analysed in [Khan09]. In UL, the initial packet arrival time (i.e., the initial time to account for the resource request and scheduling grant) is uniformly distributed and is considered to be very small, as the sub-frame duration is only 1 ms. The packet inter-arrival time is deterministic, and the packet size is assumed to follow the largest extreme value distribution, which is also known as the Fisher-Tippet distribution or the log-Weibull distribution. In DL, the same kind of distributions is applied, except for the packet arrival, which is modelled using the largest extreme value distribution.

Machine to Machine (M2M) also constitutes a broad array of services and applications that demand connectivity from mobile networks and, as such, the traffic generated by them should also be

characterised. According to [BoEH12], those services and applications can be classified as:

- Automotive, which refers to items of equipment installed in vehicles and related network applications that provide car accident emergency call service, tracking and interactive services (for example, fleet management, tourist information push and tracking and interactive stop of stolen cars) and interactive commercial and infotainment applications (such as on-demand video download, interactive gaming and internet access);
- Smart Telemetry, which deals with utility applications that interact with smart meters deployed at customer premises and other sensors that monitor and collect energy consumption information and send information about tariffs or incentives;
- Surveillance and Security, which are deployed in residential and small business premises to provide picture and video surveillance information to security alarm applications;
- Point of Sale (PoS), which includes automated teller machines (ATMs) and provides services such as cash dispensing and payments;
- Vending Machines, which are terminals that dispense goods to consumers in exchange for a fee;
- eHealth, which refers to applications that enable healthcare providers to monitor and diagnose health conditions by remotely collecting, storing, retrieving and analysing the patient's vital signs, or applications that allow a 24/7 call centre for health related assistance;
- Live Video, which is used for supervision of transport infrastructures (such as roads and railways) or city surveillance;
- Building Automation, which is based on devices used to provide services in commercial buildings;
- Industrial Automation, which supports a set of workflows and defined business processes.

Automotive applications require high data transfer rates (particularly for commercial and infotainment applications) and have high mobility and multi-bearer connectivity. Smart telemetry applications require low data transfer rates and have no mobility for stationary devices, predictable behaviour (the devices are configured to report data periodically), delay tolerance and synchronisation effect. Surveillance and security applications require cyclical exchange of information but unpredictable bursty exchanges of information when an alarm procedure is triggered, low transfer data rates (with occasional peak traffic using picture and/or video data) and multi-bearer connectivity, and have no mobility. PoS applications have limited mobility and persistent bearers and require low data transfer rates. Vending machines have no mobility, synchronisation effect and delay tolerance, and require low data transfer rates and persistent bearers. Medical applications (eHealth) have low mobility, low to medium data transfer rates, multi-bearer applications and synchronisation effect, and often require high reliability and availability. Live video applications have no mobility for stationary devices and high mobility for embarked devices, and require emergency connectivity and medium to high data transfer rates. Building and industrial automation applications have low or no mobility at all and require low data transfer rates.

Chapter 3

Models and Simulator Description

A description of the models used in this thesis is provided in this chapter, in which their mathematical formulation and implementation in the simulator is detailed. This chapter ends with a brief assessment of the model, which is done in order to check if the simulator provides results that match realistic expectations.

3.1 Model Development

This section provides a description of the models used to define the system-level performance simulation, which deals with a stochastic generation of LoS occurrences, SNR and SINR computations, calculation of achievable throughputs at the receiver, coverage and capacity considerations, radiation patterns of the antennas and influence of electrical and mechanical downtilts on the transmitter gains.

It is worth referring that no special frequency reuse scheme is considered in this thesis, which means that all the available spectrum is used everywhere. Also, one considers a three-sectorised system, where each BS is supposed to have three sector antennas, each one being positioned either in 0°, 120° or 240° of azimuth, taking the North direction as a reference. Hence, subsequent analysis are sector based, and not BS based, also because the main focus of this thesis deals with parameters intrinsic to a sector, such as the radiation pattern of the antenna.

3.1.1 LoS Occurrence

In this thesis, it is not assumed that all users are in LoS or in Non Line of Sight (NLoS) with their serving sector antenna. Instead, the existence of LoS is stochastically generated, following one of two possible approaches.

In [ViQR07], it is considered that a UE has the following probability of being in LoS:

$$P_{LoS} = \begin{cases} 1 - \dfrac{2\left(H_{B[\mathrm{m}]} - h_{m[\mathrm{m}]}\right) d_{[\mathrm{m}]} \left|\sin\left(\phi_{[^\circ]}\right)\right|}{w_{s[\mathrm{m}]}\left(h_{b[\mathrm{m}]} - h_{m[\mathrm{m}]}\right)}, & d < d_{co} \wedge s_{LoS} \geq 0 \\ 0, & d \geq d_{co} \wedge s_{LoS} < 0 \end{cases} \tag{3.1}$$

where:

- H_B: height of the buildings;
- h_m: height of the UE;
- d: distance between the BS and the UE;
- ϕ: angle of incidence of the signal in the buildings, on the horizontal plane;
- w_s: width of the streets;
- h_b: height of the BS antenna;
- d_{co}: cut-off distance;

$$s_{LoS[\mathrm{m}]} = h_{b[\mathrm{m}]} - h_{m[\mathrm{m}]} - \frac{2\left(H_{B[\mathrm{m}]} - h_{m[\mathrm{m}]}\right)}{w_{s[\mathrm{m}]}} d_{[\mathrm{m}]} \left|\sin\left(\phi_{[^\circ]}\right)\right| \tag{3.2}$$

The probability detailed in (3.1) is considered to be a realistic approach when considering the COST-231 Walfisch-Ikegami model, as it takes into account not only the distance between the BS and the UE and the height of the BS antenna above the building, but also the UE's surrounding environment.

On the other hand, in [Corr01], an alternative approach is proposed (with k equal to 1), which does not take into account such a large number of parameters as (3.1), being given by:

$$P_{LoS} = \begin{cases} k \dfrac{h_{b[\mathrm{m}]} - H_{B[\mathrm{m}]}}{h_{b[\mathrm{m}]}} \dfrac{d_{co[\mathrm{m}]} - d_{[\mathrm{m}]}}{d_{co[\mathrm{m}]}}, & d < d_{co} \wedge h_b \geq H_B \\ 0, & d \geq d_{co} \wedge h_b < H_B \end{cases} \quad (3.3)$$

where:

- k: scaling factor.

Although (3.1) is suitable to be used with the COST-231 Walfisch-Ikegami model, it only yields probabilities of LoS above 0 when the distance between the BS and the UE is extremely low (when considering the average parameters detailed in Chapter 4). As the considered scenario is the city of Lisbon, which has a very irregular structure, (3.3) is used instead, as it is an expression that depends on a smaller array of input parameters and yields significant values for a wider range of distances. However, a scaling factor k is considered in order to tune results according to measurements performed in the city of Lisbon – values for the parameters of the expression should be carefully picked so that probability of LoS does not exceed 1 (if it does, one should saturate the results to 1).

It is worth noticing that a strong limitation of both (3.1) and (3.3) is the fact that UEs closer to the façade of the building on top of which the BS antenna is positioned are the ones with the highest probability of LoS – in a real network, LoS occurrence for such UEs tends to be unlikely, as the BS antenna may be positioned in the geometric centre of the building, thus, not in line with the building's façade, and hence, in NLoS with such UEs.

3.1.2 SNR and SINR

In the initial steps of the simulation, when there are no active communications between BSs and UEs, the interfering power is not considered. As such, and in that specific situation, the SNR is used to determine the radio channel conditions for a given UE, being defined by:

$$\rho_{N[\mathrm{dB}]} = P_{Rx[\mathrm{dBm}]} - N_{[\mathrm{dBm}]} \quad (3.4)$$

where:

- P_{Rx}: power at the input of the receiver;
- N: noise power.

The power at the input of the receiver is given by (B.4), taking the link budget presented in Annex B into account and considering the COST-231 Walfisch-Ikegami propagation model presented in Annex C for path loss. The noise power is calculated using (B.6).

When there is information about the RBs distribution among users, and their corresponding SNRs, the SINR available at each UE's receiver is calculated in order to study the impact of inter-cell interference on system performance:

$$\rho_{IN[\mathrm{dB}]} = 10 \times \log\left(\frac{P_{Rx[\mathrm{mW}]}}{N_{[\mathrm{mW}]} + I_{[\mathrm{mW}]}}\right) \quad (3.5)$$

where:

- I: interfering power.

The interfering power is calculated as the sum of the power of the signals that are supported in sub-carriers placed in the same frequency as the desired signal, according to the following equation:

$$I_{[\mathrm{mW}]} = \sum_{i=1}^{N_I} I_{i[\mathrm{mW}]} \tag{3.6}$$

where:

- I_i: interfering power coming from transmitter i;
- N_I: number of interfering signals reaching the receiver.

The power of each interfering signal is also given by (B.4), considering the same propagation model and path loss expressions. As it happens with the received power from the serving sector antenna, the received signal from neighbouring sector antennas may also propagate in LoS or NLoS conditions, according to the probability given by (3.3). Only the interfering signals that have power equal or greater than the noise power are considered, as those signals are the only ones that may have a negative impact on system performance.

In a cellular system, and according to [Khan09], the SINR disparity between cell-centre and cell-edge users is usually very high, especially in a coverage limited cellular system, which leads to lower data throughputs for the cell-edge users relative to cell-centre ones, creating a large QoS inconsistency in terms of geographical coverage, as well as in terms of available data throughput within the coverage area. The reduction of inter-cell interference leads to an improvement in the cell-edge SINR.

SINR degradation is due to two main factors, as the UE moves away from the BS:

- as the path loss increases with the distance from the serving sector antenna, the received signal strength goes down;
- the increasing distance from the serving sector antenna is generally coupled with an approximation to another sector antenna, which leads to a larger inter-cell interference.

So, when computing average and standard deviation values for all the UEs being served by the system, one should expect to have a relatively high standard deviation at least for the SINR, also because there are UEs not only in LoS conditions but also in NLoS.

Results extracted from (3.5) and from measurements performed in the field are compared in Chapter 4, in order to complete the assessment of the proposed models.

3.1.3 Throughput and Capacity

Theoretical bit rates in the DL can be calculated using the following expression:

$$R_{b[\mathrm{Mbps}]} = \frac{N_{sub/RB} \times N_{sym/sub} \times N_{b/sym} \times N_{RB} \times N_{MIMO}}{T_{RB[\mu\mathrm{s}]}} \tag{3.7}$$

where:

- $N_{sub/RB}$: number of sub-carriers per RB (12 when considering a 15 kHz sub-carrier spacing, which fulfil the 180 kHz bandwidth of an RB);
- $N_{sym/sub}$: number of symbols per subcarrier (7 when the normal CP is used);

- $N_{b/sym}$: number of bits per symbol, which depends on the modulation scheme and coding rate used;
- N_{RB}: number of RBs;
- N_{MIMO}: MIMO order (2, for 2×2 MIMO);
- T_{RB}: time duration of an RB, which is 500 μs.

When inter-cell interference is considered, according to [SeTB11] and using (3.5), the achievable throughput is given by:

$$R_{b[\text{Mbps}]} = N_{RB} \times B_{RB[\text{MHz}]} \times \log_2(1 + \rho_{IN}) \quad (3.8)$$

where:

- B_{RB}: bandwidth of an RB.

In order to accomplish a more accurate evaluation of link and system levels performance, a realistic modelling of propagation characteristics is done, taking the channel models presented in [SeTB11] into account, It is also worth noticing that the propagation characteristics are strongly affected by the carrier frequency, which also has an impact on MIMO implementation, as the size of the antenna arrangement depends on the carrier wavelength.

LTE channel models are based on models already defined by the International Telecommunication Union (ITU) and 3GPP for GSM and UMTS, being associated to low, medium and large delay spreads. The Extended Pedestrian A (EPA) model provides a low delay spread (with an r.m.s. delay spread of 43 ns), being employed in an urban environment with fairly small cell sizes, while the Extended Vehicular A (EVA) and Extended Typical Urban (ETU) models are associated with medium (with an r.m.s. value of 357 ns) and large (with an r.m.s. value of 991 ns) delay spreads, respectively. These models are also applied with low (5 Hz), medium (70 Hz) and high (300 Hz) Doppler shifts, which enable the common combinations EPA 5 Hz, EVA 5 Hz, EVA 70 Hz and ETU 70 Hz.

The quality of the signal received by a UE depends on the channel quality from the serving sector, the level of interference from other sectors, and the noise level. In order to enhance capacity and coverage for a given transmission power, the transmitter tries to match the data rate for each user to the variations in received signal quality, which is referred to as link adaptation and is typically based on Adaptive Modulation and Coding (AMC). The modulation scheme and coding rate may be adapted according to the channel conditions, when using AMC.

In terms of modulation schemes, it is known that low-order modulation (e.g., QPSK) is more robust and, as such, is able to tolerate higher levels of interference, although it provides a lower transmission bit rate. It is usually selected when a low SINR is experienced. On the other hand, high-order modulation (e.g., 64QAM) offers a higher bit rate, but it is more susceptible to errors due to its higher sensitivity to noise, interference and channel estimation errors. When the SINR is sufficiently high, high-order modulations are usually chosen.

A lower code rate can be used in poor channel conditions and a higher code rate when the SINR is high. The adaptation of the code rate is implemented by applying puncturing or repetition to the output

of a mother code, to increase or reduce the code rate, respectively.

In LTE, the Modulation and Coding Scheme (MCS) is constant over the allocated frequency resources for a given UE. However, time-domain channel-dependent scheduling and AMC are supported. When multiple transport blocks are transmitted to one user in a given sub-frame using MIMO, each transport block can use an independent MCS.

The enunciated concepts are applied on the modelling of the behaviour of the system and respective simulator using the expressions provided in Annex D. In a first approach, throughputs are calculated via the existing SNR at each receiver. Then, when the SINR is considered instead, the achievable throughputs are calculated again, which enables the study of the impact of inter-cell interference on SNR/SINR or throughput reduction.

On the other hand, capacity is evaluated by the number of UEs served per sector. A UE is considered to be served if it is receiving RBs from the serving sector antenna and those RBs are able to provide a minimum throughput, depending on the type of service the UE is using.

3.1.4 Coverage and Antennas

Sector antenna's range is calculated, in a first approach, considering an NLoS scenario; when the distance to the BS increases, the probability of LoS decreases, so it is expected that UEs farther from their serving sector antenna are served in NLoS conditions in the most probable situations. A minimum throughput is considered as well, as UEs are considered to be served if they reach the minimum throughput for their wanted service. In a subsequent approach, sector antenna's range is calculated as the distance of the UE that is farther away from its serving sector:

$$R_{sector[\mathrm{m}]} = d_{\max[\mathrm{m}]} \tag{3.9}$$

where:

- d_{max}: distance of the UE farther away from its serving sector antenna.

The antennas' influence in the results is obtained through their gain, which has a direct effect on the UE's received power, being both the desired one and the one received from interfering sectors – this has an impact on the SINR. An approach similar to the one presented in [YiHH09] and [AtJo10], which makes use of antenna models proposed in [3GPP10a], is followed.

According to [3GPP10a], the horizontal radiation pattern of the antennas is given by:

$$G_{H[\mathrm{dB}]}(\varphi) = -min\left[12\left(\frac{\varphi_{[^\circ]}}{\varphi_{3dB[^\circ]}}\right)^2, A_{m[\mathrm{dB}]}\right] \tag{3.10}$$

where:

- φ: angle between the pointing direction of the antenna and the direction defined by the antenna and the UE, in the horizontal plane;
- φ_{3dB}: horizontal half-power beamwidth;
- A_m: front-to-back attenuation.

The vertical radiation pattern of the antennas is given by:

$$G_{V[\mathrm{dB}]}(\theta) = -min\left[12\left(\frac{\theta_{[°]} - \theta_{etilt[°]}}{\theta_{3dB[°]}}\right)^2, SLA_{v[\mathrm{dB}]}\right] \tag{3.11}$$

where:

- θ: angle between the pointing direction of the antenna and the direction defined by the antenna and the UE (LoS) / building (NLoS), in the vertical plane;
- θ_{etilt}: electrical antenna downtilt;
- θ_{3dB}: vertical half-power beamwidth;
- SLA_v: sidelobe attenuation.

The θ angle under study can be calculated for a UE that is in LoS conditions by:

$$\theta_{[\mathrm{rad}]} = \arctan\left(\frac{h_{b[\mathrm{m}]} - h_{m[\mathrm{m}]}}{d_{[\mathrm{m}]}}\right) \tag{3.12}$$

For a UE under NLoS conditions, θ is given by the following expression (marked in Figure C.1), where one should notice that the UE is assumed to be at the centre of the street:

$$\theta_{[\mathrm{rad}]} = \arctan\left(\frac{h_{b[\mathrm{m}]} - H_{B[\mathrm{m}]}}{d_{[\mathrm{m}]} - \frac{w_{s[\mathrm{m}]}}{2}}\right) \tag{3.13}$$

The total contribution of the two radiation patterns, hence, the total gain of the antenna, is given by:

$$G(\varphi,\theta)_{[\mathrm{dBi}]} = G_{max[\mathrm{dBi}]} - min\{-[G_{H[\mathrm{dB}]}(\varphi) + G_{V[\mathrm{dB}]}(\theta)], A_{m[\mathrm{dB}]}\} \tag{3.14}$$

where:

- G_{max}: maximum gain of the antenna.

Typically, antenna characteristics are measured in anechoic chambers (blue curves in Figure 3.1 and Figure 3.2 for the horizontal and vertical radiation patterns, respectively), which means that near-field scatterers (such as mast, mountings and roof-tops) and diffraction are usually not accounted for. In this thesis, those phenomena are not considered in the propagation models, but they are conceptually included in the effective antenna pattern defined by (3.10) and (3.11) and illustrated in the red curves of Figure 3.1 and Figure 3.2.

When electrical downtilt is considered, main, side and back lobes are tilted uniformly by changing the phases of the antenna elements. On the other hand, when mechanical downtilt is considered, the antenna main lobe is lowered on one side and the back lobe is raised on the other side, as the antenna elements are physically tilted. One should note that pure electrical downtilt produces an elevation steering of the radiation pattern that is independent of the horizontal direction (azimuth), whereas mechanical downtilt creates radiation pattern irregularities (pattern blooming), as it can be seen in Figure 3.3. In Figure 3.3, one should note that a mechanical downtilt of up to 4° results in a horizontal radiation pattern that is relatively uniform. However, when further values of mechanical downtilt are considered, the half-power beamwidth widens. At 10°, the pattern is grossly distorted [Meye10]. This situation suggests that mechanical and electrical downtilts should have a different impact on system performance.

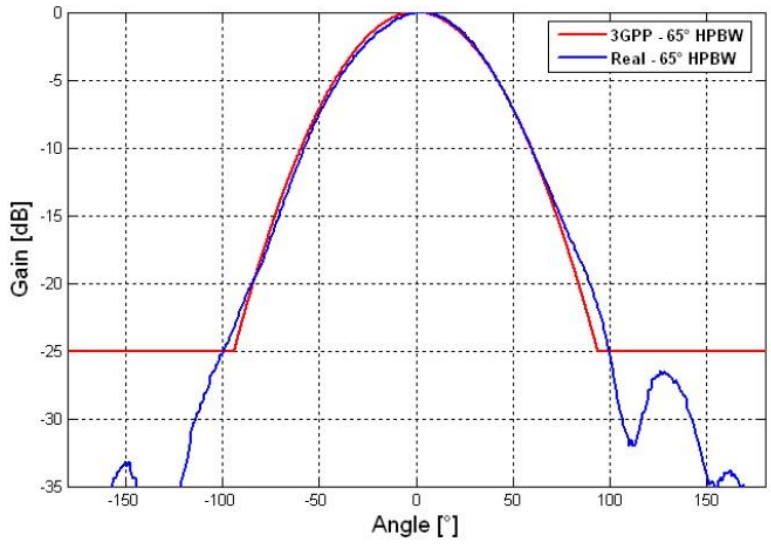

Figure 3.1. Modelling of the horizontal pattern of an antenna with $A_m = 25\text{dB}$ and $\varphi_{3dB} = 65°$ (extracted from [YiHH09]).

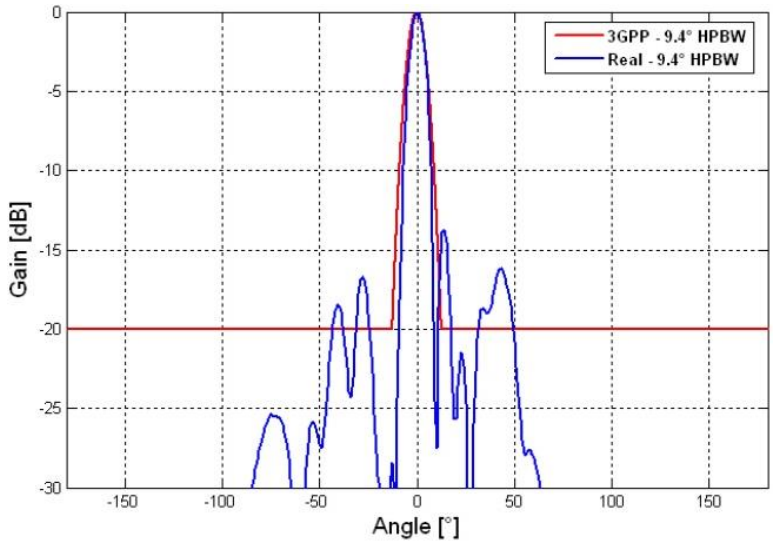

Figure 3.2. Modelling of the vertical pattern of an antenna with $SLA_v = 20\text{dB}$ and $\theta_{3dB} = 9.4°$ (extracted from [YiHH09]).

Mechanical downtilt is taken into account by using the following change of variables, according to [3GPP10a]:

$$\varphi_{[°]} = \arg\left(\cos\left(\varphi_{[°]}'\right)\sin\left(\theta_{v[°]}'\right)\cos\left(\theta_{mtilt[°]}\right) - \cos\left(\theta_{v[°]}'\right)\sin\left(\theta_{mtilt[°]}\right) + j\,\sin(\varphi_{[°]}')\sin(\theta_{v[°]}')\right) \quad (3.15)$$

where:

- φ': angle between the pointing direction of the antenna (neglecting any existing tilt) and the direction defined by the antenna and the UE, in the horizontal plane;
- θ_v': angle between the vertical direction of the antenna (neglecting any existing tilt) and the direction defined by the antenna and the UE (LoS) / building (NLoS), in the vertical plane;
- θ_{mtilt}: mechanical antenna downtilt.

$$\theta_{v[°]} = \arccos\left(\cos(\varphi')\sin\left(\theta_{v[°]}'\right)\sin\left(\theta_{mtilt[°]}\right) + \cos(\theta_{v[°]}')\cos(\theta_{mtilt[°]})\right) \quad (3.16)$$

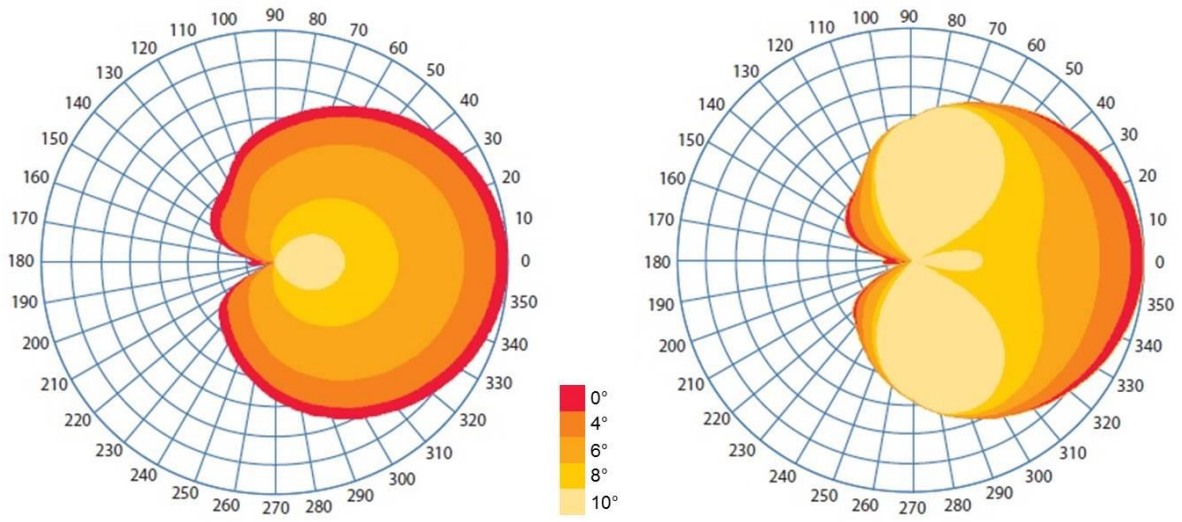

(a) Electrical downtilt (b) Mechanical downtilt

Figure 3.3. Horizontal radiation pattern associated to either electrical or mechanical downtilts (adapted from [Meye10]).

In order to have a coherent approach and to use the angles found in (3.15) and (3.16) in the gains in (3.10) and (3.11), one should consider the following equivalences and trigonometric identities:

$$\theta_{[°]} = \theta_{v[°]} - 90° \tag{3.17}$$

$$\sin(\theta_{[°]} + 90°) = \cos(\theta_{[°]}) \tag{3.18}$$

$$\cos(\theta_{[°]} + 90°) = -\sin(\theta_{[°]}) \tag{3.19}$$

Using (3.17), (3.18) and (3.19) in (3.15) and (3.16), one ends up having the following change of variables, which can be used in (3.10) and (3.11):

$$\varphi_{[°]} = \arg\left(\cos\left(\varphi_{[°]}'\right)\cos\left(\theta_{[°]}'\right)\cos\left(\theta_{mtilt[°]}\right) + \sin\left(\theta_{[°]}'\right)\sin\left(\theta_{mtilt[°]}\right) + j\,\sin(\varphi_{[°]}')\cos(\theta_{[°]}')\right) \tag{3.20}$$

$$\theta_{[°]} = \arccos\left(\cos(\varphi')\cos\left(\theta_{[°]}'\right)\sin\left(\theta_{mtilt[°]}\right) - \sin(\theta_{[°]}')\cos(\theta_{mtilt[°]})\right) - 90° \tag{3.21}$$

The antennas' parameters used in the model and corresponding simulator, for the reference scenario, are the ones obtained from [Kath12].

3.2 Model Implementation

In order to implement the models described in Section 3.1, a simulator was developed using the MapBasic and C++ programming languages. However, it was not done from scratch – instead, it was based on work developed in previous master theses, such as [Duar08] and [Pire12], followed by modifications done under the scope of the current thesis. A lot of effort was put into changing some of the algorithms and implementations, in order to get a more realistic approach of the network's behaviour – everything that deals with antenna parameters and downtilt was implemented from scratch in this thesis, as well as the possibility to have both LoS and NLoS users, a more realistic spectrum distribution among RBs, an association of users to sectors based on received power and a

throughput calculation based on the expressions provided in Annex D. Also, some other changes were made, in the sense that in this thesis only LTE is considered, so legacy parameters related to other systems were removed from the programming files, in order to get a more efficient approach and to reduce running time – the entire C++ part of the simulator was restructured also to accommodate the changes introduced in this thesis. A careful analysis of all the files was also done, which enabled the rectification of some typos that could have a negative impact on the results.

The simulator uses a snapshot approach, where results provided refer to the behaviour of the network at a given instant. Its main structure is provided in Figure 3.4.

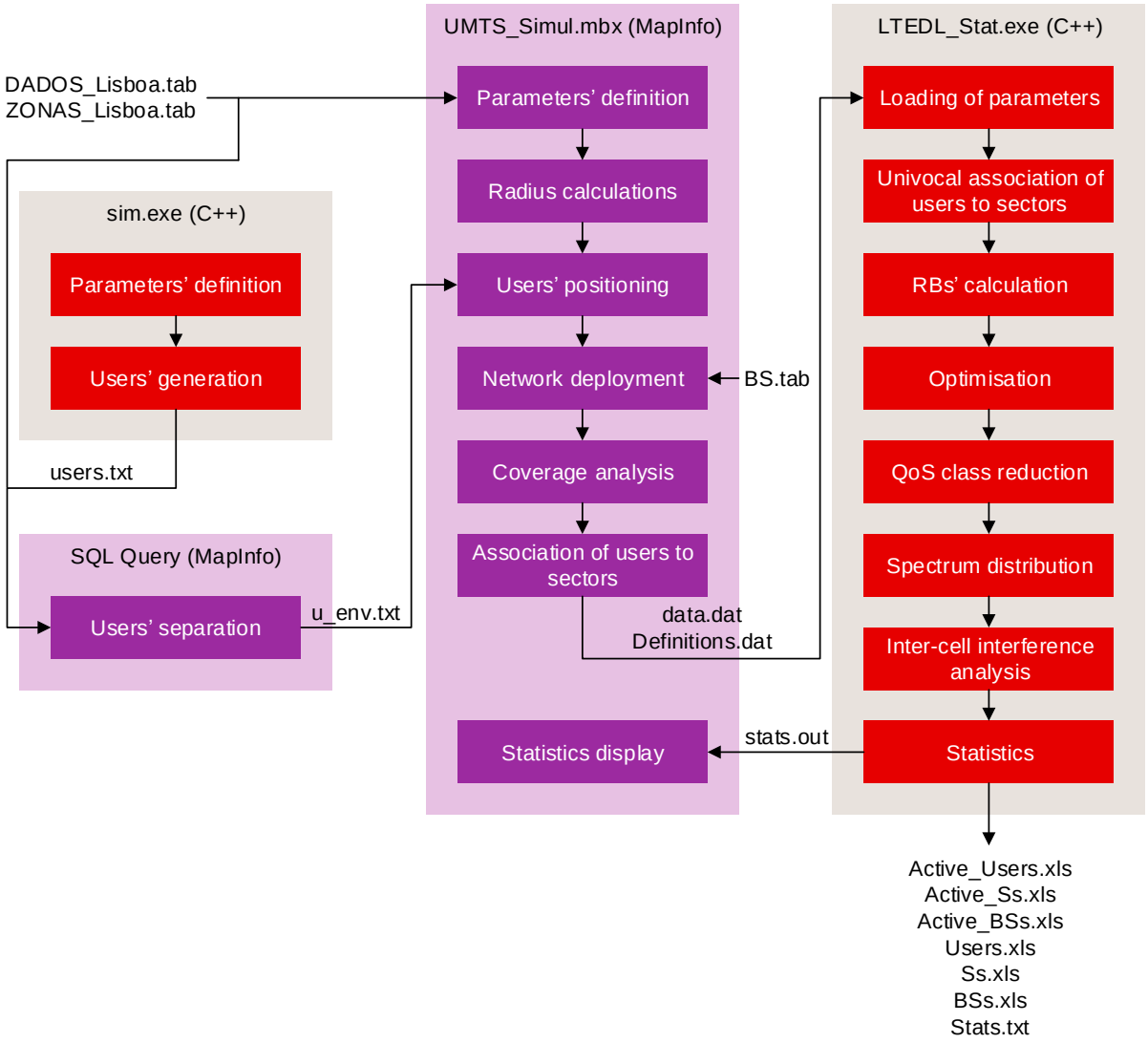

Figure 3.4. Simulator workflow.

Input data has to be explicitly given to the simulator, in order for it to work properly. The following input files must be provided:

- DADOS_Lisboa.tab, which holds information about the city of Lisbon, namely its districts;
- ZONAS_Lisboa.tab, which contains information about the area characterisation;
- BS.tab, which has information on BSs' location.

Some files' names presented in Figure 3.4 are just representative. For example, when the centre of

Lisbon is analysed concerning the 2 600 MHz band, the file BS.tab is called VodafoneCentreNetworkUpdated2600.tab, as it contains information about BSs located in the centre of Lisbon and working in the 2 600 MHz band. It has “Updated” in its name because it does not match exactly the file provided by Vodafone. It is assumed that the file provided by Vodafone contains information about all existing BSs in the city of Lisbon and work in LTE’s frequency bands. This means that, in order to have information about BSs that work in each of the frequency bands, some processing was made in that file – superimposed and BSs very close to each other were eliminated, as it was assumed that they corresponded to co-existent sites or different sectors of the same BS. It is assumed that the resulting file contains information about all BSs that work in the 2 600 MHz band. Then, that file was processed again in order to have different files for centre and off-centre of Lisbon’s BSs. After that division, copies of those files were again processed, in order to have information about the other two frequency bands. It is assumed that 2/3 of the BSs also work in the 1 800 MHz band, and 1/3 in the 800 MHz one.

There are other files that are outputs of certain modules of the simulator, and serve as inputs for others, which are:

- users.txt, which provides information about users’ location and the service each one of them is requesting;
- u_env.txt, which provides information about either centre or off-centre users’ location and the service each one of them is requesting;
- data.dat, which provides information about BSs’ location, the sectors each one of them has, and also information about users who are potentially covered by them, including their location, requested service and distance to the BS;
- Definitions.dat, which contains information about propagation model parameters, frequency band, bandwidth, services’ minimum and maximum throughputs, antennas’ parameters, type of environment, LoS probability method and whether localised or distributed resource allocation should be used;
- stats.out, which contains information obtained after the main C++ modules are executed, such as average UE’s, Sector’s and BS’s throughput and number of covered and served users.

Statistics presented in Chapter 4 are based on data contained in the following output files provided by the simulator:

- Active_Users.xls, an Excel file that provides, in each row, information about a served UE’s throughput, number of RBs, distance from the serving BS, average SNR, average SINR, average received power, average interfering power, requested service, whether it is a cell-centre or cell-edge UE and whether the UE is in LoS or NLoS conditions;
- Users.xls, which provides the same information as Active_Users.xls, except that it extends data collection to non-served UEs;
- Active_Ss.xls, which contains information about active sectors, such as served throughput, number of served users, number of served RBs and the distance of the farthest user being served;

- Ss.xls, which provides the same information as Active_Ss.xls, except that it extends data collection to sectors that became non-active after the inter-cell interference analysis took place;
- Active_BSs.xls, which provides the same information as Active_Ss.xls, except that it corresponds to a BS rather than a sector;
- BSs.xls, which contains the same information as Ss.xls, except that it refers to a BS rather than a sector;
- Stats.txt, which has information about average UE's, sector's and BS's throughput and number of RBs, number of served, covered and LoS UEs, number of UEs asking for and being served a given service, average interfered RBs per active sector, maximum coverage radius, and parameters introduced in the simulator as inputs.

The simulator defines the desired scenario from a set of defined input parameters, which are the ones presented in Chapter 4. Some input parameters' pre-processing is automatically done in the simulator, in order to ensure that inconsistencies do not occur during simulations.

The first module that needs to be run is sim.exe, which is the one studied in [SeCa04]. It creates a file with users' positioning along the entire city of Lisbon, which also contains information about the service the user is requesting, according to the percentage introduced as input. Users' distribution takes real population density along the city of Lisbon into account, but occurs in a square containing the entire city of Lisbon and some areas that do not belong to the city – about 10% of the users end up not being considered in the simulator, as it only performs an analysis over the city of Lisbon.

Then, the users file is filtered, in order to provide information for centre or off-centre users. For the users' separation into centre and off-centre users, an SQL Query created under the scope of this thesis is performed using MapInfo. Centre users are considered to be the ones who are placed in either of the following districts (according to the districts definition established before 2012): São Mamede, Santo Condestável, Prazeres, Santa Isabel, Lapa, Santos-o-Velho, Mercês, Santa Catarina, São Paulo, São Sebastião da Pedreira, Coração de Jesus, São José, Encarnação, Santa Justa, Sacramento, Mártires, São Nicolau, São Jorge de Arroios, Pena, Madalena, Sé, São Cristóvão e São Lourenço, Castelo, Santiago, Socorro, Anjos, Penha de França, Graça, Santo Estêvão, São Miguel, São Vicente de Fora and Santa Engrácia. Off-centre users are the ones that do not belong to these districts, but are still within Lisbon's premises.

After that, one should have all the input files needed in order to execute the UMTS_Simul.mbx. This program has UMTS in its name only because it is based in previous works that dealt with 3G systems, and not because UMTS is considered in this thesis. The MapBasic programmed environment, which was modified in this thesis, provides a user interface in MapInfo, so that the manual input of parameters is intuitive for the user. Those parameters are pre-processed by MapInfo before they are written in a file (Definitions.dat) to be read by LTEDL_Stat.exe. After the introduction of parameters detailed in Annex E, a preliminary study of coverage is done. It is based on a reference minimum throughput, which is translated to a minimum SNR via (D.5), taking into account that, at the cell-edge, QPSK is the modulation scheme being used, as it is the most robust, enabling realistic throughputs at

a relatively low SNR. Then, minimum SNR is translated into minimum received power, taking into account noise power. In order to get the maximum distance that guarantees the minimum received power, only the horizontal radiation pattern of the antennas presented in (3.10) and implemented in this thesis is considered (normalised vertical radiation pattern is not taken into account) – this means that coverage areas computed using this method are not very realistic, being much larger than the one that occurs in a real network. So, a more detailed analysis of coverage is done afterwards, in LTEDL_Stat.exe, which is, however, simplified by the fact that only an active set of users around each sector is considered (instead of making an analysis over the whole network). This primary coverage analysis is also used to process geographical information: users generated by the sim.exe simulator and filtered afterwards are associated to sectors based on whether they are located inside the coverage area of a given sector or not. Since there is quite an overlapping of coverage areas, users can often be associated to more than one sector.

As the most time consuming task of the simulations is the association of users to sectors, once it is done for the first time in MapInfo, other simulations using the same users and BSs are no longer called from MapInfo, but instead from the LTEDL_Stat.exe directly (which only requires a manual change of the parameters recorded in Definitions.dat). This saves a lot of time in the simulations, and has no negative side effects on the results, taking into account that coverage areas provided by MapInfo are much larger than they should be.

Input parameters introduced in UMTS_Simul.mbx are passed on to LTEDL_Stat.exe as illustrated in Figure 3.4. The C++ program starts by reading Definitions.dat and data.dat and saving their information to internal data structures. Users who are considered to be covered by more than one sector are associated to the one from which they receive the highest power – in this analysis, all users are considered to be under NLoS conditions. Whenever received power from two sectors is equal, which can happen when the user is covered by more than one sector and the antennas' gain is the same (which happens near the frontier between the sectors), the user is associated to the one that guarantees the lowest azimuth. This association method was entirely programmed under the scope of this thesis, as previous works considered only a distance based allocation that does not take important parameters into account, such as the radiation pattern of the antennas.

Each sector has a number of RBs dictated by the bandwidth being considered, according to Table 2.3. Users are given all the RBs they need in order to receive the maximum throughput that their associated service requires (check Chapter 4 for the definition of this maximum throughput), if their radio channel condition is able to support it. At this step, system capacity is not taken into account.

In order to determine the number of RBs that a user needs in order to fulfil its desired data rate, the throughput for a single RB is calculated based on the SNR given by (3.4), which is also computed for a single RB, and the expressions provided in Annex D, which were created and implemented under the scope of this thesis. As the simulator is snapshot based, allocation is not done on a sub-frame (two consecutive RBs in the time domain) basis, but instead on an RB one. At this step, it is assumed that all RBs have the highest frequency in the frequency band under study, according to Table A.3, and also according to the chosen bandwidth (the allocated spectrum is considered to be always the

one that has lower frequencies, whenever a bandwidth lower than the maximum one is picked). This is done in order to ensure that all allocations meet the user's requirements in terms of throughputs, because the top-most RB is the one that suffers the highest path loss, since it has the highest frequency. More realistic SNRs and SINRs are computed later in the simulation, after all the RBs allocations are done. The user's desired throughput is divided by the throughput for a single RB (being picked the integer ceiling value), in order to have knowledge, in a first approach, of the number of RBs requested by each user.

For the SNR computation, the received power is calculated based on the expressions provided in Annex B and Annex C, which take the antenna gain provided by (3.14), (3.10) and (3.11) into account – this was entirely implemented in this thesis. Users are classified as either LoS or in NLoS, according to the probability given by (3.3), taking k as 3 (tuned according to measurement results provided in Chapter 4), which is a feature introduced in this thesis. This has an impact not only in the expressions used to determine received power, but also on the definition of the vertical angle used to determine the antenna gain in the user's direction, according to (3.12) and (3.13), which was also implemented in the simulator for the first time.

After all the allocations are done, based on user's requested throughput, it is checked if those are coherent with the system capacity. If not, reduction has to occur, so that users are not requesting more resources than the ones the network is able to provide them.

Since the Proportional Fair algorithm is linked with the time domain, which is not considered in the simulator, an adapted version of that algorithm was implemented in [Duar08] and [Pire12]. It takes into account fairness, in the sense that resources are supposed to be assigned to all users. However, that assignment takes the type of service the user is requesting (each type of service is assigned a QoS priority, as defined in Table 4.4) into account. So, resources are allocated to all users requesting them, whether they are cell-centre or cell-edge ones, without taking system capacity into account. For the same type of service, the former usually request fewer resources, as they have better channel conditions, while the latter tend to need a lot more resources, as they have worse channel conditions. Then, system capacity is considered: if users are requesting more resources than the network can provide, their requested throughput is decreased until the minimum throughput is reached or system capacity becomes coherent. Users that are requesting the highest priority services are the last ones to have their resources reduced, while users that are requesting the lowest priority services are the first ones to have their resources reduced. Nevertheless, reduction is proportional and fair: lowest priority service users are assigned a half of the RBs they previously had, then the second lowest priority service users are assigned a half of the RBs they previously had, and so on and so forth, until system capacity is not exceeded. In the first round of reductions, if after each resource reduction users still have RBs assigned, but are not able to reach a minimum throughput, they are guaranteed minimum throughput. From the second round onwards, if that continues to happen, they are delayed (i.e., they are not served at the instant of the simulation).

Before all reductions take place, optimisation is performed (but only if there is the need to perform reductions): users that ended up being served with a throughput slightly higher than the one they

wanted are reduced one RB.

After UEs' assigned RBs are consistent with system capacity, all RBs are assigned a position on the available spectrum, following a method entirely implemented under the scope of this thesis. Resource Allocation Type 2 of localised (and contiguous) type (described in Chapter 2) takes place, because it is the only one that makes it possible to allocate either one or the maximum available RBs to a single UE. Allocation starts either at the beginning or at the end of the available spectrum, which is decided randomly for each sector (each of the options has an equal probability of occurrence).

The frequency associated to each RB is taken as the frequency of the RB's sub-carrier which is centred in the highest frequency. A 200 kHz spacing between RBs is taken, because a uniform distribution of RBs among the available bandwidth is considered, and one only considers 10, 15 and 20 MHz bandwidths in this thesis, which enable a uniform spacing of 200 kHz among RBs to fulfil the entire spectrum (the number of RBs that correspond to each bandwidth can be seen in Table 2.3).

Then, an inter-cell interference analysis takes place. For each user that is assigned at least one RB from a BS sector, it is checked if there are other sector antennas sending RBs that use the same sub-carriers as the ones used to serve the UE being considered in its sector, but to serve other users. If there are, it is checked if each of those RBs represent a received power higher than noise – if this is true, they are considered to be interfering RBs. Interfering sector antennas are also considered to be in LoS or NLoS conditions according to (3.3), this feature being implemented under the scope of this thesis. SINR is computed to take interference into account, and a new throughput for each RB is calculated (modulation is determined per RB and not per user, as it happens in a real scenario), taking it into account instead of the SNR in the expressions provided in Annex D. If the new throughput for a given UE is below the minimum throughput for its service, the UE is delayed, which means that it is not served at the instant of the simulation.

After this analysis takes place, output files are generated, a detailed analysis of the results being done by using Microsoft Excel. A window indicating a successful completion of the program is also shown in MapInfo, along with some results determined during the simulation.

The execution of the workflow presented in Figure 3.4 lasts about an hour and a half for each simulation in the 2 600 MHz band, off-centre of Lisbon and for a high load scenario, using a PC equipped with an Intel Core i5 CPU at 2.30 GHz and 6 GB of RAM. In order to shorten this simulation time, and taking into account that the most time consuming phase of the process in the MapInfo related one, after 5 users' distributions are assigned to sectors that provide them coverage, for each of the frequency bands and each of the environments, subsequent simulations can take advantage of those previously generated files, making the simulation's running time decrease a lot, to some tens of seconds. This does not have any influence on the results, because coverage areas provided by MapInfo are much larger than they actually are, since the vertical radiation pattern is not considered in this first approach.

3.3 Model Assessment

Results provided by the simulator are saved in .xls files, which are analysed using Microsoft Excel. Average and standard deviation metrics are automatically computed, and are crucial elements that support subsequent analyses. In order to ensure statistical relevance of the results, for each analysis, a certain number of simulations are considered, the total average and standard deviation for each scenario being computed by taking the ones for each simulation into account, using expressions (3.22) and (3.23), respectively.

$$\mu = \frac{1}{N}\sum_{n=1}^{N}\mu_n \tag{3.22}$$

where:

- N: number of simulations;
- μ_n: average obtained in simulation n.

$$\sigma = \sqrt{\frac{1}{N}\sum_{n=1}^{N}\sigma_n^2} \tag{3.23}$$

where:

- σ_n: standard deviation obtained in simulation n.

As each simulation takes an already high number of users in the network into account, especially in a high load scenario analysis, one should not expect the need to have a high number of simulations to ensure statistical relevance. According to Figure 3.5 and Figure 3.6, 10 and 5 simulations are done for each low load and high load scenarios analysis, respectively, as using that number of simulations one can already notice that the standard deviation over average ratio of the UE's throughput tends to a constant value. That analysis was performed using the 2 600 MHz band as a reference, but it was repeated for the other two bands considered in this thesis, which enabled similar conclusions.

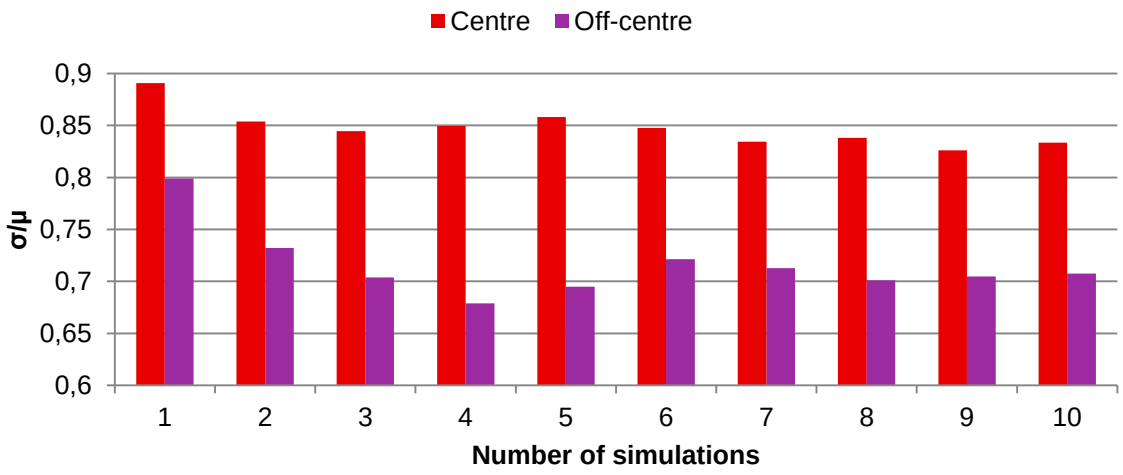

Figure 3.5. Standard deviation over average of the UE's throughput along the number of simulations for centre and off-centre environments and for the low load scenario.

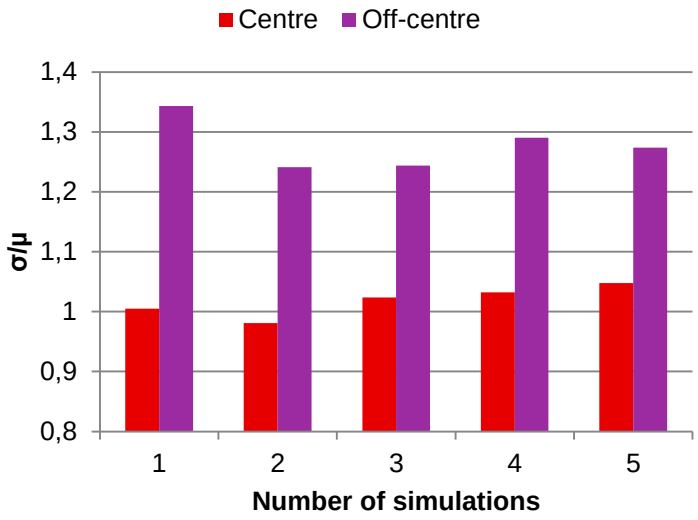

Figure 3.6. Standard deviation over average of the UE's throughput along the number of simulations for centre and off-centre environments and for the high load scenario.

Variations between consecutive simulations over the same scenario happen, because some analysis performed by the simulator are stochastic, such as the occurrence of LoS for a given user, the spectrum occupation and the distribution of users along the centre/off-centre area of Lisbon.

In order to decide on the number of users for the high load scenario, 30 simulations were performed (15 for each environment – centre and off-centre). The users' generation module was asked to generate from 1 000 up to 15 000 users, in steps of 1 000, in the entire city of Lisbon (some of them are positioned outside of the city and are not considered in further analysis), using the 2 600 MHz band, as it is the one that tends to provide the highest capacity – this is because it is the one where the highest bandwidth is available (20 MHz) and where BSs' density is higher. Those users were then separated in centre and off-centre ones, and each of those groups of users was an input to the simulator, which determined which of those were covered and then served by the system. The sum of the results from the two environments is plotted in Figure 3.7, which shows an expected trend – the higher the number of covered users, the higher the number of served users, until saturation starts to be noticed, as the system does not have infinite resources. The number of served users is also limited by interference, which tends to increase with the number of covered users being served.

Based on these results, the scenario that implied the generation of 14 000 users was picked as the reference one for the high load analysis. It is a scenario where interference and the limited number of radio resources are important factors that limit system performance. For that scenario, the number of covered users ended up being 11 069 (as some of the users are positioned outside of the city of Lisbon by the users' generation module, and others are positioned outside the coverage area of the system), while only 3 539 were served. If interference was not considered, the number of served users would be 7 357.

A simulation with a single UE in the network was done, in order to check if it was able to get the maximum throughput. A Category 3 UE (its characteristics can be found in Table 2.2) was considered,

as it is the one considered in the analyses performed in Chapter 4. The generated user was 10.41 m away from the closest sector antenna, and ended up being served by 84 RBs, which together offered a throughput of 100.73 Mbit/s, which is very close to the maximum theoretical value. The simulator determined that the UE was in LoS conditions, which is an expected result, due to the close proximity to the antenna. If one considered a Category 4 UE, the maximum theoretical throughput of about 150 Mbits/s would not be reached (the maximum UE throughput achieved by the simulator corresponds to about 120 Mbit/s), because the simulator does not consider the maximum coding rate for the 64QAM modulation scheme (check Annex D). This is due to the fact that the simulator is intended to represent a good approximation, on average, to the behaviour of a real network, and the usage of the maximum coding rates would provide an unrealistic approach.

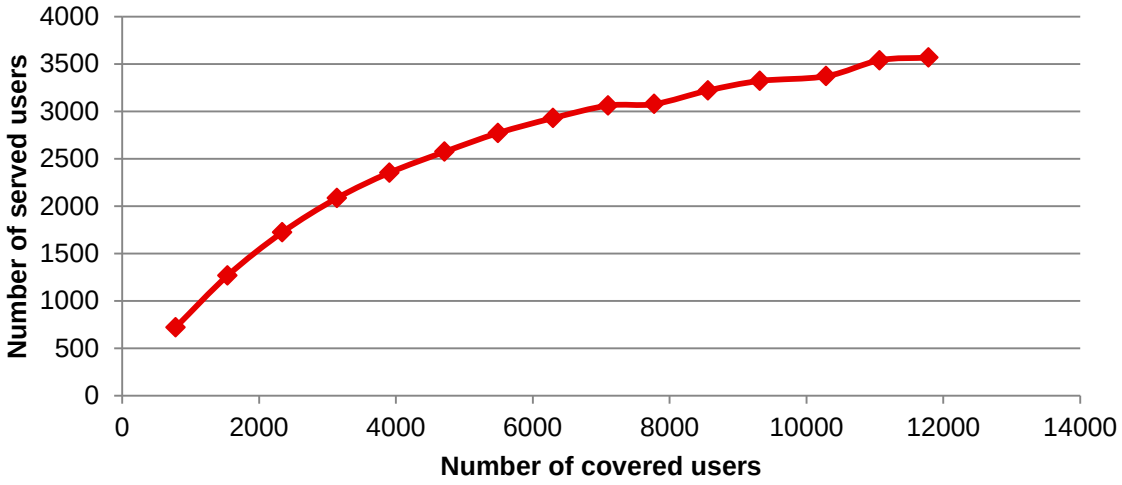

Figure 3.7. Number of served users along the number of covered users for the city of Lisbon.

The results presented in Chapter 4, such as UEs' throughputs, also show that maximum and minimum values are between the theoretical ranges. Using a debugging tool, it was also seen that all UEs' azimuths are between -60° and 60°, which is expected taking into account that a tri-sectorised system is considered, and each sector antenna's orientation is angularly separated from each other by 120°. Also, the distance of the farthest served UE never increases when one considers interference (comparing with a no-interference case), which is an expected result.

In order to study the difference between measurements and simulations, which is also used to assess the model in Chapter 4, the following relative error is considered, where measured results are taken as the reference:

$$\varepsilon_r = \frac{V_{simulated} - V_{measured}}{V_{measured}} \times 100\% \tag{3.24}$$

where:

- $V_{simulated}$: value obtained via simulation;
- $V_{measured}$: measured value.

Chapter 4

Results Analysis

This chapter starts by providing a description of the scenarios tested in the simulator. A low load scenario analysis is provided in the first place, because it also contributes to the assessment of the model, as its results are compared to measurements performed in the city of Lisbon. Then, a high load scenario analysis is presented, followed by results obtained from the variation of electrical and mechanical downtilts, height of the antennas and transmitter output powers.

4.1 Scenarios Description

The geographical scenario studied in this thesis is the city of Lisbon, and dense urban and urban environments are considered in the centre and off-centre of Lisbon, respectively.

Path loss is calculated using the COST-231 Walfisch-Ikegami propagation model provided in Annex C and the parameters shown in Table 4.1. The height of the buildings (for the urban environment), the distance between buildings' centres, the street width and the incidence angle are extracted from [Carr11]. The height of the buildings for the dense urban environment was chosen based on observations done in the centre of Lisbon, and is considered to be the one that best represents the environment where the measurements in the centre of Lisbon were performed. The heights of the BS antennas are based on [NaDA06]. The UE height is the one verified during the measurements performed in the city of Lisbon, and matches the average UE height measured among different people holding their smartphone in a typical data usage position (one should remember that the traditional voice service is not available in LTE, neither is it studied in this thesis).

Table 4.1. Configuration of parameters for the COST-231 Walfisch-Ikegami model.

Parameter	Urban	Dense urban
Height of the BS antennas (h_b) [m]	30	25
Height of the buildings (H_B) [m]	23	21
Street width (w_s) [m]	35	30
Distance between buildings' centres (w_B) [m]	75	50
Incidence angle (ϕ) [°]	90	
UE height (h_m) [m]	1.2	

Three different frequency bands associated with their maximum available bandwidths (as detailed in Annex A, except for the 1800 MHz band) are considered:

- 800 MHz band (with an associated bandwidth of 10 MHz), which provides high coverage and, as such, may suffer from high inter-cell interference;
- 1 800 MHz band (with an associated bandwidth of 15 MHz), which provides high capacity in urban areas and compatibility with a wide range of devices;
- 2 600 MHz band (with an associated bandwidth of 20 MHz), which provides high capacity.

The study of each frequency band is done separately, considering that, at the instant of the simulation, the sectors available for the given frequency band are only working on that frequency band.

Simulation parameters are summarised in Table 4.2. Concerning propagation characteristics, a fast fading margin is not considered as, according to [HoTo11], although it is typically used with UMTS due to fast power control to allow headroom for the power control operation, it is not necessary in LTE because it does not use fast power control. The slow fading margin is taken from [HoTo11].

Category 3 UEs (which are able to support DL throughputs up to 100 Mbit/s, according to Table 2.2) with a 2×2 MIMO configuration are considered. All users are considered to be EPA5 (Extended

Pedestrian A), and a Universal Frequency Reuse scheme is considered. An adapted version of Proportional Fair is considered for resource distribution, as explained in Chapter 3.

Table 4.2. Configuration of simulation parameters.

Parameter	**DL**		
Frequency band [MHz]	800	1 800	2 600
Maximum bandwidth [MHz]	10	15	20
Transmitter output power [dBm]	44.8	46	46
UE antenna gain [dBi]	1		
Modulations	QPSK, 16QAM, 64QAM		
Antenna configuration	2×2		
Electrical downtilt [°]	5		
Mechanical downtilt [°]	0		
User losses [dB]	1		
Cable losses [dB]	2		
Noise figure [dB]	7		
Slow fading margin [dB]	8.8		
Frequency reuse scheme	Universal Frequency Reuse		
Type of users	EPA5		

Transmitter output powers illustrated in Table 4.2 are given per stream – 44.8 dBm corresponds to 30 W and 46 dBm to 40 W. One considered that the transmitter output power is divided among all the RBs available in the frequency band under consideration, according to the bandwidth. Noise figure, cable losses, user losses and UE antenna gain are extracted from [Carr11].

In Table 4.3, one can check the different sector antenna parameters extracted from [Kath12]. Although some of the values present a slight variation with the antenna's electrical downtilt angle, it is assumed that (3.10) and (3.11) already take care of these variations, so the values associated with the inexistence of electrical downtilt are picked.

For the reference scenario, no mechanical downtilt is considered, and an electrical downtilt angle of 5° is taken, as this is near the maximum value supported by the used antenna in the 2 600 MHz band (which is 6°) and is the value that makes measurements' and simulations' results more alike.

LoS probability is given by (3.3) (with k assuming the value 3), as this is the approach which ends up producing a higher percentage of users is LoS, which is considered to be more realistic. However, that percentage is still relatively small, which is also considered to be realistic in a city where building density is very high and the structure is very irregular. The cut-off distance is extracted from [Corr06], being 300 m for the centre of Lisbon and 500 m for the off-centre.

Signalling and control overheads considered in the simulations are accounted for by the SINR vs. throughput equations presented in Annex D.

Table 4.3. Configuration of sector antenna parameters (adapted from [Kath12]).

Parameter	800 MHz band	1 800 MHz band	2 600 MHz band
Maximum gain [dBi]	16	18	17.8
Half-power beam width (horizontal) [°]	68	62	63
Half-power beam width (vertical) [°]	10.3	4.8	3.5
Front-to-back attenuation (horizontal) [dB]	27	25	25
Sidelobe attenuation (vertical) [dB]	18	18	18
Electrical downtilt (continuously adjustable) [°]	0–10	0–6	0–6
Mechanical downtilt [°]	0–10		

Concerning the traffic mix, six different services are considered: video streaming, chat, web browsing, FTP, e-mail and P2P. Each service is characterised by its QoS priority, minimum and maximum throughputs. The QoS priority is different for each of the services, which means that they are treated differently when users are asking for more resources than the network can provide. Although services' throughput is defined end-to-end, depending on a lot of factors that are not directly associated with the radio access of the network, minimum and maximum throughput values are used as reference, in the sense that the network is supposed to be able to offer a certain minimum throughput and is able to offer the maximum throughput available. In a real scenario, the maximum throughput allocated to the UE depends on its associated profile, being differentiated in the sense that high profile users tend to be able to get higher throughputs from the network than low profile ones. However, in this thesis, users' profile is not taken into account, so it is assumed that users ask the network for the maximum available throughput, considering the equipment they are using (Category 3 UE, which provides a maximum DL throughput of 100 Mbit/s). In the particular case of video streaming, it is assumed that a relatively high throughout value is not necessary, taking the 8 Mbit/s value as a reference for an HD video streaming (based on an approximation of the value calculated from the information available in [Veri13] for a 4G Mobile Broadband video streaming in high-definition, and also based on [Voda13]). Also, for the chat service, high peak throughputs do not need to be considered, so the values used in [Pire12] are picked. The chosen values are illustrated in Table 4.4. Whenever the 800 MHz band is used, maximum requested throughputs of 100 Mbit/s are reduced to 75 Mbit/s, as this is the maximum throughput achieved in a frequency band where a maximum bandwidth of 10 MHz is available.

The chosen percentages for the traffic mix reflect not only services usage, but also the type of service: while video streaming, FTP or P2P require a significant and continuous information download for a certain period of time, web browsing, chat and e-mail are services that usually deal with small data transfers sporadically (check Chapter 2 for a more detailed analysis of traffic models). As such, the first group of services is assumed to have a higher probability of being requesting resources from the network at a given period of time than the second one, hence, their higher percentages (an exception takes place for the web browsing, as it is considered that its usage is still very large and, hence, it has a significant probability of being used by a lot of UEs at a given instant). This should be taken into account as the simulator used in this thesis follows a snapshot approach, and should also be

complemented with the fact that services usage is different and is also reflected in the chosen percentages. It is also considered that video streaming is a major candidate to be the future LTE killer service, hence, its highest penetration.

Table 4.4. Traffic mix.

Service	QoS Priority	Minimum throughput [Mbit/s]	Maximum throughput [Mbit/s]	Penetration [%]
Video streaming	1	1.024	8	40
Chat	2	0.064	0.384	5
Web browsing	3	1.024	100	24
FTP	4	1.024	100	9
E-mail	5	1.024	100	5
P2P	6	1.024	100	17

Two major analyses are performed. The first one deals with low load scenarios, which are confronted with results extracted from field measurements, as the network presented a low load at the moment of measurements. Those simulations consider that all UEs are using the same service (FTP), asking for 100 Mbit/s from the network, in order to follow a similar approach to the measurements' one. The other approach deals with high load scenarios, where the traffic mix summarised in Table 4.4 is considered.

Taking the results provided in Section 3.3 into account, 10 simulations are performed for each low load scenario analysis, and 5 for each high load scenario analysis.

4.2 Analysis of Low Load Scenarios

Measurements were collected during several walk-tests performed in the city of Lisbon, in dense urban (centre) and urban (off-centre) areas, being summarised in Annex F. They were done using a laptop connected to a USB dongle (Vodafone Connect Pen K5005, which is manufactured by Huawei) and with an incorporated GPS receiver. Hence, the registration of location information (such as latitude and longitude) associated with the measurements was possible. The UE works with a 2×2 MIMO configuration, but it is internally limited to a peak throughput of 100 Mbit/s (Category 3), which means that the maximum capacity of the network could not be fully exploited. The UE was performing an FTP file download from Vodafone's servers. The measurement software running in the laptop was TEMS Investigation 13.1.33, which created a logfile for each one of the performed routes. Those logfiles were processed afterwards using TEMS Discovery 3.0.2.

During the walk-test, the UE was positioned approximately 1.20 m above the ground, which is considered to correspond to a typical smartphone usage when the voice service is not being considered (which is valid in an LTE scenario, where the traditional voice service is not supported).

The average moving speed was between 3 and 4 km/h. Efforts have been made in order to keep that speed as close as possible to the one that corresponds to an EPA5 scenario, which is considered in the simulations.

The regions where the measurements were carried out were carefully picked, so that it would be possible to have values for the three frequency bands (800 MHz, 1 800 MHz and 2 600 MHz) both in the centre and in the off-centre regions of Lisbon, and to illustrate the irregular nature of the city in the results. One should take into consideration the fact that the available bandwidths were not equal for the three frequency bands – 10 MHz, 15 MHz and 20 MHz were available in the 800 MHz, 1 800 MHz and 2 600 MHz bands, respectively, at the time measurements were done.

When measurements were collected, one could immediately see that services from the LTE network were not being requested by many users. So, the scenario under which measurements were performed is considered to be a low load one. In order to have coherent comparisons between measurements and simulations, that scenario was replicated in the best way possible in the simulator – 100 users are positioned in the city of Lisbon, as this number is considered to represent a compromise between a low number of users to simulate a low loaded network, and a sufficient number of users combined with a sufficient number of simulations in order to ensure statistical relevance.

In order to complement the assessment of the models implemented in the simulator, this section should also be understood as a comparison between measurements and simulations intended to validate the models, taking into account that the choice of the simulation settings and environments is the one that is able to provide the best approximations to the measurements results. Comparisons are essentially based on received power, SINR, number of allocated RBs and UEs' throughput, which are presented for the six different environments under study: DU_800, DU_1800, DU_2600, U_800, U_1800 and U_2600, where DU stands for Dense Urban (applied in the centre of Lisbon), U stands for Urban (applied in the off-centre of Lisbon) and 800, 1800 and 2600 are summarised descriptions of the 800, 1 800 and 2 600 MHz bands, respectively. Relative errors between measurements and simulations computed using (3.24) can be seen in Table 4.5. One can conclude that negative variations refer to cases where measured values are above values obtained via simulation, and positive values refer to the opposite case. Also, it can be seen that most of the highest deviations occur for the 800 MHz band.

Table 4.5. Relative errors between measured and simulated average values for different parameters and different environments.

Parameter	DU_800	DU_1800	DU_2600	U_800	U_1800	U_2600
Received Power [%]	-2.85	-4.79	2.93	14.95	-1.98	-0.06
SINR [%]	-30.73	6.63	-25.50	-26.98	11.60	17.27
Number of RBs [%]	-23.70	-12.88	-12.38	-17.75	-10.30	-11.58
Throughput [%]	-32.50	-6.02	-14.52	-40.79	5.06	3.22

As it is expected, and seen in Figure 4.1, the received power tends to decrease with the increase of

the frequency band, as the transmitter output power per RB decreases and path loss increases with the frequency band. Although the total transmitter output power does not decrease with the frequency band in every case, the number of available RBs (i.e., bandwidth) in each frequency band increases, so that one has a decrease in the power per RB. Most measured values are within the ranges defined by the simulated ones' standard deviations – however, and taking also Table 4.5 into account, the average received power for the U_800 environment shows a relative error of 14.95%, which suggests that, in this particular environment, LoS occurrence during measurements was very high, and possibly higher than the one considered in the simulations, which results in a higher received power. However, it is considered that LoS occurrence, on average along the entire centre/off-centre of Lisbon, is considered in a realistic way in the simulator, as absolute deviations between measured and simulated received powers for the other environments are lower than 5%. In any case, it should be noted that the irregular nature of the city of Lisbon's terrain is not included in the simulator.

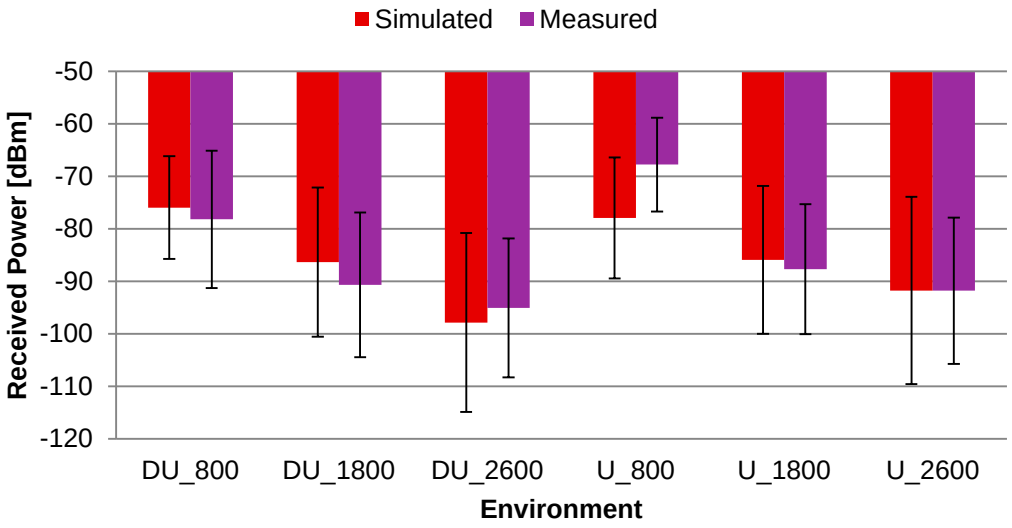

Figure 4.1. Received power for each of the environments obtained for simulations and measurements.

The behaviour of the SINR along the different frequency bands is different between simulations and measurements (although most measured values are within the standard deviation's ranges of simulated ones): instead of always decreasing with the frequency band, because of a lower received power, as it happens in measured values, the SINR obtained via simulations is lower than expected in the 800 MHz band, as one can see in Figure 4.2. This is because interference is not negligible in this simulated scenario, even when a relatively low number of users is placed in the network, and shows that this band may be the one with the highest interference problems. Measurements did not show this behaviour, probably because there were no other users using this spectrum, as it corresponds to the lowest priority one – if users try to connect to the network, they are first connected to the frequency bands that offer more capacity, such as the 2 600 MHz one, followed by the 1 800 MHz band. Only when the 800 MHz band does not co-exist with others in space, users are able to use it with the highest priority. In measurements, it was necessary to block the UE to the 800 MHz band, via software, in order to be able to perform measurements in that scenario. SINRs obtained via simulation also show higher standard deviations, because interference is not negligible in this case. Table 4.5

also shows that most deviations between measurements and simulations for the SINR are relatively high, which also suggests that the existence of interference in the simulations is higher and has a huge impact on the results.

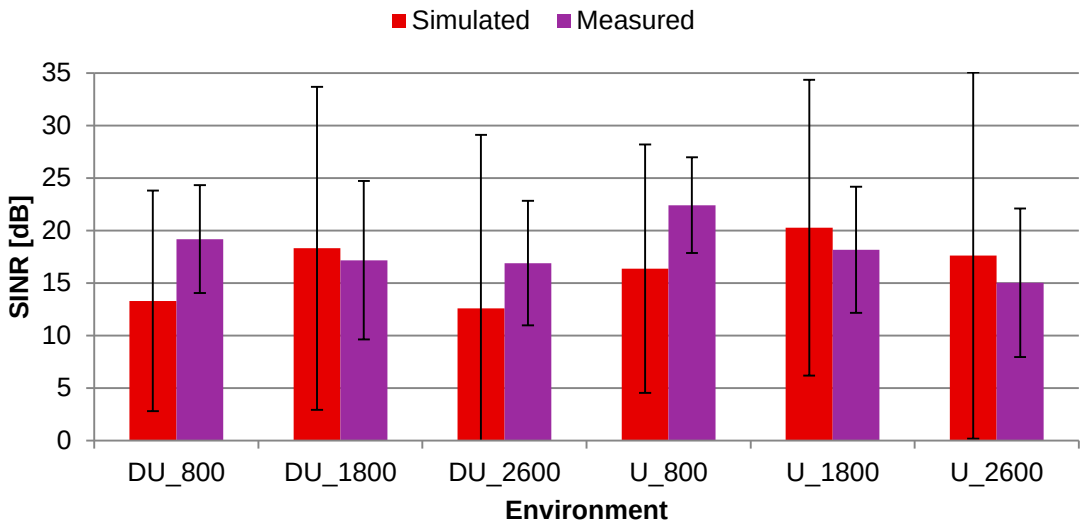

Figure 4.2. SINR for each of the environments obtained for simulations and measurements.

Figure 4.2 also shows that SINR in the off-centre of Lisbon tends to be higher than in the centre. This happens because inter-site distance in the off-centre is, on average, higher, and received power also tends to be higher (Figure 4.1).

Most of the measured values for the number of RBs are within the standard deviation's ranges of those obtained via simulation, as it is illustrated in Figure 4.3. However, there is a significant difference between the measured and the simulated number of RBs in the 2 600 MHz band, which has a practical explanation: less efficient transmission modes took place during measurements (this information was not recorded, but was checked during measurements), while simulations consider that 2×2 MIMO can always be used in DL, which is not a completely true assumption (e.g., receiver diversity can be exploited instead). As the network was not very much loaded, the UE used in the measurements was able to use all the 100 RBs almost every time in the 2 600 MHz band. As this high number of RBs is not necessary in order to achieve the peak throughput of 100 Mbit/s when good channel conditions exist, less efficient transmission modes take place, which may happen because of power consumption issues.

Taking also Table 4.5 into account, one can see that there are relatively high differences between the measured and the simulated average number of RBs, especially in the 800 MHz band. Since the network load was very low at the time measurements were performed, the UE was able to use all the necessary bandwidth almost every time. In the simulations, there were cases where two or more UEs were connected to the same sector, which meant that resources had to be shared among more than one UE. An example of this situation can be seen in Figure 4.4, where one can check that, for one of the five simulations of the DU_1800 environment, UEs either use 75 or 37 RBs, the latter being used when the same sector is serving two UEs, while in measurements, the maximum available bandwidth

was used almost every time. This leads to an average in the simulations lower than the measurements one, as well as a higher standard deviation (which happens in most cases).

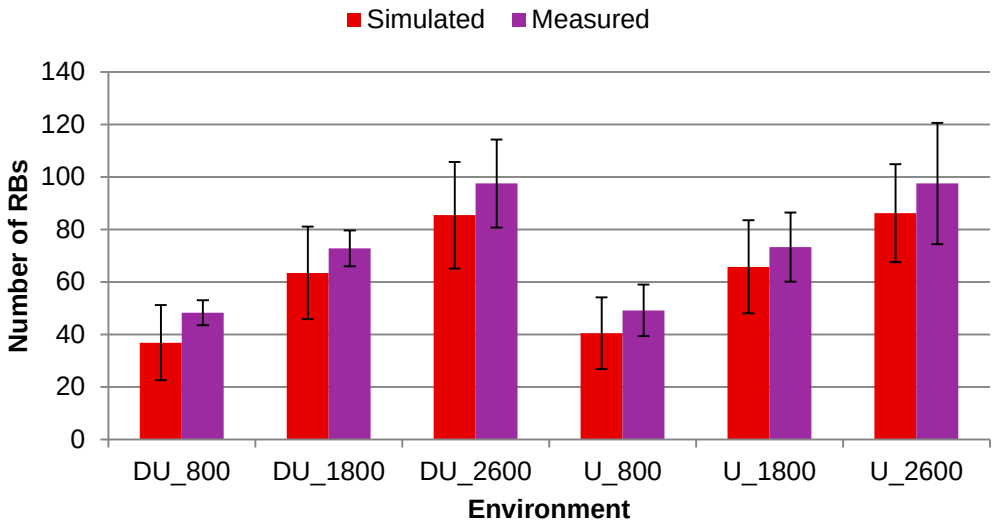

Figure 4.3. Number of RBs for each of the environments obtained for simulations and measurements.

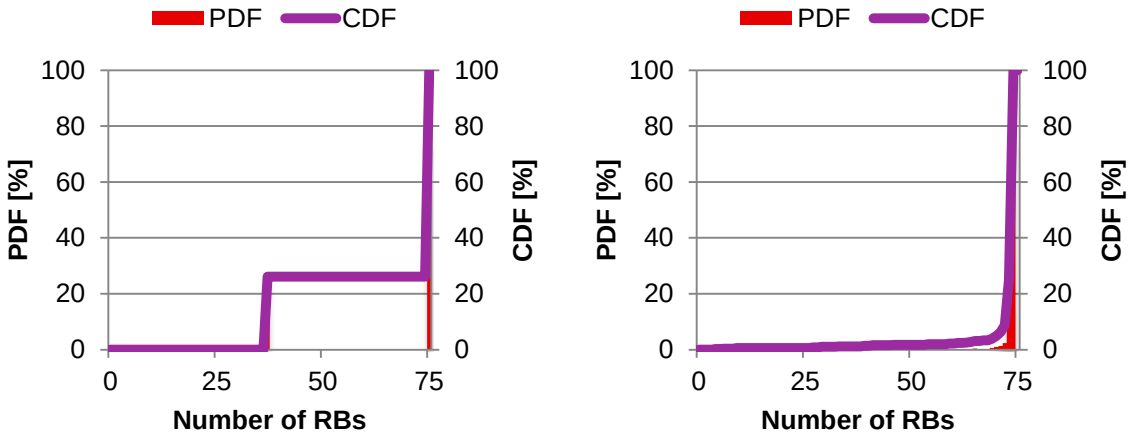

(a) Simulations (b) Measurements

Figure 4.4. PDF and CDF of the number of RBs for the DU_1800 environment obtained for simulations and measurements.

Average UEs' throughput is illustrated in Figure 4.5, for measurements and simulations and for each environment. As expected, the higher the frequency band the higher the average throughput is, as available bandwidth also increases with the frequency band. Results are according to previously discussed behaviours concerning received power, SINR and number of allocated RBs, and most measured values are within the range of the ones obtained via simulation. Taking Table 4.5 into account, one can check that the highest deviations take place for the cases where the highest deviations for the SINR and number of RBs exist, which makes sense as those factors have a strong influence on the obtained throughput. The highest difference happens in the 800 MHz band, because of previously discussed interference occurrences. As it was also previously referred, there were cases in the simulations where more than one UE was being served by the same sector, which means that

resources had to be shared among more than one UE.

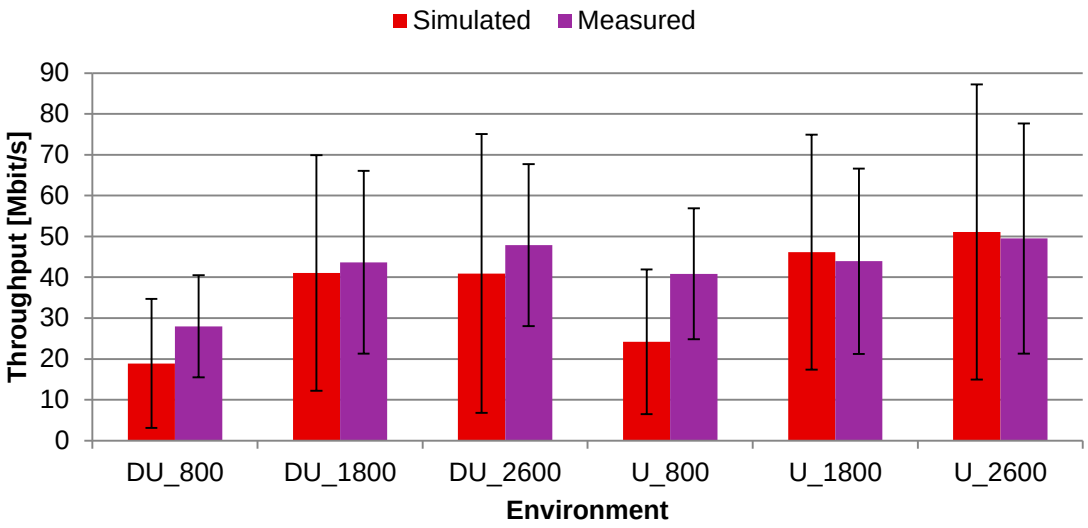

Figure 4.5. UE's throughput for each of the environments obtained for simulations and measurements.

Taking Annex C into account, where it can be seen that the validity of the propagation model used does not cover the 2 600 MHz band, one would expect to see high differences between measured and simulated results in this particular case. However, those differences are not very high, which means that the expected high deviation between measurements and simulations in that case is not sufficient to make results unrealistic.

One can also see that, although the model used to determine the probability of LoS for each UE is not ideal, especially because it does not account for the frequent NLoS condition that occurs when proximity to the building's façade is extremely high, it does enable realistic results in most cases.

It should also be noted that the number and position of the BSs considered in the simulations may not correspond to the real Vodafone network, especially for the 800 and 1 800 MHz bands case, because the assumptions taken in Section 3.2 may not be the best ones. Also, although it is considered that coverage in every band is provided along the entire city of Lisbon, this may not happen in reality.

Differences between measurements and simulations can also happen because the dimension of those two scenarios is different: measurements where performed in particular areas of the environments under study, whereas simulations take the entire city of Lisbon into account. Also, as measurements for different frequency bands were carried out in the same areas almost every time, particular characteristics of a given area were reflected in the results of more than one case. Slight variations may also be due to the fact that slow fading is stochastic in real life, whereas simulations consider it to be a constant margin.

Further studies of interference, done in the next section, may also be somehow unrealistic in some cases because the pointing direction of each sector antenna does not change from BS to BS, which does not happen in a real deployment, where sector antennas' orientation should take into account the characteristics of the particular area they are supposed to cover. It is also considered that each BS

has three sector antennas, which does not happen everywhere.

4.3 Analysis of High Load Scenarios

In this section, a detailed study of the reference scenario is performed, being followed by results obtained for the 800, 1 800 and 2 600 MHz bands after the variation of the following parameters: electrical and mechanical downtilts, height of the BS antennas and transmitter output power.

Most provided decision enabling metrics are related to the number of UEs per sector, SNR/SINR of the served UEs, and UEs' throughput. Most of those values are presented for two cases: neglecting interference and taking interference into account. It should be noted that, when values neglecting interference are presented, they refer to characteristics experienced only by the UEs that are still served after the inter-cell interference analysis takes place – an exception happens for the number of UEs per sector, as in this case, all users served when only coverage and capacity is considered are analysed.

4.3.1 Reference Scenario

For the reference scenario, the generation of 14 000 users in the users' generation module is considered. Not all of them end up being thoroughly analysed, as some of those users are placed out of the city of Lisbon, and not all of them are covered by the network. Also, those users are split into centre and off-centre regions, which are classified as dense urban and urban environments, respectively, having different characteristics worth exploiting. No mechanical downtilt is considered in the reference scenario – however, an electrical downtilt of 5° is considered.

The number of served UEs per sector is illustrated in Figure 4.6. One can see that the lower the frequency band, the higher the number of UEs served, when interference is not considered. This happens because the lower the frequency band, the higher is the sector antenna's range, as one can conclude from Figure 4.7. Inter-cell interference impact, in this particular case, can be understood as the number of UEs who end up not being served due to inter-cell interference. It can be seen that it decreases with the frequency band and from the centre to the off-centre – in the urban environment, users' density tends to be lower, as well as the BSs' density, making this case less prone to interference. In the 800 MHz band, around 80% of the users served when only coverage and capacity is considered are strongly affected by interference from neighbouring sectors/BSs, being unable to perform their requested service with a throughput above the minimum one. In the 1 800 MHz and 2 600 MHz bands, around 60 to 70% and 50% of the UEs, respectively, end up being delayed because of interference issues.

The sector antenna's range, being defined as the distance of the farthest UE served by its serving sector antenna, illustrated in Figure 4.7, is defined not only by the path loss (which increases with the frequency band), but also by the inter-site distance (which decreases with the frequency band). So,

the behaviour shown via simulation is according to the expected one.

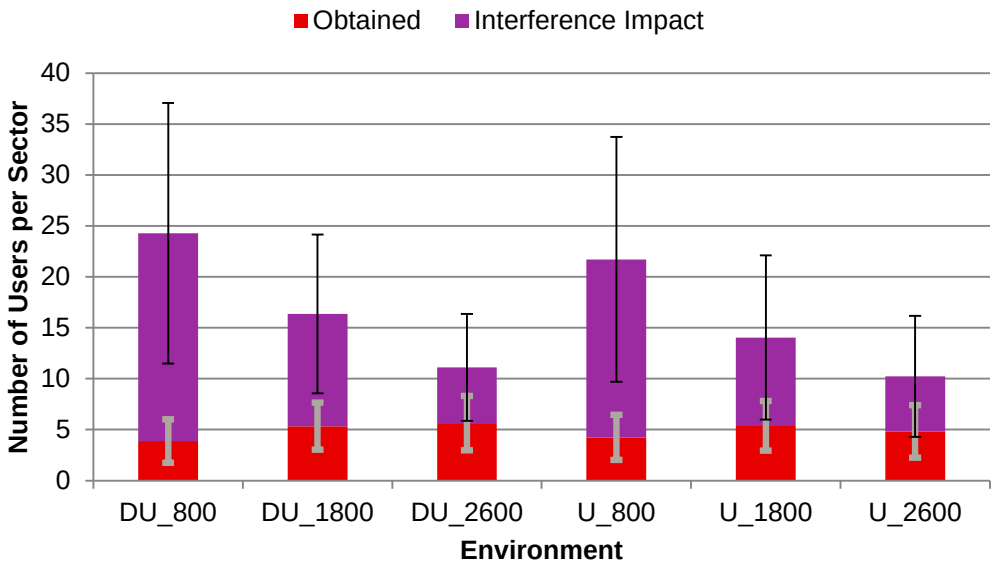

Figure 4.6. Number of served UEs per sector for each of the environments.

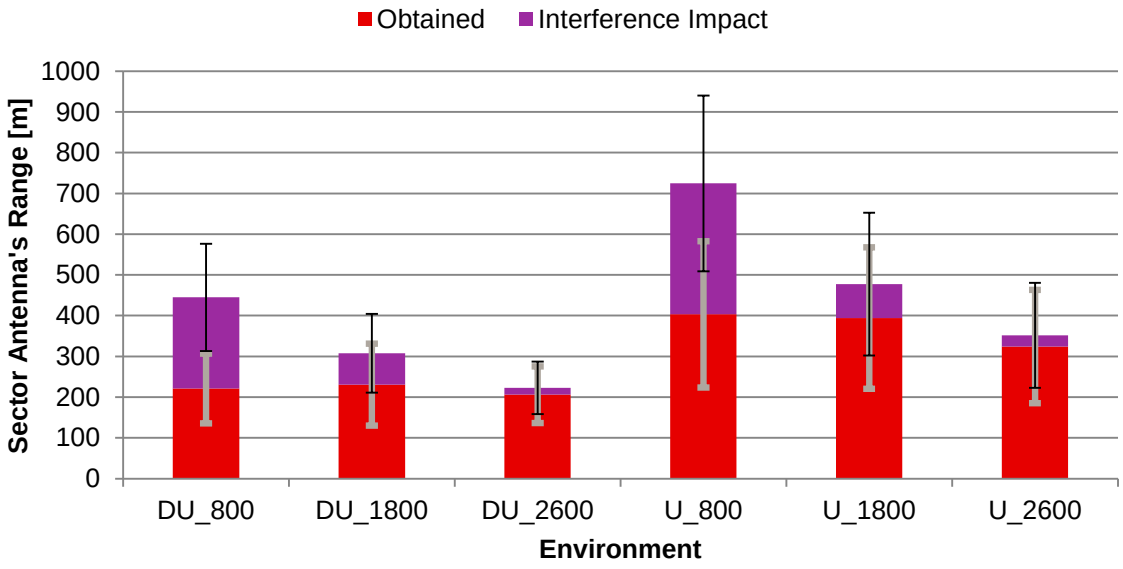

Figure 4.7. Sector antenna's range for each of the environments.

A representation of the UE's average SNR and SINR is provided in Figure 4.8. One can observe that SNR and SINR decrease with the frequency band, as the average received power also decreases. It can also be seen that inter-cell interference impact is greater for the 800 MHz band, which means that, although the received power is the highest, interference coming from neighbouring cells is also higher, leading to a higher reduction of SNR into SINR. From the average values computed for each of the environments, one can talk about an interference margin that can be used to represent inter-cell interference impact on studies about high load scenarios that deal with parameters close to the ones specified in Section 4.1. For each of the studied environments, that interference margin is represented in Table 4.6.

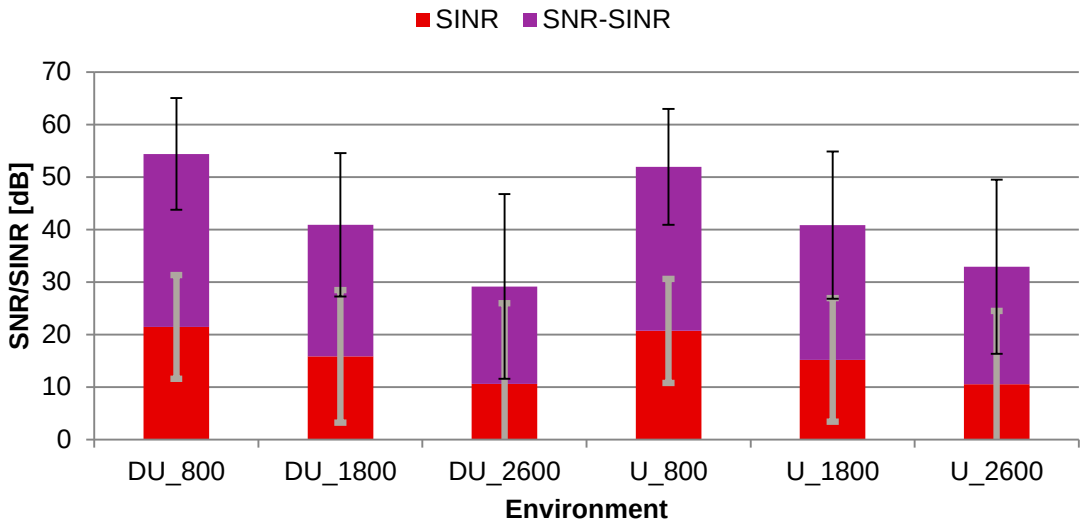

Figure 4.8. UE's average SNR/SINR for each of the environments.

Table 4.6. Interference margin as the difference between SNR and SINR for different environments.

Parameter	DU_800	DU_1800	DU_2600	U_800	U_1800	U_2600
SNR [dB]	54.39	40.90	29.14	51.92	40.85	32.91
SINR [dB]	21.44	15.82	10.61	20.69	15.16	10.55
Interference margin [dB]	32.95	25.08	18.53	31.23	25.69	22.36

The SNR/SINR behaviour along the frequency bands does not match the one obtained for the throughput, which is shown in Figure 4.9. This is because, although throughput depends strongly on the SINR, it is also influenced by the available number of RBs, which is different for each frequency band. Capacity increases with the frequency band, taking the reference scenario into account, so although a higher number of users is served the lower the frequency band is (Figure 4.6), they are served with a lower throughput, when only coverage and capacity are analysed.

Figure 4.9 also shows an expected behaviour: in a system characterised by the existence of UEs in either LoS or NLoS conditions, different distances from the serving sector, and asking for different types of services, standard deviations for the UEs' throughput are relatively high. This means that throughput distribution along each sector is not uniform, as one can check in Figure 4.10 for the U_2600 case (which presents the highest standard deviation). Most of the UEs are served with a throughput close to the minimum stipulated for each service (five of the six services have 1.024 Mbit/s as the minimum) – around 90% of the UEs obtain throughputs below 8 Mbit/s. Surprisingly, one can see that there is one UE being served with around 100 Mbit/s, which can occur in a sector where no more UEs are requesting resources, and the UE is experiencing good channel conditions – in fact, it was verified that this particular UE is not strongly affected by interference from neighbouring sectors.

The traffic mix represented in Table 4.4 was considered in all the simulations regarding the high load scenario. Figure 4.11 shows the percentage of UEs requesting and being served each of the six services considered, for the U_2600 case. Services are sorted by their priority, and one can conclude

that the percentage of UEs served does not match the percentage of UEs requesting a certain service. This happens because not all UEs requesting the service end up being covered by the network, but most importantly because not all services ask the network for the same throughput: although video streaming and chat are the highest priority services, they ask for much lower throughputs than the other services. Hence, its actual priority ends up being different, because resource distribution takes into account both the QoS priority and the throughput UEs are asking for, and considers that UEs which do not meet a certain minimum throughput are delayed. So, video streaming and chat end up being the services where serving percentage is below the requested one.

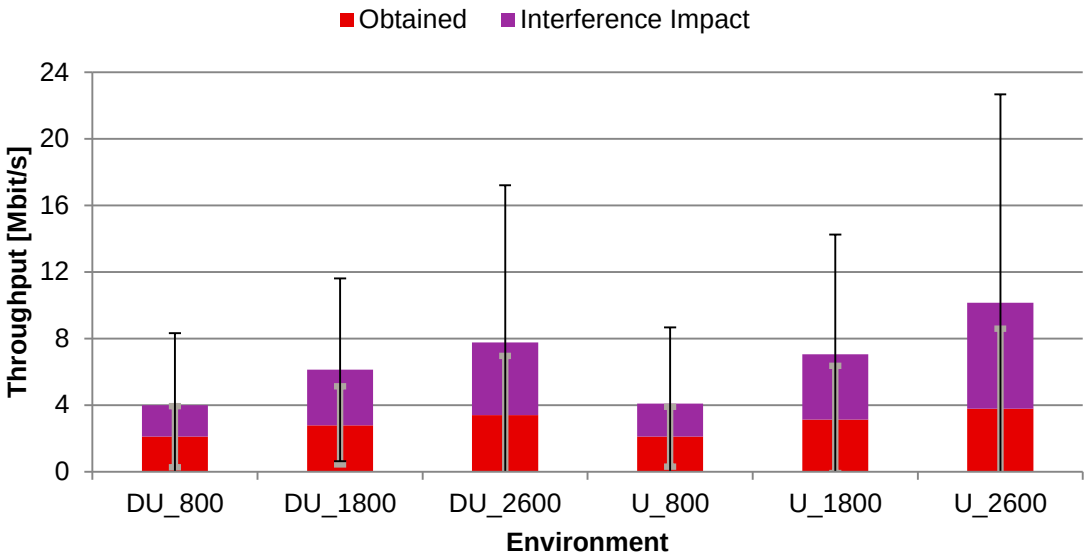

Figure 4.9. UEs' throughput for each of the environments.

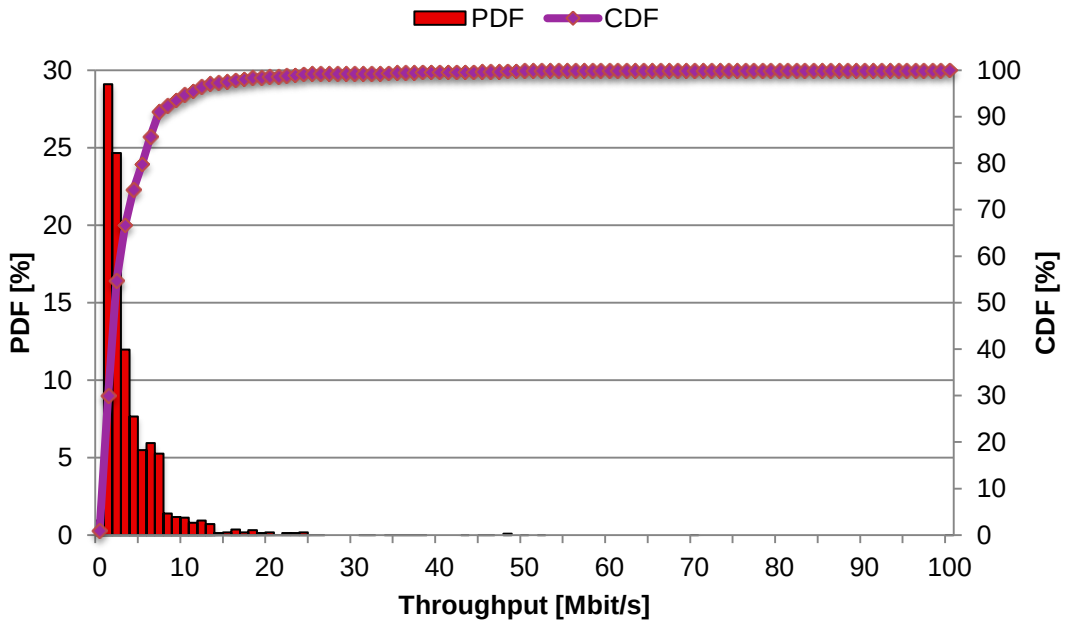

Figure 4.10. PDF and CDF of the UE's throughput for one of the simulations of the U_2600 case.

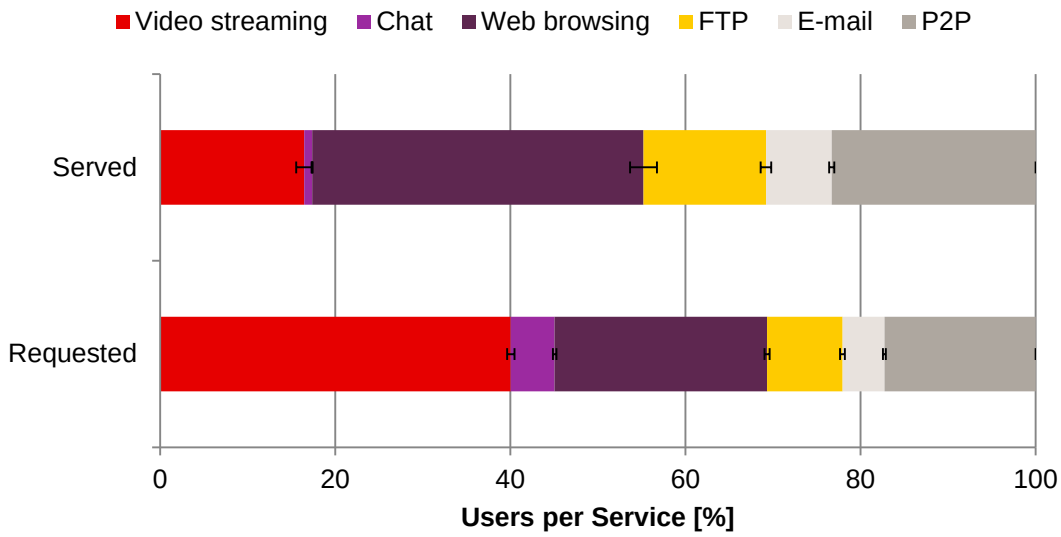

Figure 4.11. Percentage of UEs requesting and being served each of the services considered.

4.3.2 Electrical Downtilt

For the study of the electrical downtilt that minimises the inter-cell interference impact in each of the frequency bands, angles from 1° to 11° were studied, with a step of 2° between consecutive analyses. So, 1°, 3°, 5°, 7°, 9° and 11° electrical downtilt values were used to check system performance. Those values were chosen taking into account that the downtilt range of the considered antenna (Table 4.3) should not be much exceeded – it is, however, because one considers that different antennas able to provide higher electrical downtilts could be used instead.

Performance is evaluated in terms of number of served UEs per sector, average UEs' SNR/SINR and UEs' obtained throughputs. It is worth noticing that average UEs' SNRs only take into account the UEs that are still considered to be served after the inter-cell interference analysis – values for the UEs that end up not being served do not contribute for that average computation. For all the analyses that deal with parameters' variations, it was checked that the number of active sectors tends to be constant over all simulations, hence, the validity of the usage of the number of active UEs per sector.

Figure 4.12 and Figure 4.13 show the number of UEs per sector after the inter-cell interference analysis takes place for the centre and off-centre of Lisbon, respectively. It can be seen that the higher the frequency band, the sooner (in terms of lower electrical downtilt angles) and stronger a performance enhancement happens for most cases, which can be explained by the fact that the vertical half-power beamwidth decreases with the frequency band. The narrower the vertical radiation pattern, the higher the effect of downtilt variations is, as (3.11) shows.

Taking the results into account, one can conclude that an electrical downtilt of 7°, 5° and 3° for the 800, 1 800 and 2 600 MHz bands, respectively, enable the highest number of served UEs per sector, on average. This happens for both the centre and the off-centre of Lisbon, except for the 800 MHz band case – the optimal electrical downtilt for the off-centre of Lisbon is 9° instead. The increase on the number of UEs per sector, comparing with the reference scenario, are of 1.3%, 0.0% and 1.2% on

average for the 800, 1 800 and 2 600 MHz bands, respectively, for the centre of Lisbon. For the off-centre, one has an increase of 5.2%, 0.0% and 1.9%. One should take into account that, if a different electrical downtilt step was considered, results could be slightly different.

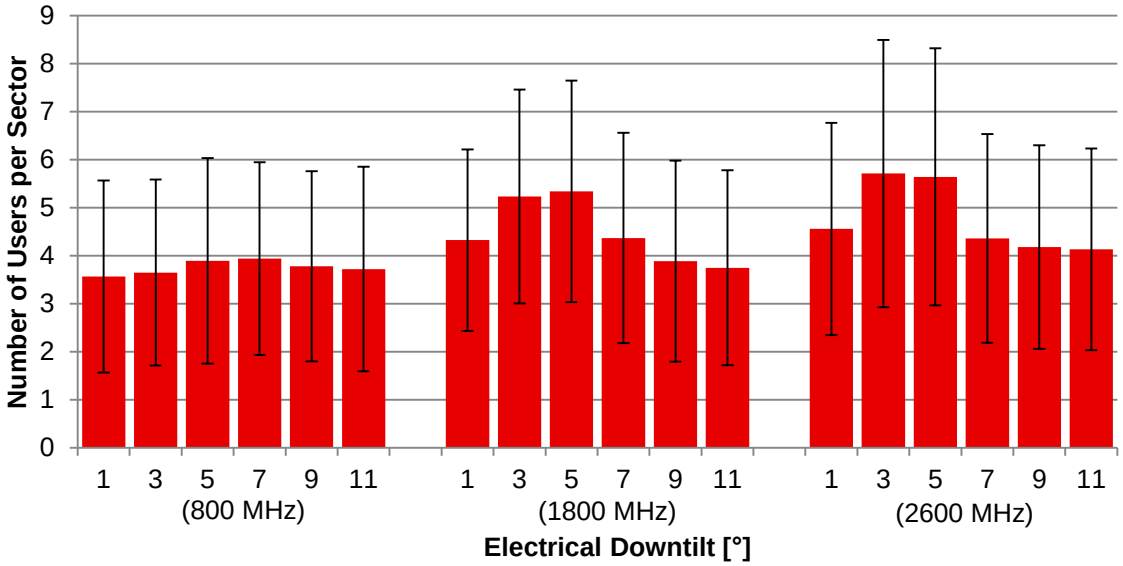

Figure 4.12. Number of served UEs per sector for different electrical downtilt values, different frequency bands and for the centre of Lisbon.

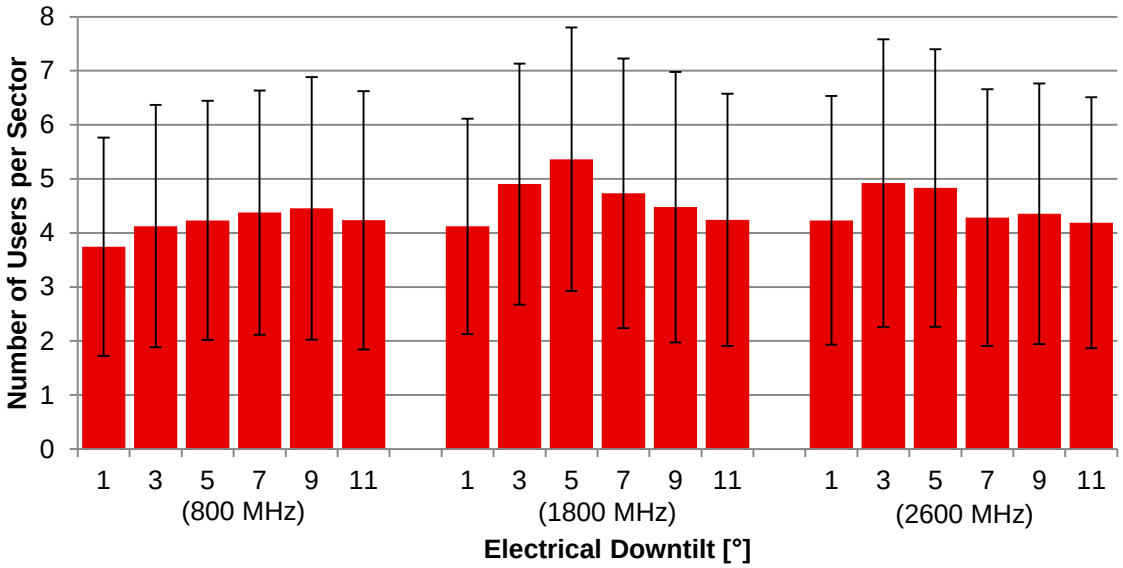

Figure 4.13. Number of served UEs per sector for different electrical downtilt values, different frequency bands and for the off-centre of Lisbon.

The optimal values may seem relatively low, but taking into account that most UEs are in NLoS conditions, especially UEs at the cell-edge (as LoS probability for a given UE decreases with distance, as shown in (3.3)), it is expected that the effect of electrical downtilt is also a function of the buildings' and BS antennas' height (vertical angle for the radiation pattern is calculated using (3.13) for NLoS conditions), hence, the relatively low value of electrical downtilt taken as the optimal one. This can also be concluded by taking into account the differences between the centre and the off-centre

environments: in off-centre, where the difference between BS antennas height and building's height is higher, there seems to be a performance enhancement for higher electrical downtilts (as it happens for the 800 MHz case).

The evolution of the SNR and SINR along variations on the electrical downtilt for the three frequency bands and for the centre and off-centre of Lisbon is summarised in Figure 4.14 and Figure 4.15, respectively. The interference margin, i.e., the difference between SNR and SINR, decreases with the electrical downtilt, on average, which makes sense, taking into account that a growing electrical downtilt leads to a lower received power for UEs far from the cell-centre – this means that UEs from neighbouring sectors tend to receive less interference power.

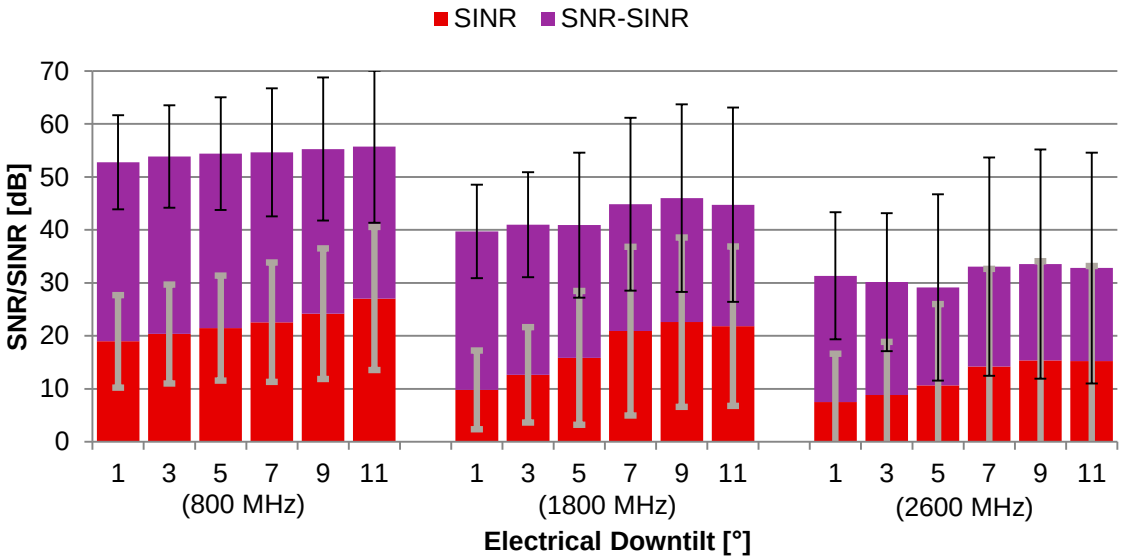

Figure 4.14. UEs' average SNR/SINR for different electrical downtilt values, different frequency bands and for the centre of Lisbon.

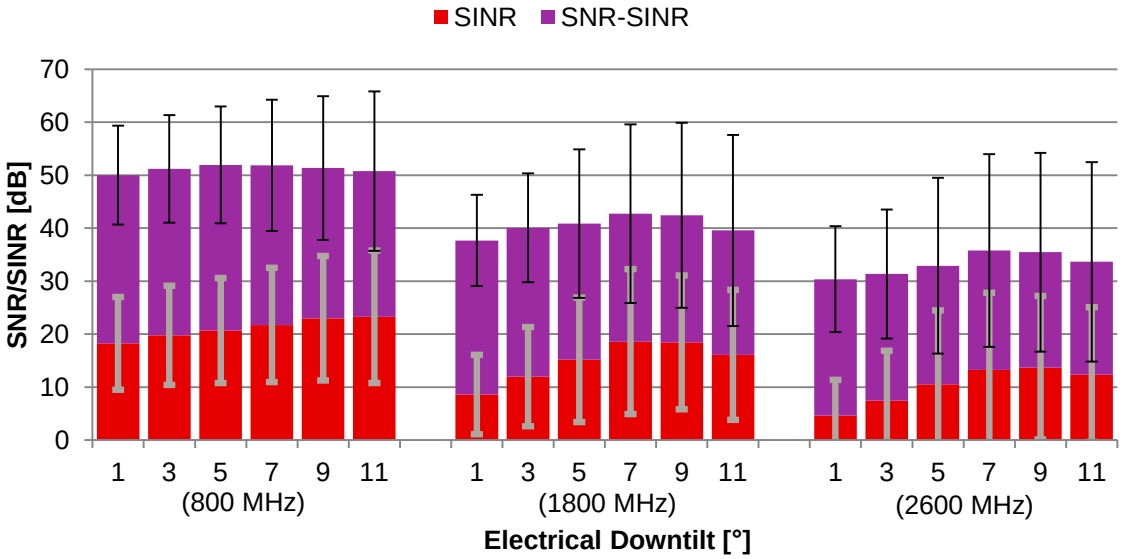

Figure 4.15. UEs' average SNR/SINR for different electrical downtilt values, different frequency bands and for the off-centre of Lisbon.

For the 1 800 and 2 600 MHz bands, an electrical downtilt of 9° maximises the SINR, on average, for the centre of Lisbon. On the other hand, for the off-centre of Lisbon, an electrical downtilt of 7° is the one that maximises SINR for the 1 800 MHz band, while the best value for the 2 600 MHz band case is the same as for the centre. The optimal value for the 800 MHz band, taking into account the electrical downtilt range studied, is 11° both for the centre and the off-centre of Lisbon. Optimal values for the SINR in the centre of Lisbon assume higher values than those of the off-centre, which can be explained by the higher BSs' density – this means that UEs tend to be closer to its serving sector antenna, as there are more BSs/sectors per square meter. Assuming that the antennas have implemented the optimal electrical downtilt for each case, the radiation pattern gain combined with a higher proximity to the serving sector antenna leads to an increase in the received power for the centre of Lisbon, which seems to be higher than the effect of inter-cell interference, because of the higher SINR.

Figure 4.16 and Figure 4.17 show UEs' throughput along the electrical downtilt for the three frequency bands and for the centre and off-centre of Lisbon, respectively. The behaviour similar to the one seen for the SINR is visible, as throughput depends on the SINR available at the UE's receiver. However, it also depends on the number of RBs that can still provide throughput (some of the RBs are unable to provide capacity to the UE because of high levels of interference), hence, some differences found between the trends of the two parameters.

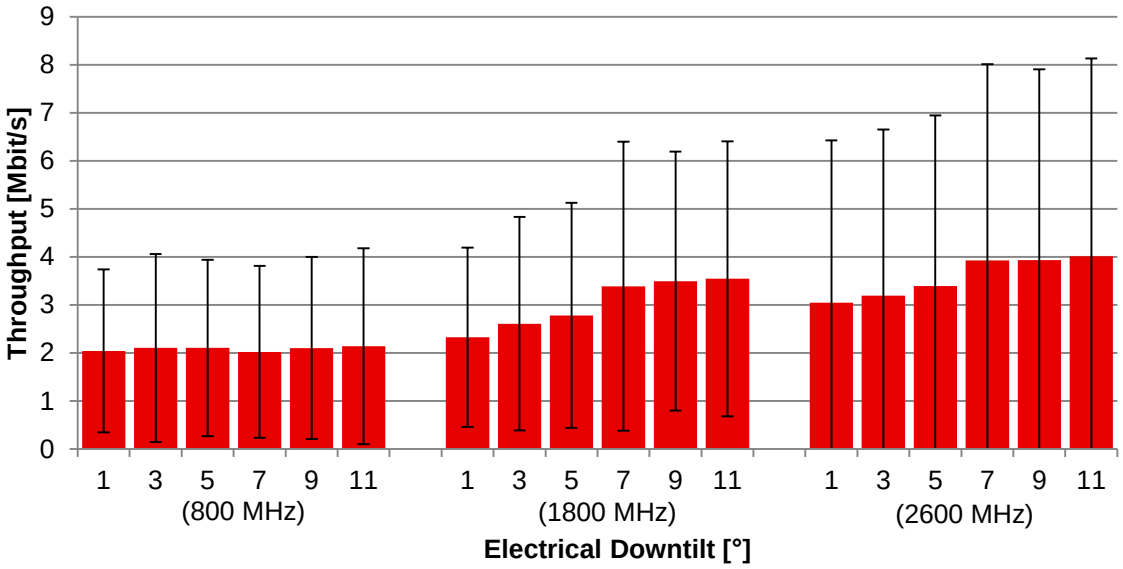

Figure 4.16. UE's throughput for different electrical downtilt values, different frequency bands and for the centre of Lisbon.

Taking average values for the UEs' throughput into account, one can see that optimal performance is achieved for 11° of electrical downtilt for the three frequency bands and for the centre of Lisbon, with performance enhancements of 1.9%, 27.3% and 18.9% for the 800, 1 800 and 2 600 MHz bands, respectively. For the off-centre of Lisbon, 11°, 9° and 9° of electrical downtilt enhance throughput for the 800, 1 800 and 2 600 MHz bands, respectively, by 4.3%, 17.2% and 20.4%.

Performance improvements achieved with optimal electrical downtilts over the reference scenario are

summarised in Table 4.7.

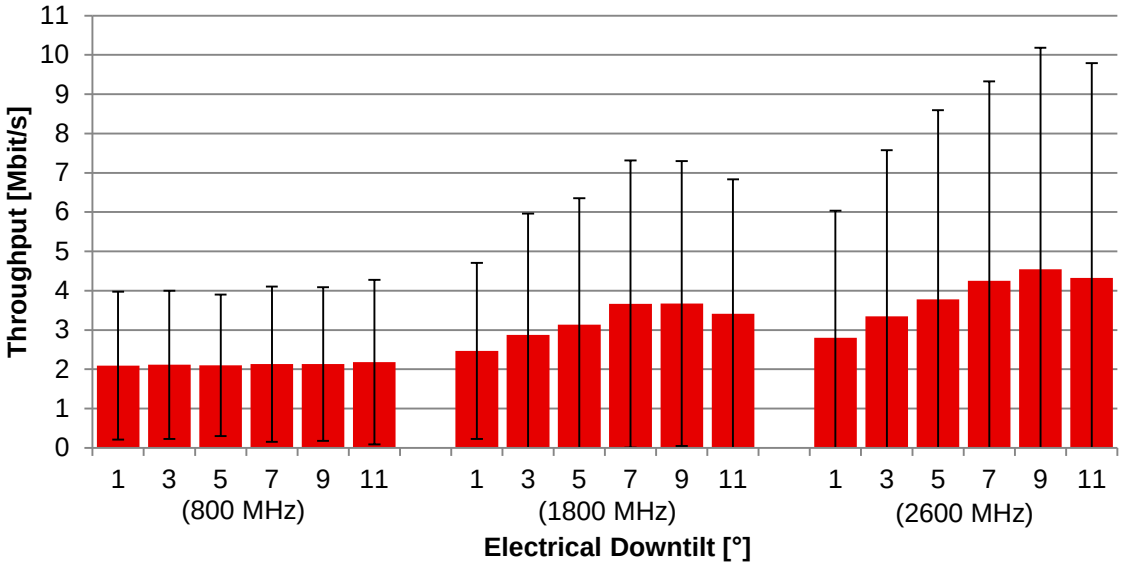

Figure 4.17. UE's throughput for different electrical downtilt values, different frequency bands and for the off-centre of Lisbon.

Table 4.7. Performance improvements over the reference scenario achieved using optimal electrical downtilt values for each environment.

Parameter	DU_800	DU_1800	DU_2600	U_800	U_1800	U_2600
Number of UEs per sector [%]	1.3	0.0	1.2	5.2	0.0	1.9
Throughput [%]	1.9	27.3	18.9	4.3	17.2	20.4

4.3.3 Mechanical Downtilt

Instead of using an electrical downtilt of the antennas, one now considers a mechanical downtilt. This has particular relevance taking into account the differences that exist at the radiation pattern level for the two types of downtilt, as illustrated in Figure 3.3. However, most of the achieved results can be interpreted in the same way as those of the electrical downtilt.

In the following analysis, electrical downtilt is considered to be 0°, while mechanical downtilt changes from 1° to 11°, with a step of 2°, as it was done for the previous scrutiny concerning electrical downtilt.

Taking average values into account, from Figure 4.18 and Figure 4.19, one can present optimal mechanical downtilt values for the highest number of served UEs per sector: 3°, 5° and 5° for the 800, 1 800 and 2 600 MHz bands in the centre of Lisbon (with improvements of -0.5%, -3.2% and 2.5% over the reference scenario), respectively, and 7°, 5° and 3° for the 800, 1 800 and 2 600 MHz bands for the off-centre of Lisbon (with enhancements of 3.3%, -4.5% and 1.0%). Not all of those optimal values of angles correspond to the ones obtained for the electrical downtilt, which is explained by the different deformations the radiation pattern suffers with the increase of the electrical or mechanical downtilts.

Figure 4.20 and Figure 4.21 show the SNR/SINR obtained for the three frequency bands and for the centre and off-centre environments, respectively. Considering the interference margin as the difference between the SNR and the SINR, it can also be seen that it decreases with the mechanical downtilt. In order to obtain optimal performance in this case, i.e., highest SINR, one should consider 11°, 9° and 11° of mechanical downtilt for the 800, 1 800 and 2 600 MHz bands, respectively, in the centre of Lisbon, and 11°, 7° and 9° for the same frequency bands but in the off-centre of Lisbon. It should also be noted that if a different range and step of mechanical downtilts was considered instead, optimal values could be different.

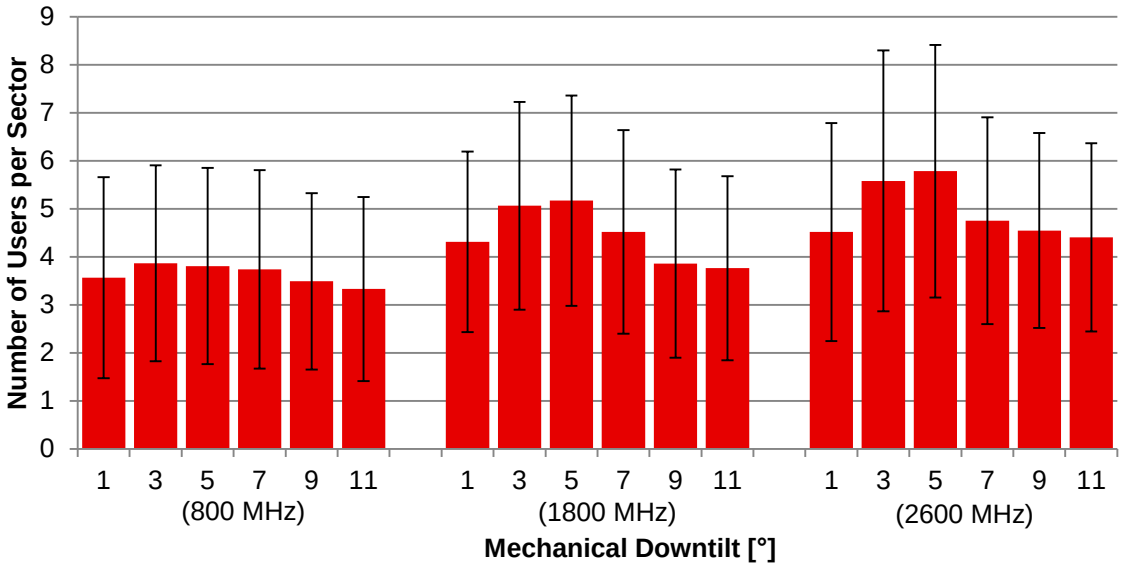

Figure 4.18. Number of served UEs per sector for different mechanical downtilt values, different frequency bands and for the centre of Lisbon.

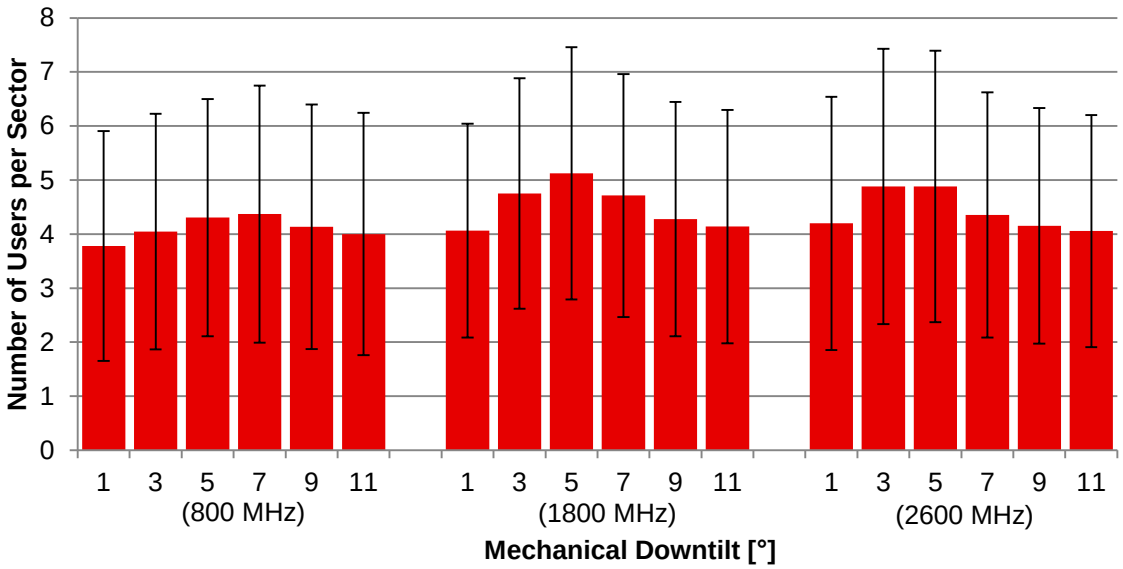

Figure 4.19. Number of served UEs per sector for different mechanical downtilt values, different frequency bands and for the off-centre of Lisbon.

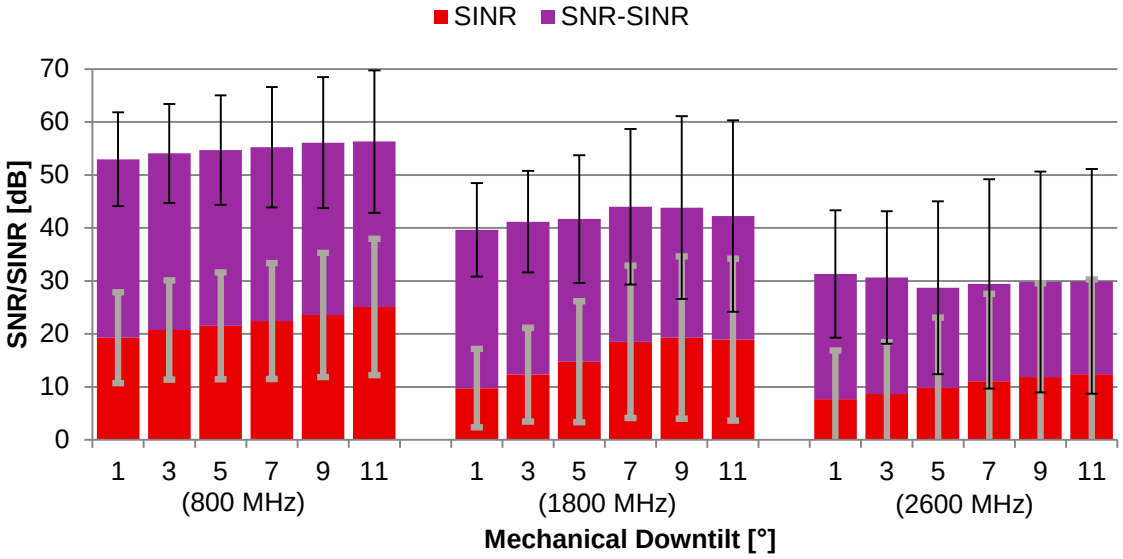

Figure 4.20. UEs' average SNR/SINR for different mechanical downtilt values, different frequency bands and for the centre of Lisbon.

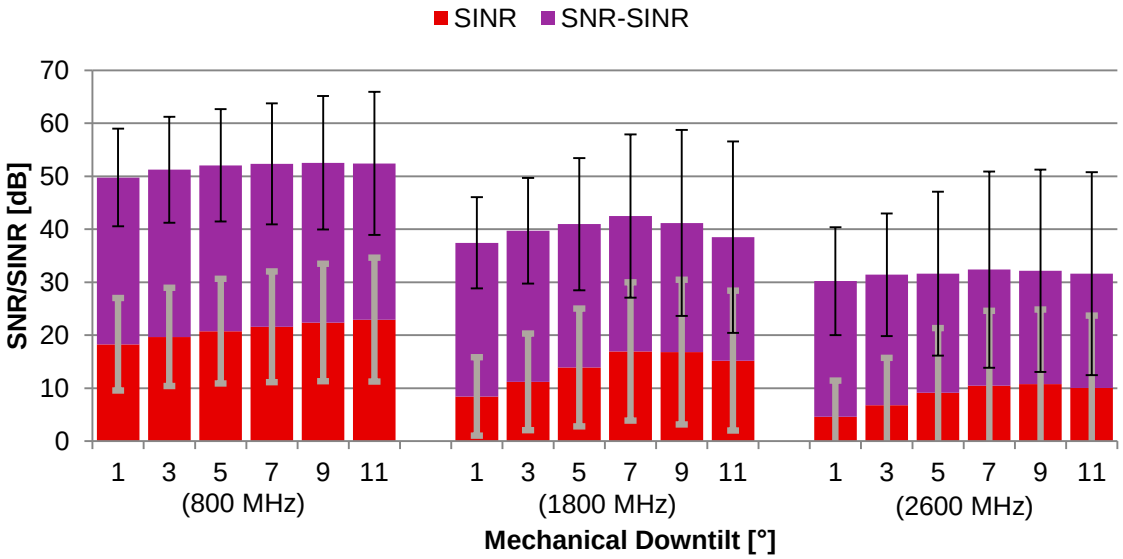

Figure 4.21. UEs' average SNR/SINR for different mechanical downtilt values, different frequency bands and for the off-centre of Lisbon.

Concerning throughput, one cannot exactly see from Figure 4.22 which is the optimal value for the 800 MHz band in the centre of Lisbon. Taking the standard deviation ranges into account, 11° is picked as the best option, which shows -1.0% improvement over the reference scenario (being negative, it represents a worse case). For the 1 800 and 2 600 MHz bands, 9° and 11° are the optimal values for the mechanical downtilt, respectively, in the centre of Lisbon (enabling performance gains of 18.0% and 10.9%). For the off-centre, and taking Figure 4.23 into account, 11°, 7° and 9° are the optimal mechanical downtilts for the 800, 1 800 and 2 600 MHz bands – which increase performance by 4.8%, 10.8% and 5.0%, comparing to the reference scenario. Again, the different deformations the radiation pattern suffers depending on whether electrical or mechanical downtilts are considered justify the different values for the optimal performance between electrical and mechanical downtilt analyses.

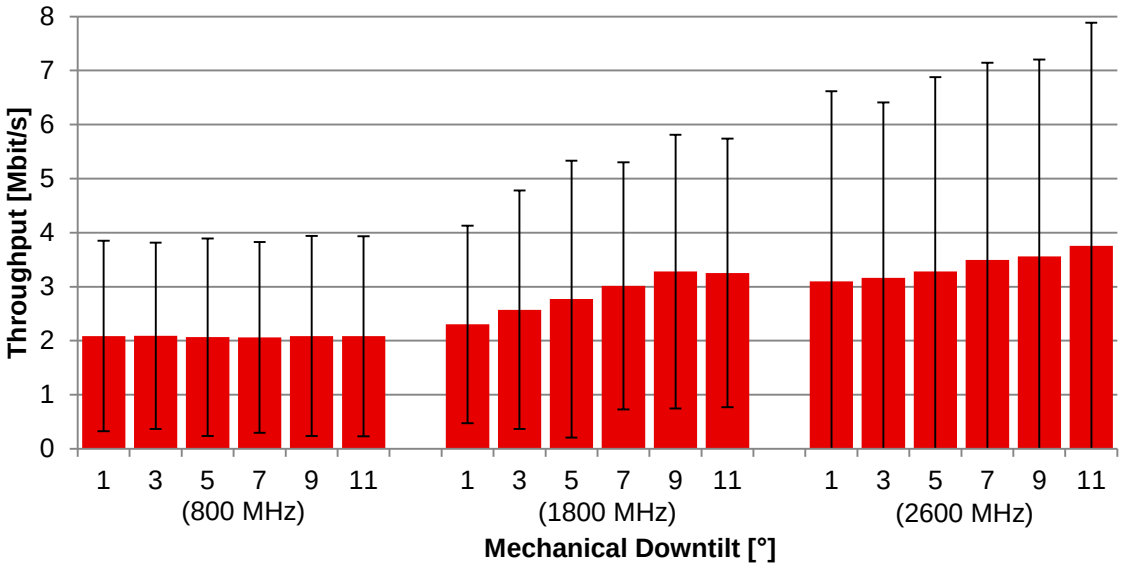

Figure 4.22. UE's throughput for different mechanical downtilt values, different frequency bands and for the centre of Lisbon.

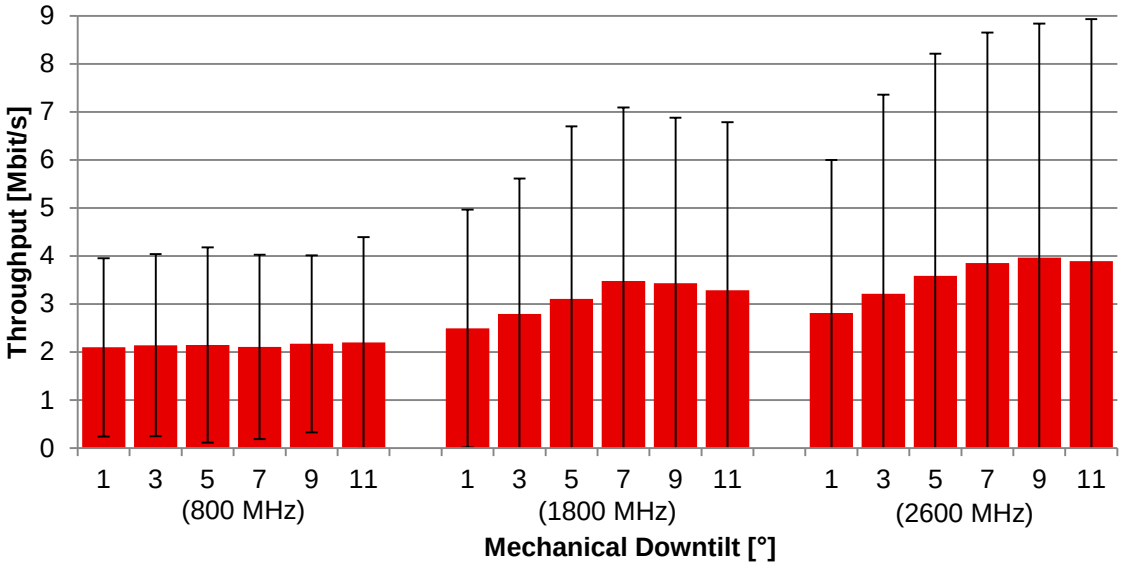

Figure 4.23. UE's throughput for different mechanical downtilt values, different frequency bands and for the off-centre of Lisbon.

Table 4.8 summarises the different performance improvements in terms of number of served UEs per sector and throughputs achieved using optimal mechanical downtilts for each environment. As for the electrical downtilt case, one should take into account that the presented values should be considered with caution, as the standard deviations of those parameters assume relatively high values. However, there is a significant trend among most results: confronting Table 4.7 with Table 4.8, it can be seen that electrical downtilt enables higher performance improvements than the mechanical one for most of the analysed cases, at least over the range of downtilts considered in this thesis. Exceptions take place for the DU_2600 and U_800 environments, for the number of served UEs per sector and obtained throughputs, respectively.

Table 4.8. Performance improvements over the reference scenario achieved using optimal mechanical downtilt values for each environment.

Parameter	DU_800	DU_1800	DU_2600	U_800	U_1800	U_2600
Number of UEs per sector [%]	-0.5	-3.2	2.5	3.3	-4.5	1.0
Throughput [%]	-1.0	18.0	10.9	4.8	10.8	5.0

4.3.4 Height of the Antennas

For the analysis of the influence of the height of the antennas in the results, different values are considered for the centre and off-centre of Lisbon. This is done in order to have not only a small step between the values considered (in order to have realistic scenarios), but also to consider the values used for the reference scenario, which are different between the environments. For the centre of Lisbon analysis, 23, 25, 27 and 29 m are considered for the height of the antennas. On the other hand, for the off-centre of Lisbon analysis, 26, 28, 30 and 32 m are considered instead as the height of the antennas. It is worth noticing that none of these values make the probability of LoS for a given user exceed one (taking into account that LoS occurrence is given by (3.3)).

One should expect the height of the antennas to have a significant impact on system performance, due to interference issues and LoS probability. In order to study the latter, one of the metrics used in this analysis is the LoS occurrence over the centre and off-centre of Lisbon. It is expected that the higher the antennas are the higher LoS occurrence becomes, as it is verified by simulation results presented in Figure 4.24 for the centre and off-centre of Lisbon. Although LoS probability for a given UE does not depend directly on the frequency band, Figure 4.24 shows variations between different frequency bands, because a different number of BSs is considered for each one – there are two times more BSs in the 1 800 MHz band and three times more BSs in the 2 600 MHz band than in the 800 MHz one. This situation has impact on inter-site distance – the average distance of the UE to its serving sector antenna in the 2 600 MHz band tends to be lower than the one for the 800 MHz case, for example, which makes the first case a situation where LoS occurrence is higher. There are also differences between the centre and the off-centre: in the centre, LoS occurrence tends to be higher for a lower value of the height of the antennas, because buildings' height is lower. Also, BSs' density is higher in the centre of Lisbon.

The analysis of the number of served UEs per sector along different heights for the antennas – illustrated in Figure 4.25 – shows that optimal values for that parameter can be proposed: for the centre of Lisbon, antennas placed 27 m above the ground lead to the maximum average number of UEs served per sector, for any of the frequency bands. In the off-centre of Lisbon, 28 and 30 m lead to the optimal performance in the 800 and 1 800 MHz bands, respectively. For the 2 600 MHz band, and taking into account the range of values analysed in the present study, 32 m seem to provide optimal performance in the off-centre. However, if a wider range had been considered, there could be a better value for the height of the BS antennas.

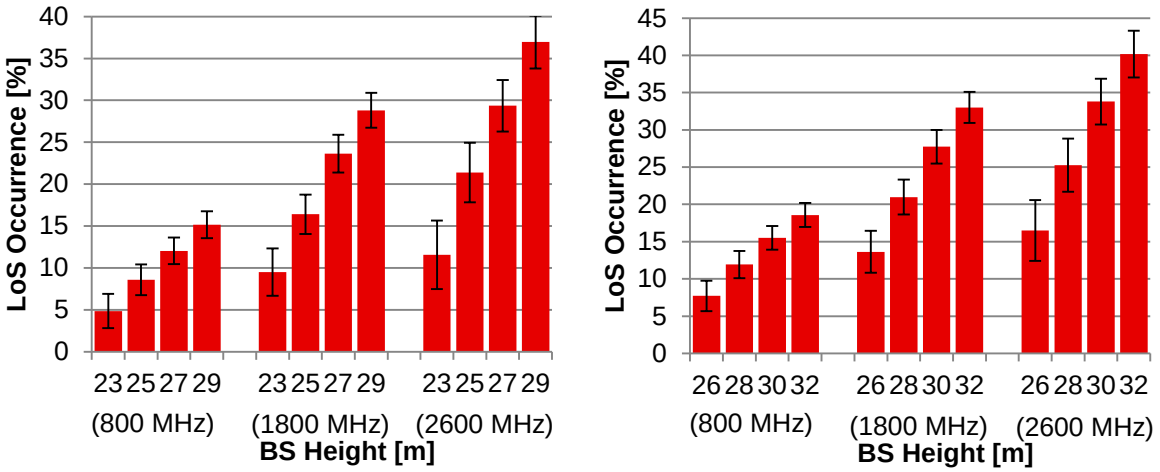

(a) Centre (b) Off-centre

Figure 4.24. LoS occurrence for all the UEs positioned in the centre and off-centre of Lisbon, whether they are or not covered by the system, along the heights of the antennas and frequency bands.

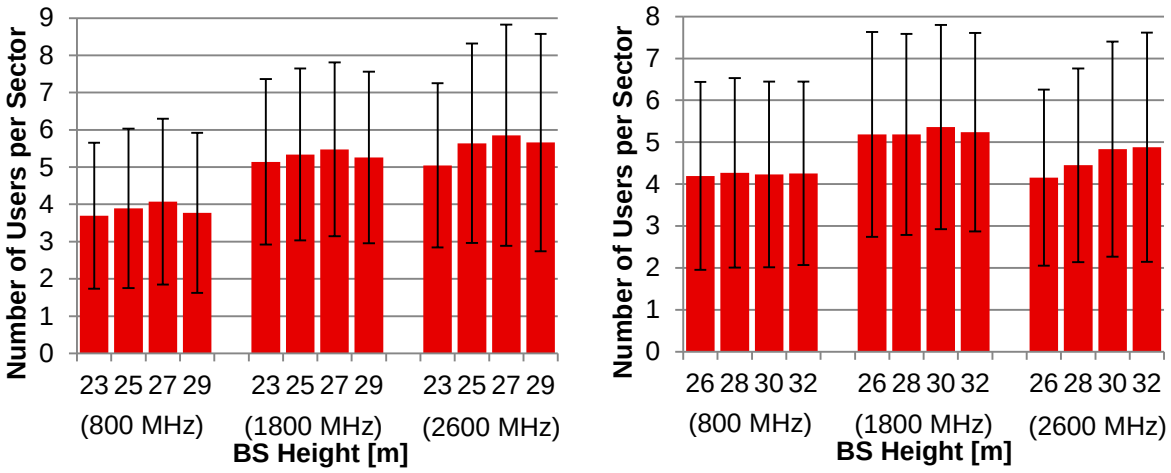

(a) Centre (b) Off-centre

Figure 4.25. Number of served UEs per sector for different heights of the antennas, different frequency bands and for the centre and off-centre of Lisbon.

Figure 4.26 and Figure 4.27 present the SNR/SINR along different values for the height of the antennas in the centre and off-centre of Lisbon, respectively. It can be seen that the difference between SNR and SINR increases with the height of the BS antenna, as SNR increases and SINR decreases. This is an expected trend, because the higher the antennas are, the higher the LoS probability is, hence, LoS occurrence increases, which leads to a higher average SNR. However, a higher LoS occurrence can have a negative impact on neighbouring sectors, whose UEs end up receiving a higher interference power, leading to a lower SINR. From (C.5), one can also see that a higher antenna also leads to a decrease in the path loss, which makes the received power higher. Taking this analysis into account, values for the height of the antennas that lead to optimal performance in terms of SINR are the lowest considered for each case, taking both average and standard deviation values into account – this analysis should, however, be taken carefully, as variations on the standard deviation are sometimes higher than those of the average.

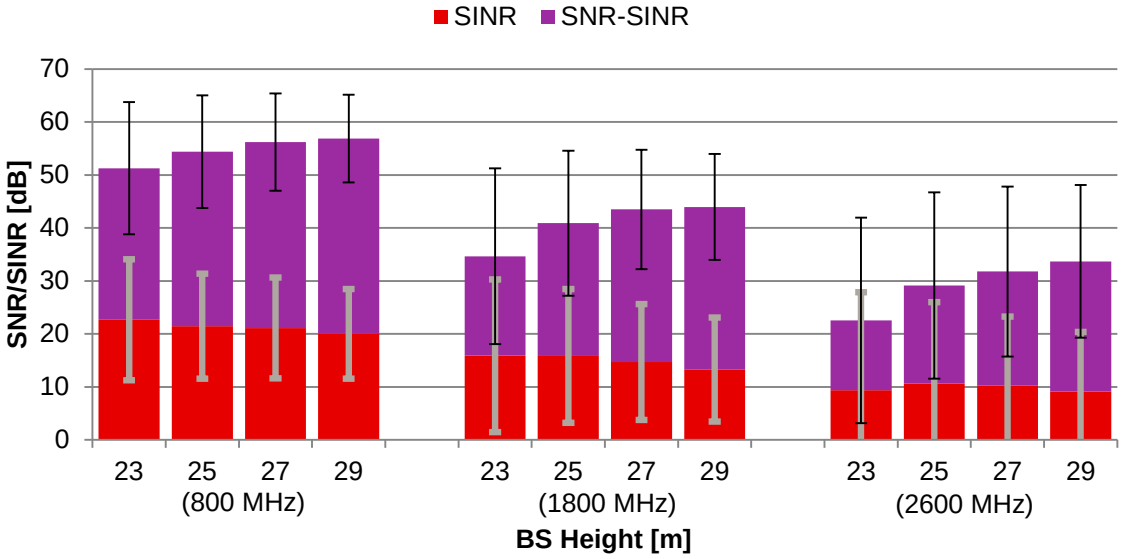

Figure 4.26. UEs' average SNR/SINR for different heights of the antennas, different frequency bands and for the centre of Lisbon.

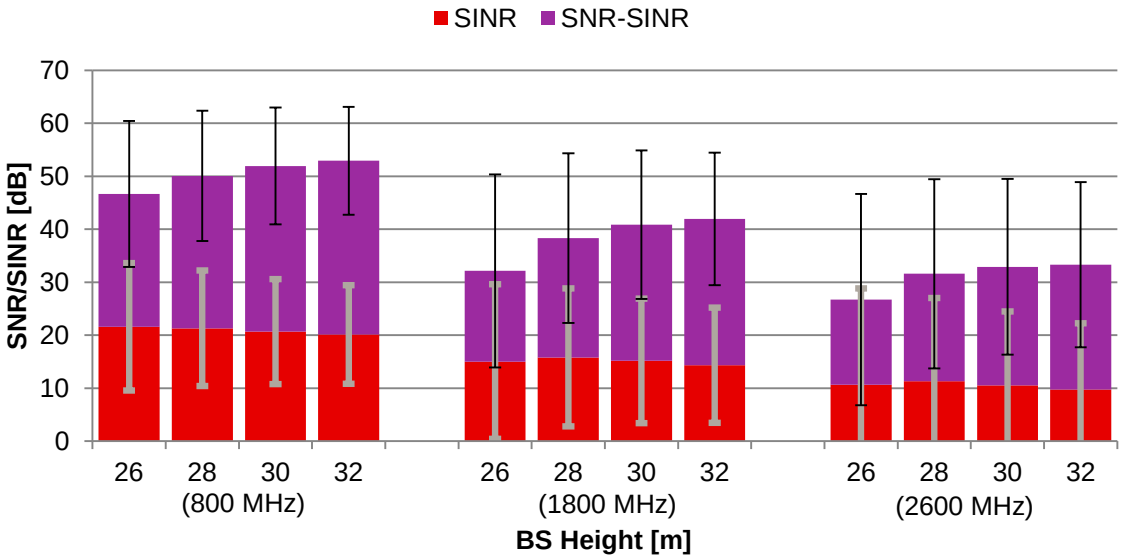

Figure 4.27. UEs' average SNR/SINR for different heights of the antennas, different frequency bands and for the off-centre of Lisbon.

Obtained throughputs for different heights of the antennas, illustrated in Figure 4.28, show a behaviour similar to the SINR's one, hence the same conclusions are maintained, including the same values that lead to optimal performance and the necessary precautions, except for the optimal value for the U_1800 case – in this particular situation, the value picked as the optimal is 28 m, solely based on an average values analysis, because the performance improvement study, summarised in Table 4.9, is based on average values. It is, however, worth noticing that throughput increases with the frequency band as available capacity also increases with the frequency band, taking the reference scenario into account. As the number of served UEs per sector is lower in the off-centre, obtained throughput is higher because sector's capacity does not change from centre to off-centre of Lisbon.

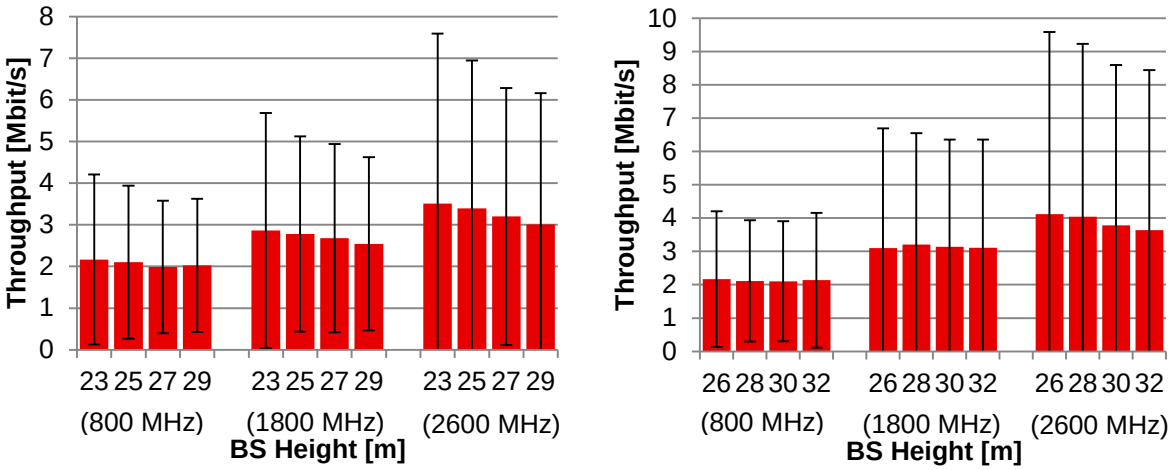

(a) Centre (b) Off-centre

Figure 4.28. UE's throughput for different heights of the antennas, different frequency bands and for the centre and off-centre of Lisbon.

Table 4.9. Performance improvements over the reference scenario achieved using optimal heights of the antennas for each environment.

Parameter	DU_800	DU_1800	DU_2600	U_800	U_1800	U_2600
Number of UEs per sector [%]	4.9	2.6	3.7	0.9	0.0	1.0
Throughput [%]	3.3	2.9	3.5	3.3	1.9	9.0

4.3.5 Transmitter Output Power

For the analysis of the influence of the transmitter output power on system performance, four values are simulated: 10 W (40 dBm), 20 W (43 dBm), 30 W (44.8 dBm) and 40 W (46 dBm). Only values equal or below the maximum value taken for the reference scenario were considered, as power consumption tends to be a major focus of studies in order to reduce network operation costs. So, higher values are considered to be not as beneficial as the ones considered in this thesis.

The impact of the transmitter output power on the number of served UEs per sector is illustrated in Figure 4.29. For the 1 800 MHz band, for both the centre and the off-centre of Lisbon, there is a clear trend: the lower the transmitter output power, the higher is the number of UEs served per sector. This suggests that a lower output power leads to a lower number of UEs being strongly affected by interference, which means that more UEs are able to be served. For the other frequency bands, its behaviour does not show the same significance. However, one can see that the higher the output power, the higher is the number of UEs served in the 2 600 MHz band for both centre and off-centre, which suggests that a higher received power from the serving sector antenna at the UE has more impact on system performance than the interfering power coming from neighbouring sectors. For the 800 MHz band, it is difficult to select an optimal value given the considered range.

Concerning the SNR/SINR analysis, based on Figure 4.30 and Figure 4.31, one can see that the

difference between SNR and SINR increases with the transmitter output power for every frequency band and every environment. SNR clearly increases with the output power, because a higher power is received at the UE, but there is no clear trend for the evolution of the SINR.

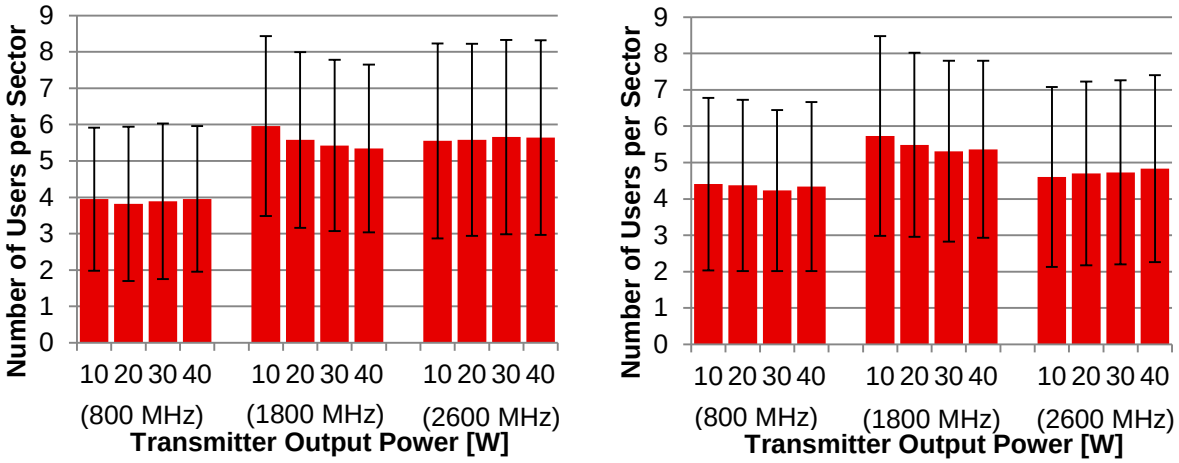

(a) Centre (b) Off-centre

Figure 4.29. Number of served UEs per sector for different transmitter output powers, different frequency bands and for the centre and off-centre of Lisbon.

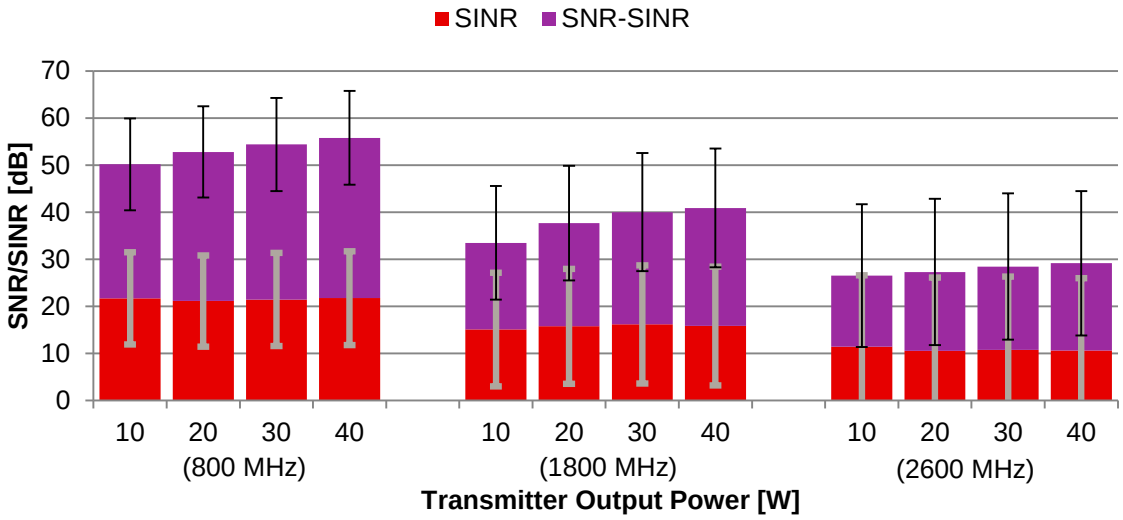

Figure 4.30. UEs' average SNR/SINR for different transmitter output powers, different frequency bands and for the centre of Lisbon.

Obtained throughputs along the transmitter output power for the three frequency bands and for the centre and off-centre of Lisbon can be seen in Figure 4.32. The lower the output power the higher the obtained throughput is, on average, for the 2 600 MHz band in the centre and off-centre – this was expected, as a relatively constant SINR and an increasing number of served UEs per sector along the transmitter output power leads to less UEs asking for resources from the network for the lower output powers, hence, served UEs are able to use more resources, achieving higher throughputs. For the 1 800 MHz band, the highest throughput is met when the output power is 30 W – this is clearer for the off-centre case than for the centre one. For the 800 MHz band, 20 W seem to be the optimal output power value for the centre of Lisbon taking only average values into account – however, the standard

deviation variation for that case is exceptionally higher than for the other cases, hence, this optimal value is considered to be impossible to determine in the considered range. For the off-centre case, it is also difficult to pick an optimal value given the considered range.

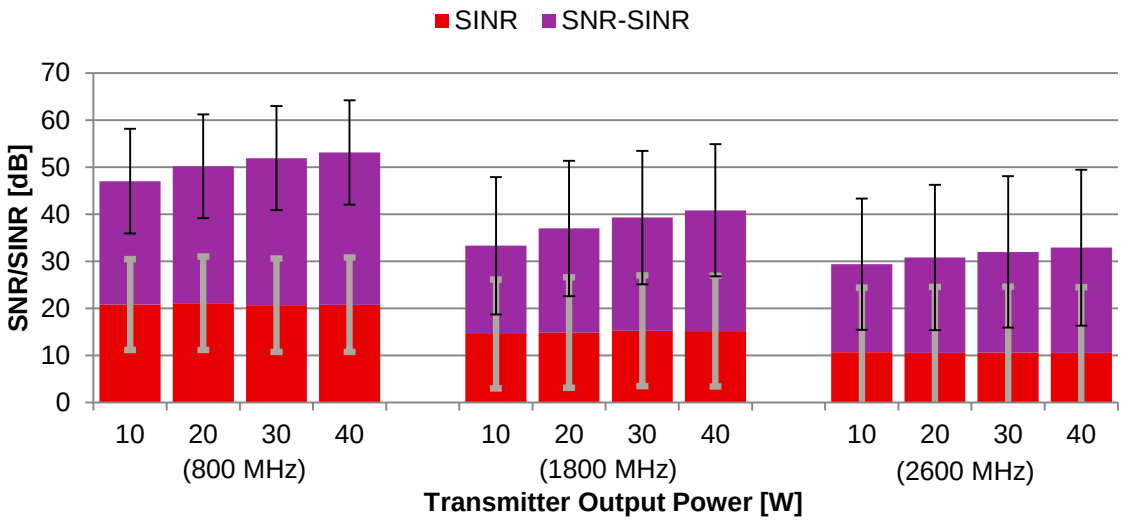

Figure 4.31. UEs' average SNR/SINR for different transmitter output powers, different frequency bands and for the off-centre of Lisbon.

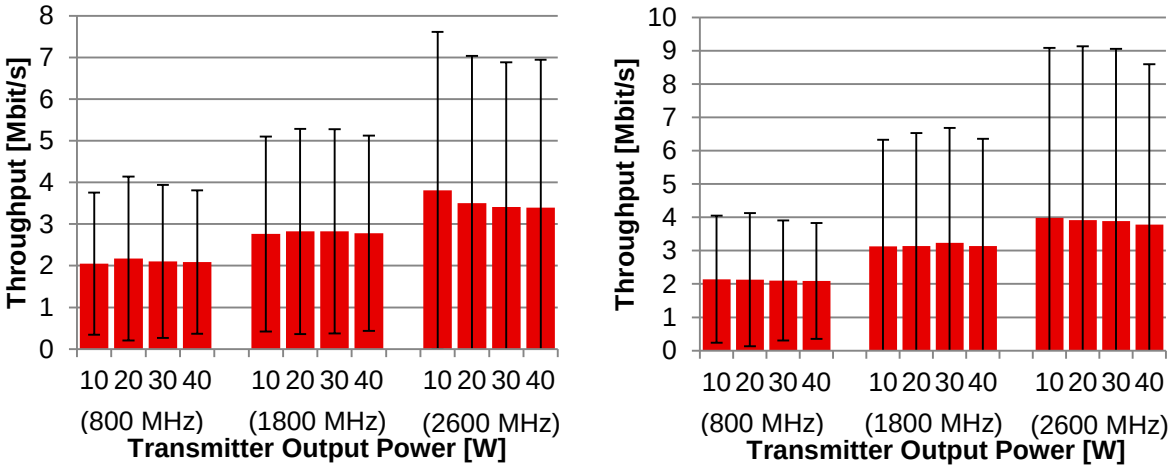

(a) Centre

(b) Off-centre

Figure 4.32. UE's throughput for different transmitter output powers, different frequency bands and for the centre and off-centre of Lisbon.

Improvements obtained over the reference scenario are summarised in Table 4.10.

Table 4.10. Performance improvements over the reference scenario achieved using optimal transmitter output powers for each environment.

Parameter	DU_800	DU_1800	DU_2600	U_800	U_1800	U_2600
Number of UEs per sector [%]	-	11.6	0.0	-	6.9	0.0
Throughput [%]	-	1.8	12.4	-	2.9	5.6

Chapter 5

Conclusions

In this chapter, a summary of all the work carried out under the scope of this thesis is provided. Then, some important conclusions are highlighted, and should provide network operators some useful guidelines on how to minimise inter-cell interference. In the end, hints for future works are given.

The main goal of this thesis was the study of the inter-cell interference impact on LTE performance in urban scenarios, and how it could be minimised, via antennas' electrical and mechanical downtilts, height and output power. An initial analysis of low load scenarios intended to compare measurements performed in the city of Lisbon and simulations was performed, being followed by a high load scenarios analysis that also addressed the pattern for the electrical and mechanical downtilts, height and output power of the antennas.

In the first chapter, a superficial description of the mobile communications systems evolution over time and of the growing consumer and traffic demand is presented, followed by an explanation about the motivation and contents of this thesis.

Chapter 2 provides a theoretical background on LTE's network architecture, radio interface, and coverage and capacity aspects. Particular relevance is given to resource allocation types, as it was found out that, in order to be able to allocate either one RB or the maximum available bandwidth to a single user, only one type of allocation should be used: Resource Allocation Type 2 of localised type, which presents a contiguous allocation over the spectrum. Interference issues and mitigation techniques are also pointed out in the second chapter, along with a brief state of the art concerning interference models. The main focus of this thesis is also addressed, namely the antennas' downtilt angle and already developed studies on that field. The chapter ends with a description of services and applications' characteristics and the description of some traffic models intended to help the definition of the traffic mix used later on, under the scope of the simulations to be performed in the high load scenarios.

As part of the theoretical analysis, some extensive research was done in order to find out the frequency bands, bandwidths and exact portions of the spectrum allocated to each Portuguese network operator, as a result of the multi-band auction supported by ANACOM, this being detailed in Annex A. This was performed in order to have a realistic RB positioning along the spectrum, which was intended to be done over Vodafone's assigned bandwidths.

Chapter 3 presents the model and equations that allow the simulator to emulate reality in the most realistic way possible, as well as a description of the simulator workflow and a model assessment. The developed model has three important aspects that were implemented from scratch in this thesis, and involved a lot of restructuring of the simulator files: the existence of users who experience either LoS or NLoS conditions, a contiguous spectrum allocation, and an association of users to sectors based on the received power. For the definition of a user being in LoS or NLoS conditions, two models were studied. However, only the one that offers higher LoS probabilities for a given user was picked, and even that model was adapted, using a scaling factor, in order to be able to provide a more realistic approach. It was later verified that that model provides a good approximation to results extracted from measurements in the city of Lisbon. A contiguous spectrum allocation was considered, because it is the one that enables the allocation of either a single RB to a given UE or the whole bandwidth. The association of users to sectors is based on received power, and not only on distance, because one of the focuses of this thesis is related to the antenna's radiation pattern, which has a strong influence on the received power along the sector. Also, it is closer to what happens in a real network, where users

tend to be connected to the sector antenna that offers them a higher received power.

Concerning the received power calculation, it was done using the link budget provided in Annex B, which does not consider stochastic generations for fast and slow fadings – in this thesis, only slow fading was considered, and it assumed a fixed value. Path loss was computed using the COST-231 Walfisch-Ikegami model, detailed in Annex C. Transmitter antenna gain was calculated based on 3GPP proposed models for the horizontal and radiation pattern of the antennas, which are able to be shaped according to electrical and/or mechanical downtilt values given as inputs. It was seen, based on research, that mechanical downtilt effect on the radiation pattern is much more irregular than the electrical downtilt's one.

In order to establish a realistic relationship between SINR and achieved throughput, expressions for throughput calculation were developed in this thesis. Expressions were defined taking the generalised logistic function into consideration (the best fit approach of that function to real data collected by 3GPP was encountered) and provide a simple modelling of the throughput evolution along the SINR, according to the modulation scheme being considered. Intermediate coding rates in each modulation were considered, in order to have a realistic representation of the UE's throughput on average.

In the third chapter, a model assessment is also provided, being important in the definition of the high load scenario (in terms of number of users considered) and the number of simulations that should be performed for the low load scenario (10) and for the high load scenario (5).

Chapter 4 starts by providing a description of the scenarios used in this thesis, followed by the low and high load scenarios analyses. The parameters of the antennas were picked taking a given antenna as reference, and the three frequency bands used by Portuguese operators to provide coverage were all used in the reference scenario, because they have particular characteristics worth exploiting: different path loss (due to different frequencies), different available bandwidth, different output power per RB, different BSs' density along the city, and different parameters for the antennas, namely vertical half-power beamwidth. Two different environments were considered for the city of Lisbon: dense urban, for the centre, and urban, for the off-centre. The differences between the two environments are essentially based on different parameters for the propagation model, such as the heights of the antennas, and different BSs' and users' density.

For the low load scenario analysis, several walk-tests, detailed in Annex F, were performed along centre and off-centre regions of Lisbon, using each of the frequency bands at a time. Results obtained in those measurements were compared to simulations performed under a scenario intended to be a good representation of the real one. Taking average values into account, relative errors for the received power are below 5% for each of the considered environments, except for the usage of the 800 MHz band in the off-centre of Lisbon – this happens because LoS occurrence in the particular area where measurements were performed is higher than the average considered for the whole network. Higher relative errors were obtained for the SINR comparison, especially for the 800 MHz band, which shows that this band, even when a relative low number of active UEs in the network is considered, it the one that suffers the highest interference impact. Those differences also influence UEs' throughput relative errors between measurements and simulations, which are also impacted by

the existing differences in the number of allocated RBs per UE – this is due to the fact that, in the simulations, there were cases where two or more UEs were being served by the same sector, while in the measurements those cases did not happen or, if they did, they happened for a very short period of time which was diluted in the overall analysis.

In the high load scenarios analysis, a study of the reference scenario was performed in the first place. It shows that the interference impact in the number of served UEs per sector, the sector antenna's range, and the reduction of SNR into SINR decreases with the frequency band. For this last parameter, called interference margin in this thesis, several values were proposed to help further studies on LTE scenarios where inter-cell interference should be considered: for the reference scenario, and for the centre of Lisbon, one can consider an interference margin of 32.95, 25.08 and 18.53 dB for the 800, 1 800 and 2 600 MHz bands, respectively, and 31.23, 25.69 and 22.36 dB for the same bands but for the off-centre. It was also verified that inter-cell interference impact on throughput increases with the frequency band. The reference scenario scrutiny ends with a result that shows a limitation of the algorithms considered in the simulator: the percentage of UEs served by a given service does not match the percentage of UEs requesting that service for all cases, being evident what is happening in the system: although video streaming and chat are the highest priority services, they end up being the ones whose serving percentage is reduced the most because they do not ask the network for the same maximum throughput, as it happens with the remaining services. As RBs' allocation to UEs is based on QoS priority and requested throughput, actual priorities of those services end up being changed, enabling other services to have higher serving percentages because they asked for much higher throughputs in the beginning. Future studies done with the same simulator as the one used in this thesis should be improved in the sense that services penetration for served UEs should be similar to the requested one, or it may even stabilise in the same value for all services when a very high load network is considered, for example. Other limitations of this work are related to the fact that the same buildings' height, street width and distance between buildings' centres are considered for each of the environments – these parameters are only dependent on the type of environment (urban or dense urban). Also, terrain undulation is not considered, neither the fact that Lisbon has a very irregular structure, which includes different buildings that may impose limitations to coverage areas and received power levels. It was also considered that all BSs are tri-sectorised, which does not happen for all of them, and that the network for the 1 800 MHz and 800 MHz bands is composed by 2/3 and 1/3 of the BSs that work in the 2 600 MHz one, respectively.

Variations of some parameters, like electrical and mechanical downtilts of the antennas, their height and their output power, were considered in order to check if system performance could be enhanced. That performance enhancement over the reference scenario was thoroughly analysed for the number of served UEs per sector and their obtained throughput. Overall, most performance enhancements are reached when electrical downtilt variations are considered, followed by the height of the antennas, the transmitter output power and mechanical downtilt. It is also noticeable that different behaviours of inter-cell interference impact along variations in the electrical downtilt are observed for the three frequency bands, mainly because they have different vertical half-power beamwidths – the narrower the beamwidth the higher the electrical downtilt impact is.

If one wants to improve the number of served UEs per sector, taking into account the variations' range considered in this thesis and highest performance enhancements for each of the six environments, one should consider:

- an electrical downtilt of 9° (5.2% improvement) and 3° (1.9% improvement) for the 800 and 2 600 MHz bands, respectively, in the off-centre;
- 27 m for the height of the antennas in the 800 (4.9% improvement) and 2 600 MHz (3.7% improvement) bands for the centre of Lisbon;
- a transmitter output power of 10 W for the 1 800 MHz band on both the centre (11.6% improvement) and off-centre (6.9% improvement) of Lisbon.

A lower output power value (10 W) than the one considered (40 W) for the 1 800 MHz band as the optimal solution suggests that if full capacity (20 MHz) was taken instead for this particular band, the interference impact would be lower than the one seen for the reference scenario, because output power per RB would be lower.

On the other hand, if one wishes to improve the UEs' obtained throughput, one should consider the following:

- an electrical downtilt of 11° for the 1 800 (27.3% improvement) and 2 600 MHz (18.9% improvement) in the centre, and 9° for the 1 800 (17.2% improvement) and 2 600 MHz (20.4% improvement) in the off-centre;
- 23 m for the height of the antennas in the 800 MHz band in the centre of Lisbon (3.3% improvement);
- a mechanical downtilt of 11° for the 800 MHz band in the off-centre (4.8% improvement).

There is no clear optimal value for the transmitter output power for the range considered in the 800 MHz band analysis, because there are no significant changes between consecutive values (at least for the number of served UEs per sector). So, one can propose the minimum considered as the best one, because it leads to lower power consumption, which reduces the network operation's costs.

Optimal values of electrical downtilt for the increase of the number of served UEs per sector are within the ranges supported by the reference antennas. This does not happen for the optimal values of either electrical or mechanical downtilt for the increase of UEs' throughput, which are still valid as a different antenna could be used instead.

Besides the improvement of a real priority based RBs distribution among UEs, future works could consider an even better antenna modelling, especially in the vertical radiation pattern, as the one used in this thesis does not provide a very accurate modelling of secondary lobes. Beamforming techniques could also be studied in future works, in order to know if they represent good or bad approaches in a real system, and a combined variation of electrical and mechanical downtilts could also be studied. A better modelling of throughput as a function of SINR could also be developed, taking into account different transmission modes and/or different coding rates in each modulation. The UL should also be analysed, as users tend to become more and more *prosumers* – they are not only consumers of data, but are also starting to be active producers of content. This will eventually lead to the consideration of

photo or video upload to social networks in the traffic mix, for example. As there are a lot of frequency bands overlapping along the city of Lisbon, a study where this is exploited could also be conducted, addressing performance gains achieved when carrier aggregation in an LTE-A scenario is considered.

In any case, it is suggested that future master theses continue to contemplate a measurements campaign in the field, as it provides a better understanding of how a real network behaves, giving a general perspective of the influence of certain parameters on system performance.

Annex A

Frequency Allocations in Portugal

This annex provides an overview of the frequency allocations in Portugal, taking into account the frequency bands that are typically allocated in European countries.

According to [HoTo11], there are 31 E-UTRA frequency bands defined: 22 for FDD, and 9 for TDD. However, the eNodeB radio frequency (RF) requirements are defined in a frequency band agnostic way, and there are also some exceptions for the UE RF specifications. So, if the need arises, further LTE frequency bands may be defined, which will only affect isolated parts of the RF specifications.

Not all of the frequency bands are available worldwide, and its general management and distribution is done according to four main regions of the world: Americas, Asia, Europe and Japan. This means that LTE deployments in a global perspective may use different frequency bands from the beginning.

In Europe, FDD is the widely adopted duplex mode. Table A.1 shows the usage and definition of the frequency bands in Europe. The most relevant bands are the following:

- Band 3, or the 1 800 MHz band, which is partially used by GSM and, as such, may suffer refarming of some of its frequencies to provide an extended LTE coverage in the future;
- Band 7, or the 2 600 MHz band;
- Band 8, or the 900 MHz band, which is used mostly by GSM (making LTE refarming a possibility in the future), due to its lower propagation losses that make it a preferred choice from a coverage point of view;
- Band 20, or the 800 MHz band, which is even more attractive from a coverage point of view.

Table A.1. E-UTRA frequency bands used in Europe (adapted from [HoTo11]).

Band	Uplink	Downlink	Duplex Mode
1	[1920;1980] MHz	[2110;2170] MHz	FDD
3	[1710;1785] MHz	[1805;1880] MHz	
7	[2500;2570] MHz	[2620;2690] MHz	
8	[880;915] MHz	[925;960] MHz	
20	[832;862] MHz	[791;821] MHz	
22	[3410;3500] MHz	[3510;3600] MHz	

Following a trend among other European countries, the regulator of the communications sector in Portugal (ANACOM) issued unified titles of rights of use of frequencies for terrestrial electronic communication services, as a result of a multi-band auction, according to [ANAC12c]. Although the frequency lots were not specifically auctioned for LTE allocation purposes, due to the principles of neutrality, the large majority of them should be used in such a way, as they belong to the frequency bands referred in Table A.1. Table A.2 refers to those allocations, which were assigned to the three major network operators in Portugal (Optimus, TMN and Vodafone). Each of these players paid a significant amount of money to earn the rights to use the frequencies bought. Vodafone was the one who bought the most frequency lots, having spent a total of 146 M€, according to [ANAC11].

In the assignment phase, each operator selected the exact frequencies that corresponded to the acquired lots, following an order dictated by the final ranking of winning bidders and ANACOM's criteria [ANAC12a], except for the 1 800 MHz band. As stated in [ANAC12c], the three operators which obtained lots in the 1 800 MHz band made an agreement among them to determine the exact

location of their acquisitions in this frequency band. The agreement, which was subsequently approved by ANACOM [ANAC12b], included the redistribution of the frequency lots that operators already had in that frequency band (2×6 MHz each), in order to get a contiguous distribution of the spectrum attributed to each operator. All the attributions that correspond to LTE FDD purposes are summarised in Table A.3. Nevertheless, some operators may still have a portion of the 1 800 MHz band allocated for GSM1800 purposes.

Table A.2. Allocations made as a result of the multi-band auction (based on [ANAC12c]).

<table>
<tr><th>Lots</th><th>Owner</th><th>Frequency Band</th><th>Size of Each Lot</th></tr>
<tr><td>B1, B2</td><td>TMN</td><td rowspan="3">800 MHz</td><td rowspan="5">2 × 5 MHz</td></tr>
<tr><td>B3, B4</td><td>Vodafone</td></tr>
<tr><td>B5, B6</td><td>Optimus</td></tr>
<tr><td>C2</td><td>Vodafone</td><td>900 MHz</td></tr>
<tr><td>D1, D2</td><td>TMN</td><td rowspan="6">1 800 MHz</td></tr>
<tr><td>D3, D4</td><td>Vodafone</td><td></td></tr>
<tr><td>D5, D6</td><td>Optimus</td><td></td></tr>
<tr><td>E1</td><td>TMN</td><td rowspan="3">2 × 4 MHz</td></tr>
<tr><td>E2</td><td>Vodafone</td></tr>
<tr><td>E3</td><td>Optimus</td></tr>
<tr><td>G1, G2, G3, G4</td><td>TMN</td><td rowspan="4">2 600 MHz</td><td rowspan="3">2 × 5 MHz</td></tr>
<tr><td>G5, G6, G7, G8</td><td>Vodafone</td></tr>
<tr><td>G9, G10, G11, G12</td><td>Optimus</td></tr>
<tr><td>H1</td><td>Vodafone</td><td>25 MHz</td></tr>
</table>

Table A.3. Exact allocations made as a result of the multi-band auction (based on [ANAC12a] and [ANAC12c]).

Frequency Band	Owner	Frequency Interval (UL)	Frequency Interval (DL)
800 MHz	TMN	[832;842] MHz	[791;801] MHz
	Vodafone	[842;852] MHz	[801;811] MHz
	Optimus	[852;862] MHz	[811;821] MHz
1 800 MHz	Vodafone	[1710;1730] MHz	[1805;1825] MHz
	Optimus	[1730;1750] MHz	[1825;1845] MHz
	TMN	[1750;1770] MHz	[1845;1865] MHz
2 600 MHz	Vodafone	[2510;2530] MHz	[2630;2650] MHz
	Optimus	[2530;2550] MHz	[2650;2670] MHz
	TMN	[2550;2570] MHz	[2670;2690] MHz

Annex B

Link Budget

A description of the path loss calculation and its influence in the link budget is done in this annex.

In order to calculate the maximum path loss in a cell, which is useful to estimate the sector antenna's range, the link budget has to be taken into account.

According to [Corr13], the power received by the UE is given by the following expression:

$$P_{r[\mathrm{dBm}]} = P_{EIRP[\mathrm{dBm}]} + G_{r[\mathrm{dBi}]} - L_{p,total[\mathrm{dB}]} \quad \text{(B.1)}$$

where:

- P_r: power available at the receiving antenna;
- P_{EIRP}: Effective Isotropic Radiated Power (EIRP);
- G_r: gain of the receiving antenna;
- $L_{p,total}$: path loss.

The EIRP depends on the link. In DL, it is defined as follows:

$$P_{EIRP[\mathrm{dBm}]} = P_{Tx[\mathrm{dBm}]} - L_{c[\mathrm{dB}]} + G_{t[\mathrm{dBi}]} \quad \text{(B.2)}$$

where:

- P_{Tx}: transmitter output power;
- L_c: losses in the cable between the transmitter and the antenna;
- G: gain of the transmitting antenna.

In UL, the EIRP is defined by the following expression:

$$EIRP_{[\mathrm{dBm}]} = P_{Tx[\mathrm{dBm}]} - L_{u[\mathrm{dB}]} + G_{[\mathrm{dBi}]} \quad \text{(B.3)}$$

where:

- L_u: losses due to the user, which take a value between 0 and 3 dB for data.

The power at the receiver, in DL, is given by:

$$P_{Rx[\mathrm{dBm}]} = P_{r[\mathrm{dBm}]} - L_{u[\mathrm{dB}]} \quad \text{(B.4)}$$

where:

- P_{Rx}: power at the input of the receiver.

The power at the receiver, in UL, is given by:

$$P_{Rx[\mathrm{dBm}]} = P_{r[\mathrm{dBm}]} - L_{c[\mathrm{dB}]} \quad \text{(B.5)}$$

The average noise power can be estimated from the following expression, according to [Corr13] and [SeTB11]:

$$N_{[\mathrm{dBm}]} = 10\log\left(\frac{k_{[\mathrm{JK}^{-1}]} \times T_{[\mathrm{K}]}}{10^{-3}}\right) + 10\log\left(B_{N[\mathrm{Hz}]}\right) + F_{[\mathrm{dB}]} \quad \text{(B.6)}$$

where:

- k: Boltzmann's constant ($1.380662 \times 10^{-23}\ \mathrm{JK}^{-1}$);
- T: temperature of the receiver (assumed to be 15℃, hence, 288.2 K);
- B_N: noise bandwidth;
- F: noise figure.

Taking into account the assumed value for T in LTE specifications, kT is defined to be -174 dBm/Hz –

no account is taken of the small variations in temperature over normal operating conditions (typically $15℃$ to $35℃$) or extreme operating conditions ($-10℃$ to $55℃$), according to [SeTB11].

The noise bandwidth is given by:

$$B_{N[\mathrm{Hz}]} = N_{RB} \times B_{RB[\mathrm{Hz}]} \quad \text{(B.7)}$$

where:

- N_{RB}: number of RBs;
- B_{RB}: bandwidth of one RB, which is 180 kHz.

The total path loss can be calculated by:

$$L_{p,total[\mathrm{dB}]} = L_{p[\mathrm{dB}]} + M_{SF[\mathrm{dB}]} + M_{FF[\mathrm{dB}]} \quad \text{(B.8)}$$

where:

- L_p: path loss from the COST-231 Walfisch-Ikegami model;
- M_{SF}: slow fading margin;
- M_{FF}: fast fading margin.

Annex C

COST-231 Walfisch-Ikegami Model

This annex provides a description of the propagation model used to determine the path loss between transmitter and receiver.

The path loss experienced by a signal travelling between the BS and the UE can be calculated using the COST-231 Walfisch-Ikegami model, which is applied when dealing with small distances (below 5 km) and urban or suburban environments, according to [Corr13].

For LoS propagation in a street, and $d > 0.02$ km, path loss is given by:

$$L_{p[\mathrm{dB}]} = 42.6 + 26\log\left(d_{[\mathrm{km}]}\right) + 20\log\left(f_{[\mathrm{MHz}]}\right) \quad \text{(C.1)}$$

where:

- d: distance between the BS and the UE;
- f: frequency of the signal being propagated.

For all other cases, path loss is defined as:

$$L_{p[\mathrm{dB}]} = \begin{cases} L_{0[\mathrm{dB}]} + L_{rt[\mathrm{dB}]} + L_{rm[\mathrm{dB}]}, L_{rt} + L_{rm} > 0 \\ L_{0[\mathrm{dB}]} \quad , L_{rt} + L_{rm} \leq 0 \end{cases} \quad \text{(C.2)}$$

where:

- L_0: free space propagation path loss;
- L_{rt}: attenuation due to propagation from the BS to the last rooftop;
- L_{rm}: attenuation due to diffraction from the last rooftop to the UE.

The path loss experienced in a free space propagation case is given by:

$$L_{0[\mathrm{dB}]} = 32.44 + 20\log\left(d_{[\mathrm{km}]}\right) + 20\log\left(f_{[\mathrm{MHz}]}\right) \quad \text{(C.3)}$$

The propagation from the BS to the last rooftop experiences the following loss:

$$L_{rt[\mathrm{dB}]} = L_{bsh[\mathrm{dB}]} + k_a + k_d\log\left(d_{[\mathrm{km}]}\right) + k_f\log\left(f_{[\mathrm{MHz}]}\right) - 9\log\left(w_{B[\mathrm{m}]}\right) \quad \text{(C.4)}$$

where:

- w_B: distance between buildings' centres;

$$L_{bsh[\mathrm{dB}]} = \begin{cases} -18\log\left(h_{b[\mathrm{m}]} - H_{B[\mathrm{m}]} + 1\right), h_b > H_B \\ 0 \quad , h_b \leq H_B \end{cases} \quad \text{(C.5)}$$

in which:

- h_b: height of the BS antenna;
- H_B: height of the buildings.

$$k_a = \begin{cases} 54 \quad , h_b > H_B \\ 54 - 0.8\left(h_{b[\mathrm{m}]} - H_{B[\mathrm{m}]}\right) \quad , h_b \leq H_B \wedge d \geq 0.5\ km \\ 54 - 1.6\left(h_{b[\mathrm{m}]} - H_{B[\mathrm{m}]}\right)d_{km}, h_b \leq H_B \wedge d < 0.5\ km \end{cases} \quad \text{(C.6)}$$

$$k_d = \begin{cases} 18 \quad , h_b > H_B \\ 18 - 15\dfrac{h_{b[\mathrm{m}]} - H_{B[\mathrm{m}]}}{H_{B[\mathrm{m}]}}, h_b \leq H_B \end{cases} \quad \text{(C.7)}$$

$$k_f = \begin{cases} -4 + 0.7\left(\dfrac{f_{[\mathrm{MHz}]}}{925} - 1\right), \text{urban and suburban scenarios} \\ -4 + 1.5\left(\dfrac{f_{[\mathrm{MHz}]}}{925} - 1\right), \text{dense urban scenarios} \end{cases} \quad \text{(C.8)}$$

The loss due to diffraction from the last rooftop to the UE is given by:

$$L_{rm[\mathrm{dB}]} = -16.9 - 10\log\left(w_{s[\mathrm{m}]}\right) + 10\log\left(f_{[\mathrm{MHz}]}\right) + 20\log\left(H_{B[\mathrm{m}]} - h_{m[\mathrm{m}]}\right) + L_{ori[\mathrm{dB}]} \quad \text{(C.9)}$$

where:

- w_s: width of the streets;
- h_m: height of the UE;

$$L_{ori[\mathrm{dB}]} = \begin{cases} -10.0 + 0.354\phi_{[^\circ]} & ,0^\circ < \phi < 35^\circ \\ 2.5 + 0.075\left(\phi_{[^\circ]} - 35\right), & 35^\circ \le \phi < 55^\circ \\ 4.0 - 0.114\left(\phi_{[^\circ]} - 55\right), & 55^\circ \le \phi \le 90^\circ \end{cases} \quad \text{(C.10)}$$

in which:

- ϕ: angle of incidence of the signal in the buildings, on the horizontal plane.

The COST-231 Walfisch-Ikegami model is valid for the following values:

- $f_{[\mathrm{MHz}]} \in [800, 2000]$
- $d_{[\mathrm{km}]} \in [0.02, 5]$
- $h_{b[\mathrm{m}]} \in [4, 50]$
- $h_{m[\mathrm{m}]} \in [1, 3]$

Since the presented frequency range does not contain all of the frequency bands analysed in this thesis, one should understand that the results may present higher relative errors than expected.

The standard deviation of the model takes values in [4, 7] dB, and the error increases when h_b decreases relative to H_B. Some of the parameters used in this model are illustrated in Figure C.1.

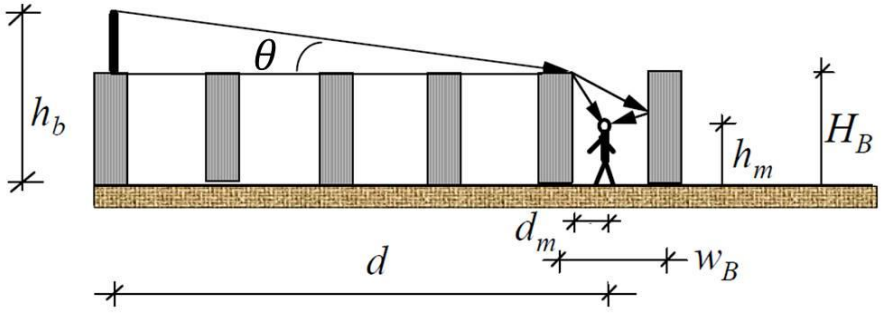

Figure C.1. COST-231 Walfisch-Ikegami model parameters (adapted from [Corr13]).

Annex D

SINR versus Throughput

The LTE models used to determine the SINR and throughput for a given set of system configurations are provided in this annex.

In order to establish a relationship between SNR/SINR and throughput, three expressions were derived for the three modulation types considered in the DL: QPSK, 16QAM and 64QAM. Those expressions are the logistic functions which provide the best fit approach to a set of values collected by 3GPP based on throughput performance tests done by manufacturers and presented in [3GPP11a]. Nine different manufacturers provided results in each of the three test scenarios, so an average among the different manufacturers' values was considered. Those values were processed using Wolfram Mathematica, which provided the best fit expressions to the generalised logistic curve provided below, as the plot of the values suggested that this would provide a good approximation:

$$R_{b[\text{bps}]} = \frac{A}{B + e^{-C\rho_{IN}[\text{dB}]}} \tag{D.1}$$

Results were obtained using 2×2 MIMO, a 10 MHz bandwidth (50 RBs, as one can check in Table 2.3), FDD, the settings provided in Table D.1 and other assumptions also provided in [3GPP11c], which are out of the focus of this master thesis. Testing was done using a transmission mode which is only first supported in LTE Release 10. However, this only has implications on the type of reference, synchronisation and control signals used as overhead, which substitute others previously used. As the amount of overhead is highly variable, the results are coherent with Release 8 and Release 9 scenarios considered in this thesis.

A comparison with previously derived expressions provided in [Duar08], [Jaci09], [Carr11] and [Pire12], which were done based on previous 3GPP results and other assumptions in order to get values for the same modulation types and MIMO configuration, was done, and showed that maximum values obtained in the two approaches are similar.

Table D.1. Test settings (extracted from [3GPP11c]).

Test	Modulation	Target coding rate	Propagation condition	UE category
1	QPSK	1/3	EVA5	1–8
2	64QAM	1/2	EPA5	2–8
3	16QAM	1/2	EPA5	2–8

In order to have a realistic approach of the behaviour of a real network, the three modulation schemes where considered to be associated to median values of coding rates. All possible MCS taking into account the CQI reported by the UE are illustrated in Table D.2 – these were compared with Table D.1, and enabled the following assumptions:

- for QPSK, the target coding rate of 1/3 is maintained;
- for 16QAM, the target coding rate of 1/2 is maintained;
- for 64QAM, a target coding rate of 3/4 is considered instead, as it is considered to be a better average over the values achieved in a real network.

A simple extrapolation of the results was considered in order to change the target coding rate for the 64QAM modulation scheme. The obtained expression was divided by its associated target coding rate and multiplied by the new one. Also, as the only propagation scenario considered in this thesis is the EPA5, an extrapolation of EVA5 to EPA5 was considered in the QPSK case, based on Table D.3.

Table D.2. CQI table (adapted from [SeTB11]).

CQI index	Modulation	Coding rate
0	Out of range	
1	QPSK	0.0762
2	QPSK	0.117
3	QPSK	0.188
4	QPSK	0.300
5	QPSK	0.438
6	QPSK	0.588
7	16QAM	0.369
8	16QAM	0.479
9	16QAM	0.602
10	64QAM	0.455
11	64QAM	0.554
12	64QAM	0.650
13	64QAM	0.754
14	64QAM	0.853
15	64QAM	0.926

Table D.3. Extrapolation EVA 5 Hz – EPA 5 Hz (extracted from [Duar08]).

Modulation	$\frac{\text{EPA 5 Hz}}{\text{EVA 5 Hz}}$	$\bar{\varepsilon_r}[\%]$
QPSK	1.027	5.3

3GPP collected results are presented as the obtained throughputs per frame, so they are divided by 20, as there are 20 RBs in a radio frame (a frame has 10 sub-frames, and each sub-frame has 2 RBs), so that one can compute values of throughput per RB.

For 2×2 MIMO, QPSK and coding rate of 1/3, throughput in the DL is given by:

$$R_{b[\text{bps}]} = \frac{2.34201 \times 10^6}{14.0051 + e^{-0.577897\rho_{IN[\text{dB}]}}} \quad \text{(D.2)}$$

For 2×2 MIMO, 16QAM and coding rate of 1/2, throughput in the DL is given by:

$$R_{b[\text{bps}]} = \frac{47613.1}{0.0926275 + e^{-0.295838\rho_{IN[\text{dB}]}}} \quad \text{(D.3)}$$

For 2×2 MIMO, 64QAM and coding rate of 3/4, throughput in the DL is given by:

$$R_{b[\text{bps}]} = \frac{26405.8}{0.0220186 + e^{-0.24491\rho_{IN[\text{dB}]}}} \quad \text{(D.4)}$$

For 2×2 MIMO, QPSK and coding rate of 1/3, SNR in the DL is given by the following expression, taking into account (D.2):

$$\rho_{IN[\mathrm{dB}]} = -\frac{1}{0.577897}\ln\left(\frac{2.34201\times 10^{6}}{R_{b[\mathrm{bps}]}} - 14.0051\right) \quad \text{(D.5)}$$

One can check in Table D.4 that for all the best fit approaches, coefficient of determination values are very close to 1, which means that the obtained curves provide good approximations to the results published by 3GPP.

Table D.4. Coefficient of determination.

Case	R^2
QPSK 1/3	0.998728
16QAM 1/2	0.999211
64QAM 1/2	0.998265

Annex E

User's Manual

A brief overview of the simulator, along with an explanation on how to run a simulation, is provided in this annex.

Whenever UMTS_Simul.mbx is opened, two consecutive windows ask for the following files:

- DADOS_Lisboa.tab, which holds information about the city of Lisbon, namely its districts;
- ZONAS_Lisboa.tab, which contains information about the area characterisation.

Then, one should access the “System” tab on the upper bar of MapInfo, select “LTE-DL” and then click on the available features, one at a time: "Propagation Model”, “Traffic Properties”, “Network Settings” and “Services”. Each click opens the corresponding window.

The “Propagation Model” window is presented in Figure E.1. It provides the appropriate choices to select the propagation model parameters such as the height of the BS antennas, the buildings’ height, street width, distance between buildings’ centres, departing angle from the closest building, UE height and type of environment (urban or dense urban).

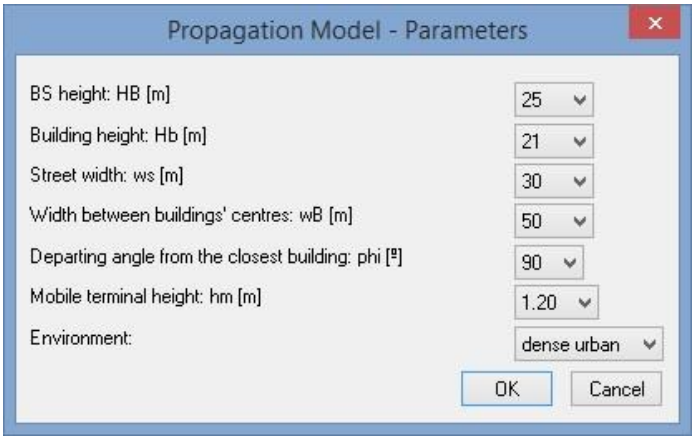

Figure E.1. Propagation model parameters.

The “Traffic Properties” window, represented in Figure E.2, enables the choice of the priority of each service being considered. Absolute values for the priority are not that relevant – what matters is their relative value taking into account all the services.

Figure E.2. Traffic properties.

The “Network Settings” window, also called “LTE-DL Settings” and represented in Figure E.3, is where most of the parameters that characterise the system are introduced. Values of throughput for the reference service are used to determine coverage areas for the centre (Reference Service 2) and off-centre (Reference Service 1) of Lisbon, and the LoS Probability section refers to (3.3) and (3.1). Resource Allocation selection refers to a contiguous (localised) distribution of RBs among the

available spectrum or random (distributed) positioning of RBs in the frequency spectrum.

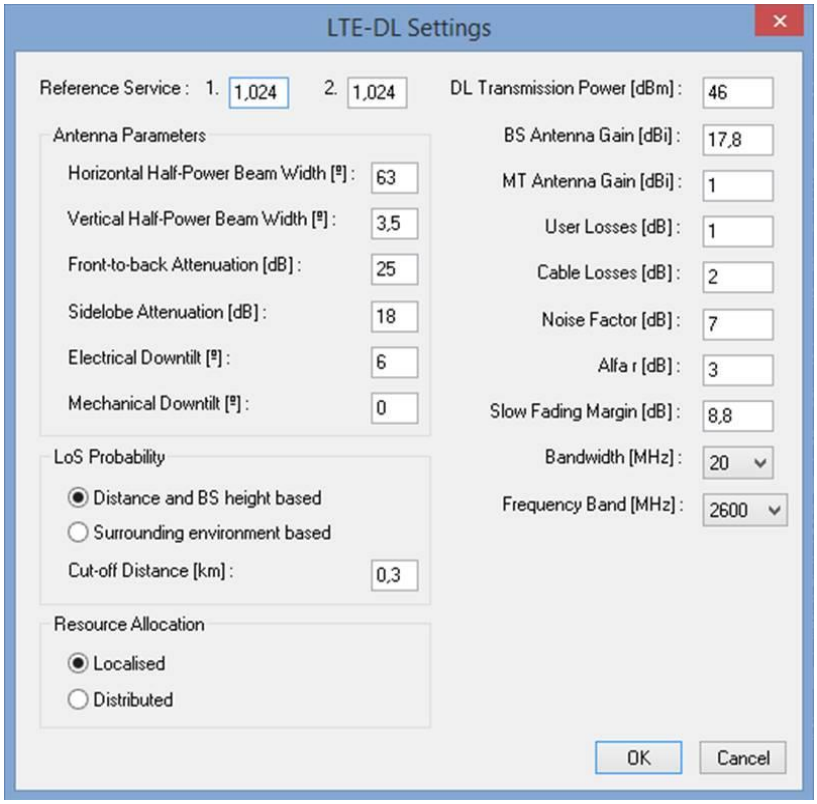

Figure E.3. LTE DL settings.

In the “LTE DL User Profile” window presented in Figure E.4 (which is available after the data presented in Figure E.1, Figure E.2 and Figure E.3 is filled in), requested and minimum throughputs for each of the considered services are introduced. Then, “Insert Users” becomes an available option, being selected in order to introduce a file containing the users positioning along the city of Lisbon. After that, “Deploy Network” also becomes selectable, and it asks for a file containing BSs’ identification and position information. When this file is loaded, “Run Simulation” can be pressed in order to perform a simulation.

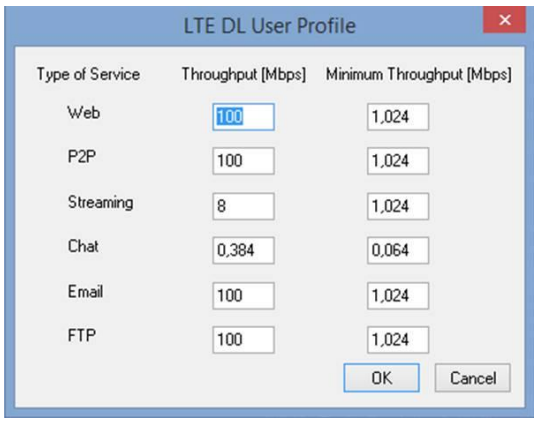

Figure E.4. LTE DL user profile.

Annex F

Walk-Test Results

A summary of the walk-tests that took place in the city of Lisbon is provided in this Annex. The most relevant results are illustrated per frequency band and per environment, and refer to received power, interference power, SNR, number of allocated RBs and achieved throughputs.

A set of measurements was performed in the city of Lisbon, in centre and off-centre areas, and in the three frequency bands that Portuguese operators use to provide LTE coverage. Seven different walk-tests took place: three in the centre of Lisbon (one for each frequency band) and four in the off-centre of Lisbon (one for each frequency band, except for the 1 800 MHz band case, where two walk-tests were done. Many walk-tests were done in the same area, as one can check in Figure F.1 (which shows where information about different frequency bands was collected), hence the need to divide the results in different sets of pictures, so that there is no superimposed information. According to [Voda13], the 1275 serving cell DL EARFCN corresponds to the 1 800 MHz band, the 2950 refers to the 2 600 MHz band, and the 6300 corresponds to the 800 MHz band.

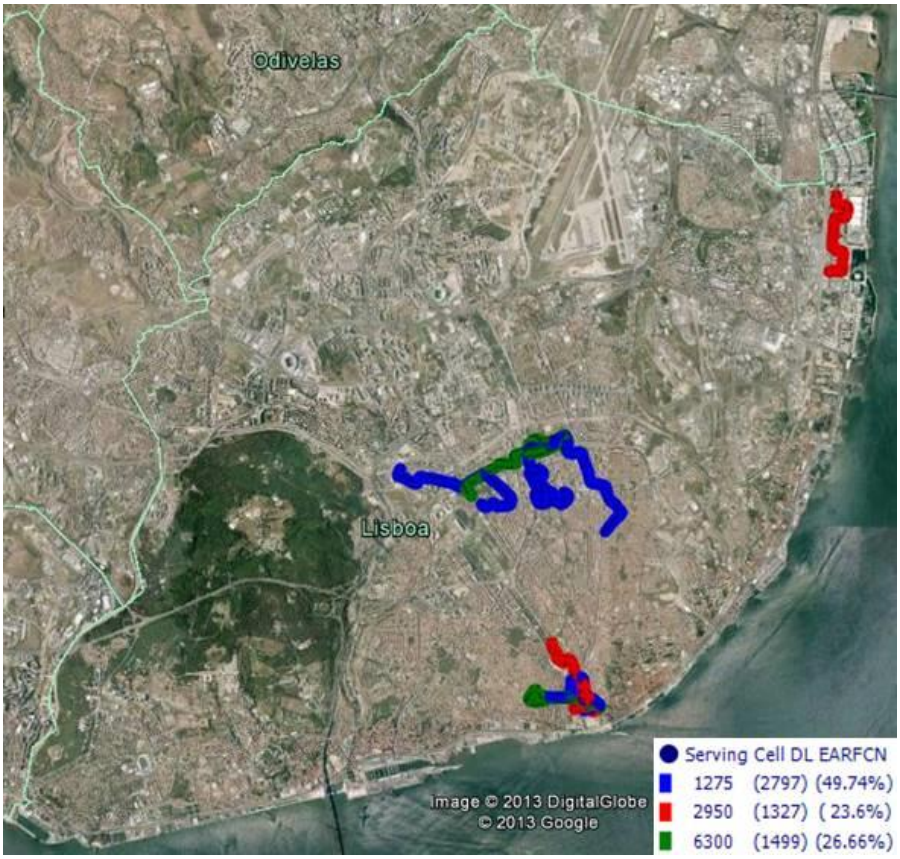

Figure F.1. Frequency bands where the walk-tests took place.

For the centre of Lisbon case, walk-tests were done in Restauradores, Baixa and Chiado areas, which are densely populated areas and, as such, are considered to be good representations of a dense urban environment. On the other hand, for the off-centre of Lisbon, measurements were done in Campolide and Campo Pequeno, for the 800 MHz band, in Campolide, Campo Pequeno, Saldanha and the vicinity of Instituto Superior Técnico for the 1 800 MHz case, and in Parque das Nações for the 2 600 MHz band. These areas have relatively high buildings close to others which are similar to centre of Lisbon ones, and have street widths larger than those of the centre of Lisbon. So, although they have an irregular configuration, which is supposed to be a good approximation to the off-centre of Lisbon, because of its irregular characterisation, they are also considered to represent a correct characterisation of an urban environment. Either way, one should take into account that some measurements in the 1 800 MHz band for the off-centre case were done in areas which are

considered to be under the dense urban category in the simulations.

Measured RSRP, which is the average of the power measured (and average between receiver branches) of the resource elements that contain cell-specific reference signals, according to [HoTo11], is indicated in Figure F.2, Figure F.3, and Figure F.4 for the 800, 1 800 and 2 600 MHz bands, respectively. It is worth noticing that the higher the frequency band, the lower is the RSRP on average, as it is expected, because transmitter output power per RB decreases with the frequency band, and there is also an increase in path loss. For all the cases, in the off-centre environment, RSRP tends to be higher on average, which may be due to a higher percentage of LoS occurrences. It was checked that points where RSRP was higher are areas where proximity to the serving sector antenna is very high and LoS occurrence is very likely.

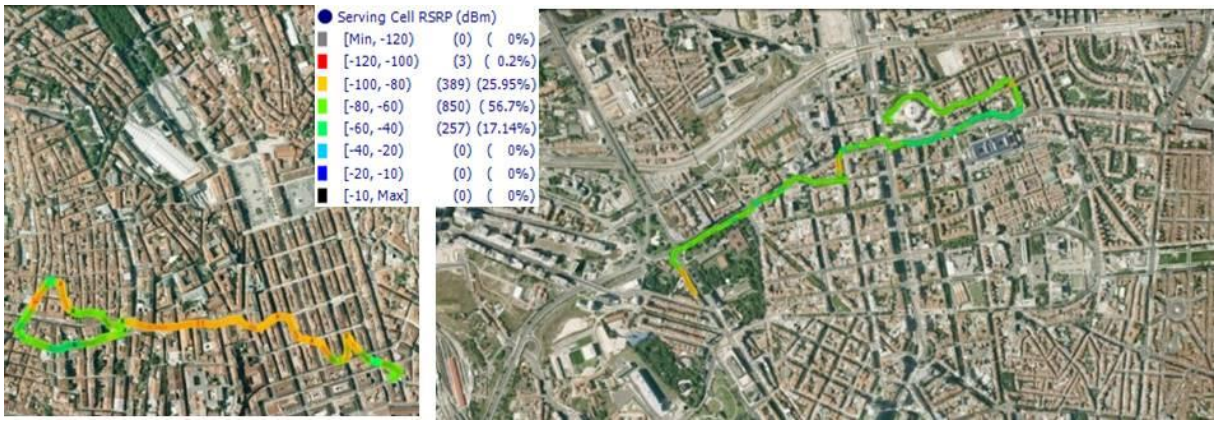

(a) Centre (b) Off-centre

Figure F.2. Measured RSRP in the 800 MHz band for centre and off-centre areas.

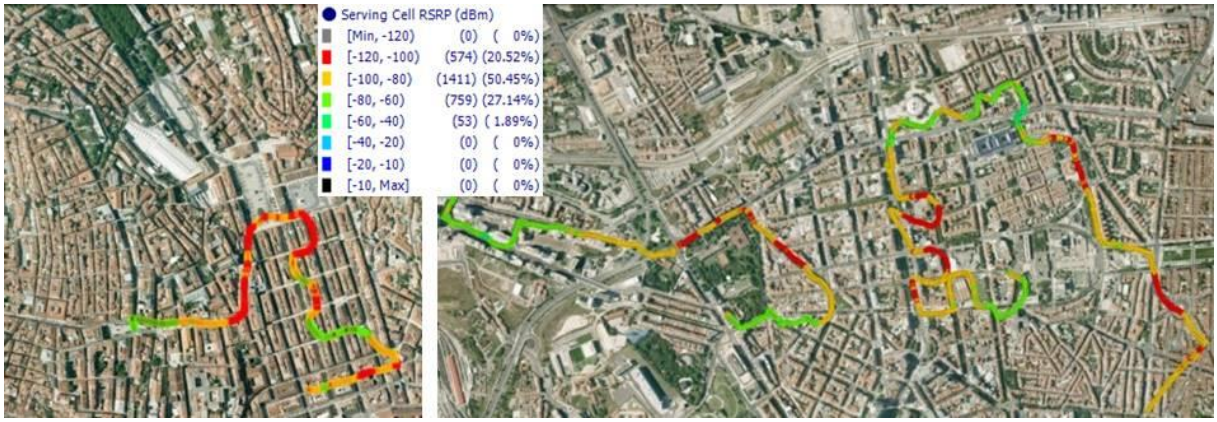

(a) Centre (b) Off-centre

Figure F.3. Measured RSRP in the 1 800 MHz band for centre and off-centre areas.

Highest measured interference power reaching the UE is presented in Figure F.5, Figure F.6, and Figure F.7 for the 800, 1 800 and 2 600 MHz bands, respectively. One can immediately notice that interference power is either similar or lower than measured RSRP from the serving sector, which is an expected trend, as if it was not that way, interfering sectors would then become serving sectors, because sector selection is also based on RSRP. It is also worth noticing that interference power is, on average, higher for the 800 MHz band, which is an expected result.

(a) Centre (b) Off-centre

Figure F.4. Measured RSRP in the 2 600 MHz band for centre and off-centre areas.

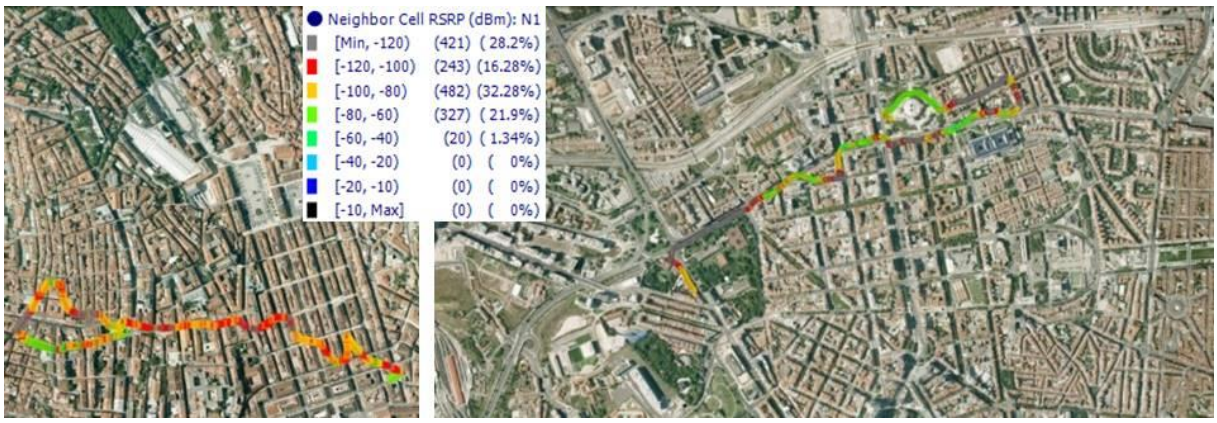

(a) Centre (b) Off-centre

Figure F.5. Highest measured neighbour cell RSRP in the 800 MHz band for centre and off-centre areas.

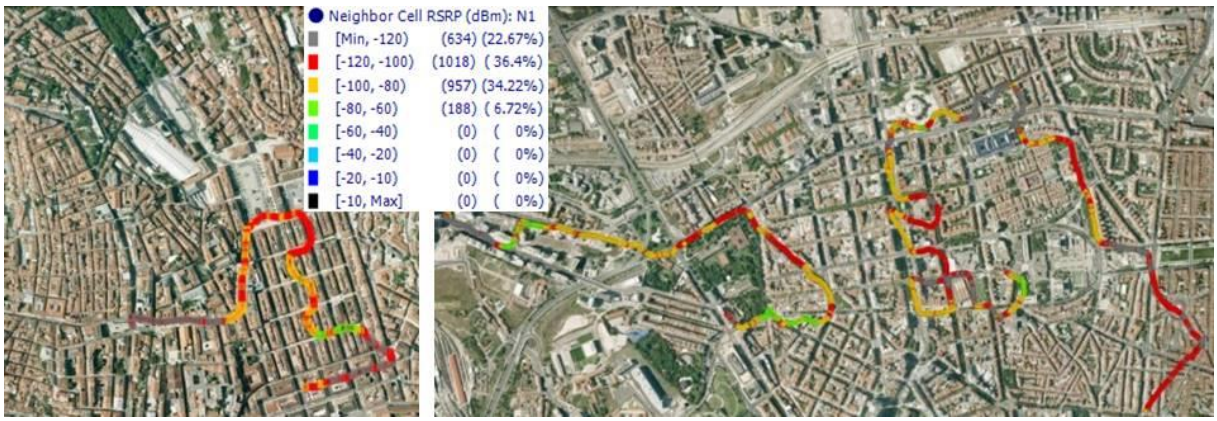

(a) Centre (b) Off-centre

Figure F.6. Highest measured neighbour cell RSRP in the 1 800 MHz band for centre and off-centre areas.

Figure F.8, Figure F.9 and Figure F.10 show the measured Reference Signal Signal-to-Noise Ratio (RS SNR) for the 800, 1 800 and 2 600 MHz bands, respectively. Taking the RSRP and highest interference power analyses into account, results are according to what should be expected: areas

where RSRP is low and highest interference power is high have a lower RS SNR. The 800 MHz case also seems to be the one where RS SNR is higher, on average, which suggests that interference was not an important constraining factor of system performance, meaning that the number of UEs using that part of the spectrum near the areas where measurements were done was not significant. RS SNRs above 30 dB were not registered, which suggests that data processing or even data collection saturates at around 30 dB, which means that RS SNRs above that value are registered as being close to 30 dB. This is assumed to happen because, in a noise limited system, in LoS conditions and when the user is very close to the BS, higher SNRs are supposed to be registered.

(a) Centre (b) Off-centre

Figure F.7. Highest measured neighbour cell RSRP in the 2 600 MHz band for centre and off-centre areas.

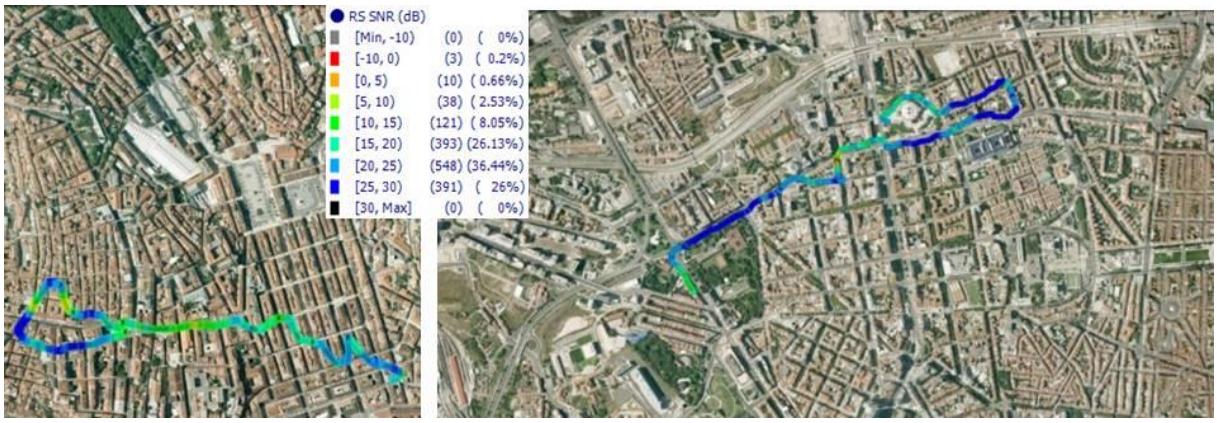

(a) Centre (b) Off-centre

Figure F.8. Measured SNR in the 800 MHz band for centre and off-centre areas.

In Figure F.11, Figure F.12, and Figure F.13, one can see the number of allocated RBs along the different measurement paths for the 800, 1 800 and 2 600 MHz bands, respectively. There are no important differences between centre and off-centre areas, but there are differences between frequency bands: as expected, the number of RBs in the 800 MHz band is around 50 almost every time, around 75 in the 1 800 MHz band and around 100 in the 2 600 MHz band. This means that full capacity of the network was achieved almost every time during measurements. Situations where the number of RBs drops considerably correspond to cell reselections and connection losses.

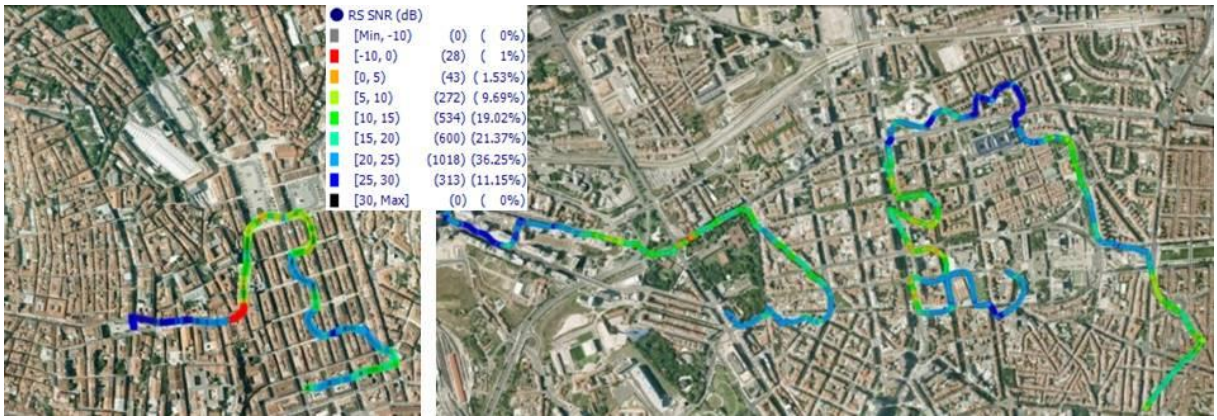

(a) Centre (b) Off-centre

Figure F.9. Measured SNR in the 1 800 MHz band for centre and off-centre areas.

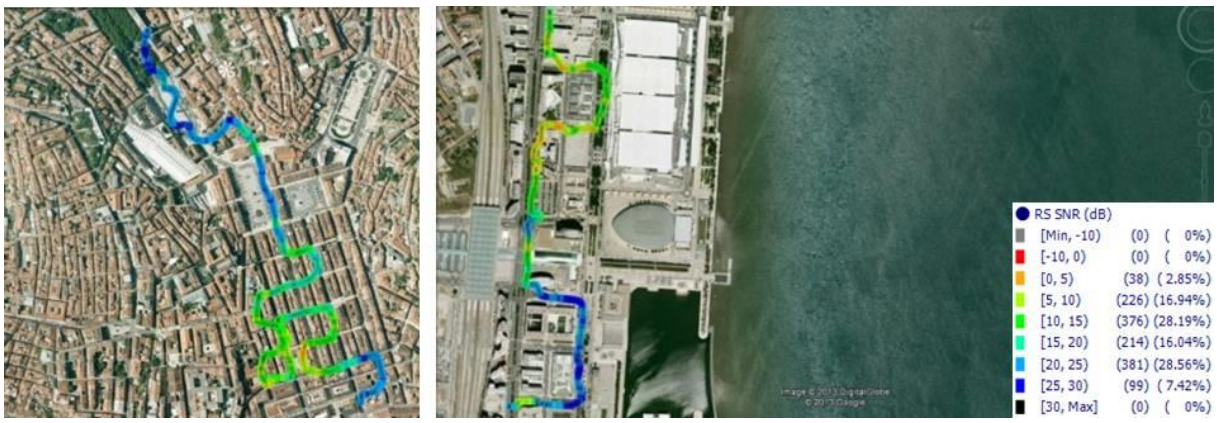

(a) Centre (b) Off-centre

Figure F.10. Measured SNR in the 2 600 MHz band for centre and off-centre areas.

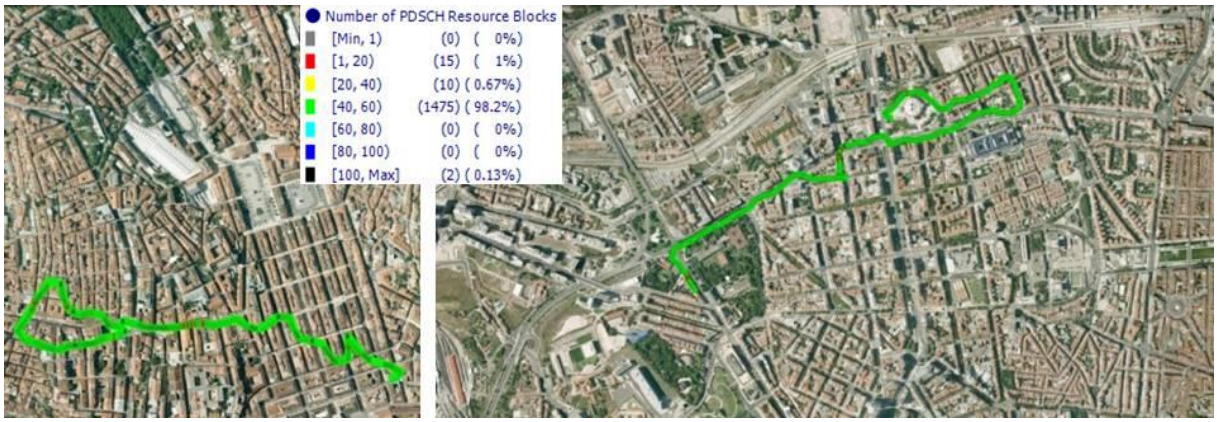

(a) Centre (b) Off-centre

Figure F.11. Number of allocated RBs in the 800 MHz band for centre and off-centre areas.

Measured PDSCH Physical Layer Throughput is represented in Figure F.14, Figure F.15 and Figure F.16 for the 800, 1 800 and 2 600 MHz bands, respectively. It can be seen that throughput assumes lower values in areas where the worst RS SNRs are felt. On average, throughput increases with frequency, because system capacity also increases with frequency. It is worth noticing that, in the 800 MHz band, there are no throughputs above 80 Mbit/s (except for a single point which presents an

abnormally high value of throughput, which may have been caused by a registration error), which is coherent with the fact that, in this frequency band, maximum theoretical throughput is around 75 Mbit/s in DL.

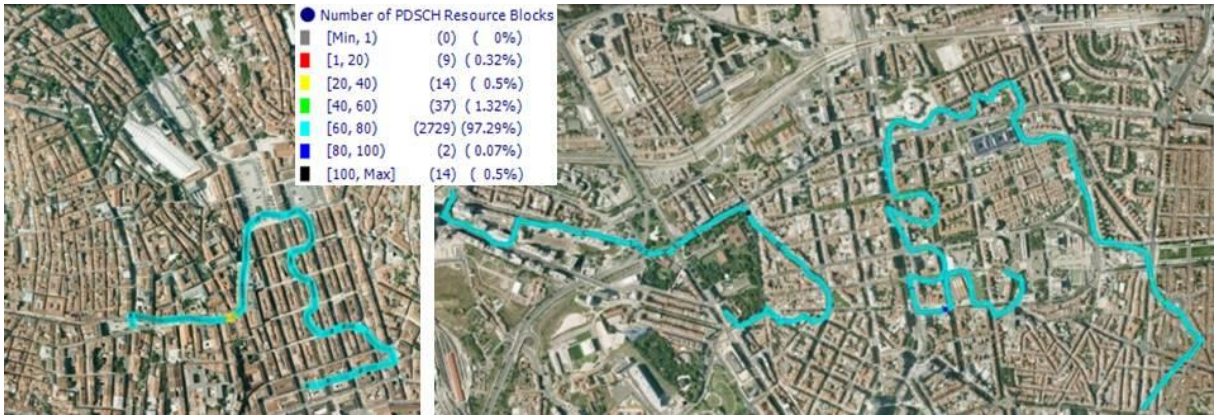

(a) Centre (b) Off-centre

Figure F.12. Number of allocated RBs in the 1 800 MHz band for centre and off-centre areas.

(a) Centre (b) Off-centre

Figure F.13. Number of allocated RBs in the 2 600 MHz band for centre and off-centre areas.

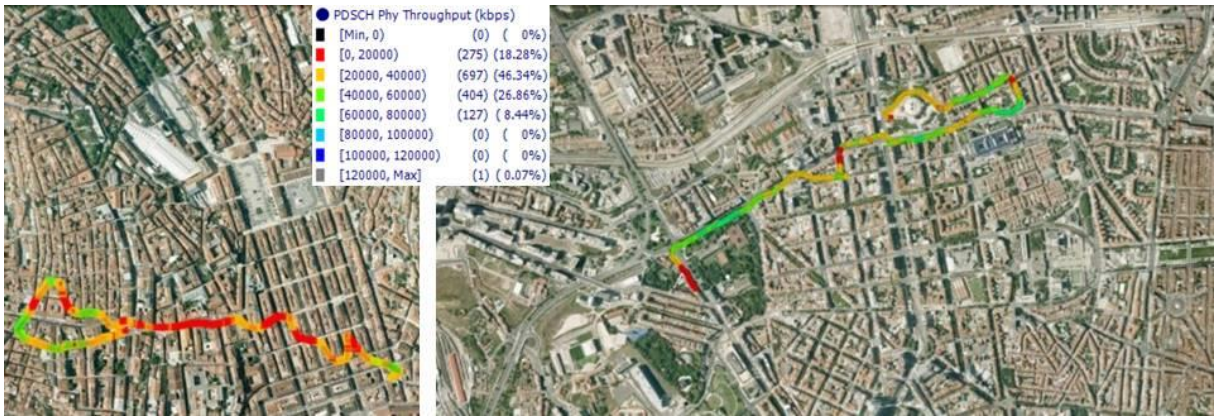

(a) Centre (b) Off-centre

Figure F.14. Measured throughput in the 800 MHz band for centre and off-centre areas.

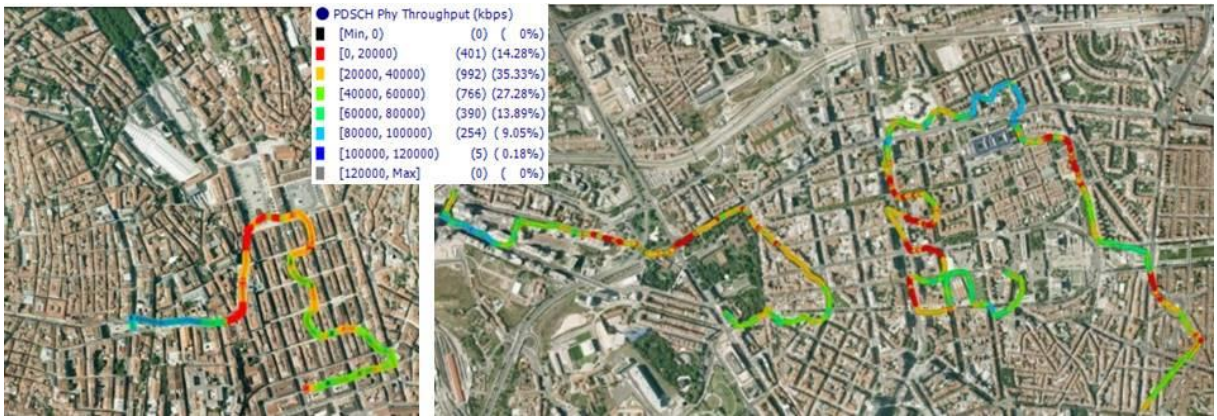

(a) Centre (b) Off-centre

Figure F.15. Measured throughput in the 1 800 MHz band for centre and off-centre areas.

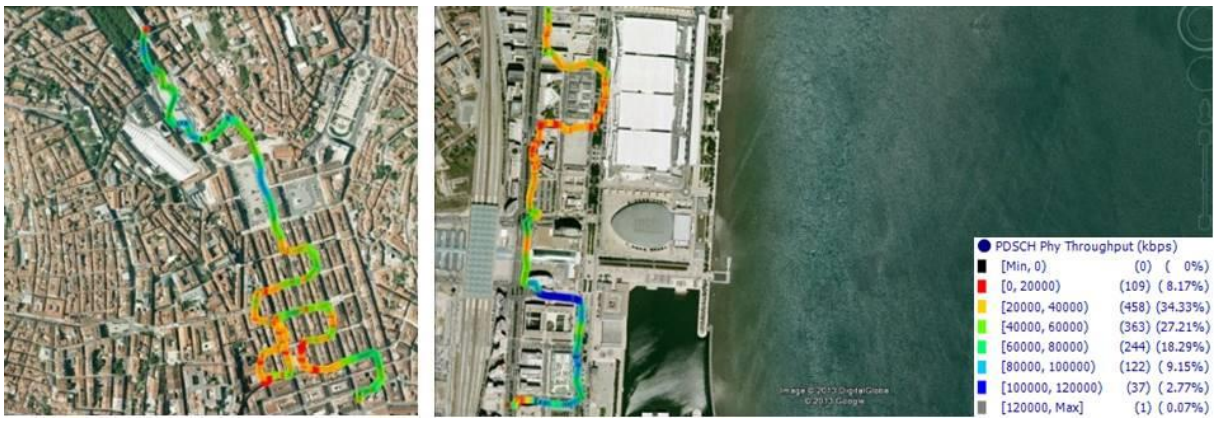

(a) Centre (b) Off-centre

Figure F.16. Measured throughput in the 2 600 MHz band for centre and off-centre areas.

References

[3GPP10a] 3GPP, Technical Specification Group Radio Access Network, *Further advancements for E-UTRA physical layer aspects (Release 9)*, Report TR 36.814, V9.0.0, Mar. 2010 (http://www.3gpp.org/ftp/Specs/html-info/36814.htm).

[3GPP10b] 3GPP, Technical Specification Group Radio Access Network, *Physical channels and modulation (Release 9)*, Report TS 36.211, V9.1.0, Mar. 2010 (http://www.3gpp.org/ftp/specs/html-INFO/36211.htm).

[3GPP10c] 3GPP, Technical Specification Group Radio Access Network, *Physical layer procedures (Release 9)*, Report TS 36.213, V9.3.0, Sep. 2010 (http://www.3gpp.org/ftp/Specs/html-info/36213.htm).

[3GPP11a] 3GPP, Technical Specification Group – RAN WG4, *Summary of alignment and impairment results for eDL-MIMO demodulation requirements*, Report R4-112713, Barcelona, Spain, May 2011.

[3GPP11b] 3GPP, *Digital cellular telecommunications system (Phase 2+); Universal Mobile Telecommunications System (UMTS); LTE; Quality of Service (QoS) concept and architecture*, ETSI TS, No. 23.107, Ver. 10.1.0, June 2011 (http://www.3gpp.org).

[3GPP11c] 3GPP, Technical Specification Group – RAN WG4, *Simulation results for eDL-MIMO demodulation requirements*, Report R4-114209, Athens, Greece, Aug. 2011.

[ANAC11] ANACOM, *Information on multi-band spectrum auction (3)*, Public Consultation, Lisbon, Portugal, Dec. 2012 (http://www.anacom.pt/render.jsp?contentId=1106646&languageId=1).

[ANAC12a] ANACOM, *Final Report of the Auction*, Public Consultation, Lisbon, Portugal, Jan. 2012 (http://www.anacom.pt/streaming/Final_Report_Auction.pdf?contentId=1115304&field=ATTACHED_FILE).

[ANAC12b] ANACOM, *Decision to approve agreement on location of spectrum in the 1800 MHz band* (in Portuguese), Public Consultation, Lisbon, Portugal, Mar. 2012 (http://www.anacom.pt/streaming/Decisao_ReshufflingMarco2012.pdf?contentId=1120288&field=ATTACHED_FILE).

[ANAC12c] ANACOM, *Decision to issue unified titles of rights of use of frequencies for terrestrial electronic communication services, subsequent to auction*, Public Consultation, Lisbon, Portugal, Mar. 2012 (http://www.anacom.pt/streaming/final_Decision_unified_titles09march2012.pdf?contentI

d=1121207&field=ATTACHED_FILE).

[AtJo10] Athley,F. and Johansson,M., “Impact of Electrical and Mechanical Antenna Tilt on LTE Downlink System Performance”, in *Proc. of VTC2010-Spring – 71st IEEE Vehicular Technology Conference*, Taipei, Taiwan, May 2010.

[BoEH12] Boswarthick,D., Elloumi,O. and Hersent,O., *M2M Communications – A Systems Approach*, John Wiley & Sons, Chichester, UK, Apr. 2012.

[Carr11] Carreira,P., *Data Rate Performance Gains in UMTS Evolution to LTE at the Cellular Level*, M. Sc. Thesis, Instituto Superior Técnico, Lisbon, Portugal, Oct. 2011.

[Corr01] Correia,L.M., *Wireless Flexible Personalised Communications: COST 259, European Co-operation in Mobile Radio Research*, John Wiley & Sons, Chichester, UK, 2001.

[Corr06] Correia,L.M., *Mobile Broadband Multimedia Networks – Techniques, Models and Tools for 4G*, Academic Press, Oxford, UK, May 2006.

[Corr13] Correia,L.M., *Mobile Communications Systems – Lecture Notes*, Instituto Superior Técnico, Lisbon, Portugal, Feb. 2013.

[DGBA12] Dhillon,H.S., Ganti,R.K., Baccelli,F. and Andrews,J.G., “Modeling and Analysis of K-Tier Downlink Heterogeneous Cellular Networks”, *IEEE Journal on Selected Areas in Communications*, Vol. 30, No. 3, Apr. 2012, pp. 550-560.

[Duar08] Duarte,S., *Analysis of Technologies for Long Term Evolution in UMTS*, M. Sc. Thesis, Instituto Superior Técnico, Lisbon, Portugal, Sep. 2008.

[EcKG11] Eckhardt,H., Klein,S. and Gruber,M., “Vertical Antenna Tilt Optimisation for LTE Base Stations”, in *Proc. of VTC2011-Spring – 73rd IEEE Vehicular Technology Conference*, Budapest, Hungary, May 2011.

[Eric13] Ericsson, *Ericsson Mobility Report*, Public Consultation, Stockholm, Sweden, June 2013 (http://www.ericsson.com/ericsson-mobility-report).

[FKRR09] Fodor,G., Koutsimanis,C., Rácz,A., Reider,N., Simonsson,A. and Müller,W., "Intercell Interference Coordination in OFDMA Networks and in the 3GPP Long Term Evolution System", *Journal of Communications*, Vol. 4, No. 7, Aug. 2009, pp. 445-453.

[GMRM12] Ghosh,A., Mangalvedhe,N., Ratasuk,R., Mondal,B., Cudak,M., Visotsky,E., Thomas,T.A., Andrews,J.G., Xia,P., Jo,H.S., Dhillon,H.S. and Novlan,T.D., "Heterogeneous Cellular Networks: From Theory to Practice", *IEEE Communications Magazine*, June 2012, pp. 54-64.

[HoTo11] Holma,H. and Toskala,A., *LTE for UMTS: Evolution to LTE Advanced (2nd Edition)*, John Wiley & Sons, Chichester, UK, Mar. 2011.

[Jaci09] Jacinto,N., *Performance Gains Evaluation from UMTS/HSPA+ to LTE at the Radio Network Level*, M. Sc. Thesis, Instituto Superior Técnico, Lisbon, Portugal, Nov. 2009.

[Kath12] Kathrein, “80010675 Antenna Fact Sheet”, Apr. 2013 (http://www.kathrein.de/svg/download/9363879b.pdf).

[Khan09] Khan,F., *LTE for 4G Mobile Broadband – Air Interface Technologies and Performance*, Cambridge University Press, New York, USA, Apr. 2009.

[Ku11] Ku,G., *Resource Allocation in LTE*, Drexel University, Pennsylvania, USA, Nov. 2011 (http://www.ece.drexel.edu/walsh/Gwanmo-Nov11-2.pdf).

[LeGu07] Lee,J. and Gupta,M., *A New Traffic Model for Current User Web Browsing Behaviour*, Internal Report, Intel Corporation, Hillsboro, USA, 2007 (http://blogs.intel.com/wp-content/mt-content/com/research/HTTP%20Traffic%20Model_v1%201%20white%20paper.pdf).

[LeSC13] Lee,P., StewartD. and Calugar-Pop,C., *Technology, Media & Telecommunications 2013*, Public Consultation, London, UK, Jan. 2013 (http://www.deloitte.com/view/en_GX/global/industries/technology-media-telecommunications/tmt-predictions-2013/index.htm?id=gx_theme_Pred13).

[Meye10] Meyer,L.J., *Electrical and Mechanical Downtilt and their Effects on Horizontal Pattern Performance*, Public Consultation, Andrew – A CommScope Company, North Carolina, USA, 2010 (http://docs.commscope.com/Public/electrical_and_mechanical_downtilt_effect_on_pattern_performance.pdf).

[NaDA06] Nawrocki,M.J., Dohler,M. and Aghvami,A.H., *Understanding UMTS Radio Network Modelling, Planning and Automated Optimisation – Theory and Practice*, John Wiley & Sons, Chichester, UK, 2006.

[PaNS11] Pauli,V., Nisar,M.D. and Seidel,E., "Reproducible LTE uplink performance analysis using precomputed interference signals", *EURASIP Journal on Advances in Signal Processing*, Vol. 2011, Sep. 2011.

[Paol12] Paolini,M., *Interference management in LTE networks and devices*, White paper, Senza Fili Consulting, Sammamish, USA, 2012 (http://www.senzafiliconsulting.com/Blog/tabid/64/articleType/ArticleView/articleId/86/Managing-interference-in-LTE-networks-and-devices.aspx).

[Pire12] Pires,R., *Coverage and Efficiency Performance Evaluation of LTE in Urban Scenarios*, M. Sc. Thesis, Instituto Superior Técnico, Lisbon, Portugal, Nov. 2012.

[PoPo10] Porjazoski,M. and Popovski,B., "Analysis of Intercell Interference Coordination by Fractional Frequency Reuse in LTE", in *Proc. of 2010 SoftCOM – International Conference on Software, Telecommunications and Computer Networks*, Split, Croatia, Sep. 2010.

[SeCa04] Sebastião,D. and Cardeiro,J., *Traffic Modelling and Dimensioning of the UMTS Radio Interface (in collaboration with Vodafone)* (in Portuguese), Dipl. Thesis, Instituto Superior

Técnico, Lisbon, Portugal, Oct. 2004.

[SeTB11] Sesia,S., Toufik,I. and Baker,I., *LTE - The UMTS Long Term Evolution: From Theory to Practice (2nd Edition)*, John Wiley & Sons, Chichester, UK, Aug. 2011.

[TGBC11] Tabia,N., Gondran,A., Baala,O. and Caminada,A., "Interference Model and Evaluation in LTE Networks", in *Proc. of 4th Joint IFIP Wireless and Mobile Networking Conference*, Toulouse, France, Oct. 2011.

[ViQR07] Vieira,P., Queluz,P. and Rodrigues,A., "A Dynamic Propagation Prediction Platform over Irregular Terrain and Buildings for Wireless Communications", in *Proc. of VTC2007-Fall – 66th IEEE Vehicular Technology Conference*, Baltimore, USA, Oct. 2007.

[Veri13] http://www.verizonwireless.com/b2c/splash/datacalculatorPopup.jsp, Aug. 2013.

[Voda13] Vodafone Portugal, *Internal communication*, 2013.

[YiHH09] Yilmaz,O., Hämäläinen,S. and Hämäläinen,J., "Comparison of Remote Electrical and Mechanical Antenna Downtilt Performance for 3GPP LTE", in *Proc. of VTC2009-Fall – 70th IEEE Vehicular Technology Conference*, Anchorage, USA, Sep. 2009.

[ZMSR08] Zheng,N., Michaelsen,P., Steiner,J., Rosa,C. and Wigard,J., "Antenna Tilt and Interaction with Open Loop Power Control in Homogeneous Uplink LTE Networks", in *Proc. of 2008 IEEE International Symposium on Wireless Communication Systems*, Reykjavík, Iceland, Oct. 2008.